

AD

TECHNICAL REPORT ARCCB-TR-95014

PREDICTION OF SHOT IMPACT USING
DYNAMIC ANALYSIS AND FIRING RESULTS
FOR THE M1A1 TANK



RONALD G. GAST

MARCH 1995



US ARMY ARMAMENT RESEARCH,
DEVELOPMENT AND ENGINEERING CENTER
CLOSE COMBAT ARMAMENTS CENTER
BENÉT LABORATORIES
WATERVLIET, N.Y. 12189-4050



APPROVED FOR PUBLIC RELEASE; DISTRIBUTION UNLIMITED

DTIC QUALITY INSPECTED 3

19950613 153

DISCLAIMER

The findings in this report are not to be construed as an official Department of the Army position unless so designated by other authorized documents.

The use of trade name(s) and/or manufacturer(s) does not constitute an official indorsement or approval.

DESTRUCTION NOTICE

For classified documents, follow the procedures in DoD 5200.22-M, Industrial Security Manual, Section II-19 or DoD 5200.1-R, Information Security Program Regulation, Chapter IX.

For unclassified, limited documents, destroy by any method that will prevent disclosure of contents or reconstruction of the document.

For unclassified, unlimited documents, destroy when the report is no longer needed. Do not return it to the originator.

REPORT DOCUMENTATION PAGE

Form Approved
OMB No. 0704-0188

Public reporting burden for this collection of information is estimated to average 1 hour per response, including the time for reviewing instructions, searching existing data sources, gathering and maintaining the data needed, and completing and reviewing the collection of information. Send comments regarding this burden estimate or any other aspect of this collection of information, including suggestions for reducing this burden, to Washington Headquarters Services, Directorate for Information Operations and Reports, 1215 Jefferson Davis Highway, Suite 1204, Arlington, VA 22202-4302, and to the Office of Management and Budget, Paperwork Reduction Project (0704-0188), Washington, DC 20503.

1. AGENCY USE ONLY (Leave blank)			2. REPORT DATE March 1995		3. REPORT TYPE AND DATES COVERED Final		
4. TITLE AND SUBTITLE PREDICTION OF SHOT IMPACT USING DYNAMIC ANALYSIS AND FIRING RESULTS FOR THE M1A1 TANK			5. FUNDING NUMBERS AMCMS: 6126.24.H180.0 PRON: M147A074M11A				
6. AUTHOR(S) Ronald G. Gast							
7. PERFORMING ORGANIZATION NAME(S) AND ADDRESS(ES) U.S. Army ARDEC Benét Laboratories, AMSTA-AR-CCB-O Watervliet, NY 12189-4050			8. PERFORMING ORGANIZATION REPORT NUMBER ARCCB-TR-95014				
9. SPONSORING/MONITORING AGENCY NAME(S) AND ADDRESS(ES) U.S. Army ARDEC Close Combat Armaments Center Picatinny Arsenal, NJ 07806-5000			10. SPONSORING/MONITORING AGENCY REPORT NUMBER				
11. SUPPLEMENTARY NOTES							
12a. DISTRIBUTION / AVAILABILITY STATEMENT Approved for public release; distribution unlimited			12b. DISTRIBUTION CODE				
13. ABSTRACT (Maximum 200 words) Conventional tank battles are an important aspect of current and future warfare techniques. Even though our mechanized weaponry is extremely accurate, we should not embrace the mindset that the best in tank gun accuracy has been achieved. We can and should do more! The 'fleet zero' concept brought about by the downsizing trend in today's army means that zeroing exercises will be conducted for the entire fleet using only a few tanks and gun tubes. The contribution of individual tubes to a tank's accuracy is no longer determined. Therefore, for the concept to work, variability in tube-to-tube manufacture (or more importantly the variability that contributes to accuracy) must be minimized or accounted for through the use of computer simulation. This report presents a comprehensive study into the relationship among the characteristics of gun tubes, projectiles, gun mounts, and ballistics and their effect upon dynamics at the muzzle and shot accuracy. The data is provided from the dynamic index tube test conducted in the early 1990s. Modelling is performed using Benét's gun vibration model and a recently purchased gun vibrations code. The overall goal is to provide aiming point correction factors based upon system dynamics and an empirically determined exit jump offset for a specific round and ballistic load. In this type of analysis, the values of uncertain or unknown parameters are randomly drawn from an expected statistical distribution. Therefore, a given distribution of input values results in a distribution of output responses having its own characteristics. The likelihood that a response occurs is cast in terms of a probability distribution. For the test data used and the analysis run, fifty percent of the samples show promise for the use of this semi-elliptical method of shot impact prediction. Further study including more rounds and gun tubes is recommended with the intent of gaining improved accuracy across the full family of rounds for the M1A1 tank.							
14. SUBJECT TERMS Gun Dynamics, M1A1, Tank Gun Accuracy, Modal Analysis, Probabilistic Analysis, M256 Tank Cannon, Kinetic Energy Projectile				15. NUMBER OF PAGES 94			
				16. PRICE CODE			
17. SECURITY CLASSIFICATION OF REPORT UNCLASSIFIED		18. SECURITY CLASSIFICATION OF THIS PAGE UNCLASSIFIED		19. SECURITY CLASSIFICATION OF ABSTRACT UNCLASSIFIED		20. LIMITATION OF ABSTRACT UJ	

TABLE OF CONTENTS

INTRODUCTION	1
DYNAMIC INDEXING OF GUN TUBES AND TEST RESULTS	2
Dynamic Indexed Tube Test	2
DYNAMIC MODELLING AND ACCURACY	24
Simulation of Barrel Dynamics (SIMBAD) Vibration Model	24
Uniform Segments Method (USM) Vibrations Model	26
PARAMETERS OF THE ACCURACY STUDY	27
Gun Mount Specifications	27
Projectile Stiffness Specifications	29
Projectile Eccentricity Specifications	31
Ballistic Uncertainties	31
SENSITIVITY TO VARIATION IN SYSTEM PARAMETERS	32
Parameter Values	32
Response Presentation	33
Response Discussion	33
PROBABILISTIC ANALYSIS AND ITS RELATIONSHIP TO ACCURACY	57
Parameter Statistics and Distributions	57
Response Discussion	58
Correlation of Dynamic Results to COI Test Data	81
DISCUSSION AND CONCLUSIONS	86
REFERENCES	89

Tables

1. Sabot Stiffness For Generic Kinetic Energy Round	31
2. Projectile Jump Extremes, Flexible Round, DIT Tubes	34
3. Projectile Jump Extremes, Flexible Round, STD Tubes	46
4. Probabilistic Distribution of Bore Rider Stiffness	58

Distribution	
Availability Codes	
Dist	Avail and/or Special
A-1	

5. Probabilistic Distribution of Projectile Imbalance	58
---	----

List of Illustrations

1a. Profile and curvature vertical plane tube #4098	4
1b. Profile and curvature vertical plane tube #4100	5
1c. Profile and curvature vertical plane tube #4102	6
1d. Profile and curvature vertical plane tube #4104	7
1e. Profile and curvature vertical plane tube #4106	8
1f. Profile and curvature vertical plane tube #4988	9
1g. Profile and curvature vertical plane tube #4990	10
1h. Profile and curvature vertical plane tube #4992	11
1i. Profile and curvature vertical plane tube #4994	12
1j. Profile and curvature vertical plane tube #4996	13
2a. Profile and curvature horizontal plane tube #4098	14
2b. Profile and curvature horizontal plane tube #4100	15
2c. Profile and curvature horizontal plane tube #4102	16
2d. Profile and curvature horizontal plane tube #4104	17
2e. Profile and curvature horizontal plane tube #4106	18
2f. Profile and curvature horizontal plane tube #4988	19
2g. Profile and curvature horizontal plane tube #4990	20
2h. Profile and curvature horizontal plane tube #4992	21
2i. Profile and curvature horizontal plane tube #4994	22
2j. Profile and curvature horizontal plane tube #4996	23
3. Centers of impact (COI) for DIT test	25
4. 120-mm M256 cannon and mount	28

5. 120-mm generic kinetic energy round	30
6a. COI data and calculated gun jump: tube #4098	35
6b. COI data and calculated projectile jump: tube #4098	36
7a. COI data and calculated gun jump: tube #4100	37
7b. COI data and calculated projectile jump: tube #4100	38
8a. COI data and calculated gun jump: tube #4102	39
8b. COI data and calculated projectile jump: tube #4102	40
9a. COI data and calculated gun jump: tube #4104	41
9b. COI data and calculated projectile jump: tube #4104	42
10a. COI data and calculated gun jump: tube #4106	43
10b. COI data and calculated projectile jump: tube #4106	44
11a. COI data and calculated gun jump: tube #4988	47
11b. COI data and calculated projectile jump: tube #4988	48
12a. COI data and calculated gun jump: tube #4990	49
12b. COI data and calculated projectile jump: tube #4990	50
13a. COI data and calculated gun jump: tube #4992	51
13b. COI data and calculated projectile jump: tube #4992	52
14a. COI data and calculated gun jump: tube #4994	53
14b. COI data and calculated projectile jump: tube #4994	54
15a. COI data and calculated gun jump: tube #4996	55
15b. COI data and calculated projectile jump: tube #4996	56
16a. Probabilistic analysis of gun jump: tube #4098	60
16b. Probabilistic analysis of projectile jump: tube #4098	61
17a. Probabilistic analysis of gun jump: tube #4100	62

17b. Probabilistic analysis of projectile jump: tube #4100	63
18a. Probabilistic analysis of gun jump: tube #4102	64
18b. Probabilistic analysis of projectile jump: tube #4102	65
19a. Probabilistic analysis of gun jump: tube #4104	66
19b. Probabilistic analysis of projectile jump: tube #4104	67
20a. Probabilistic analysis of gun jump: tube #4106	68
20b. Probabilistic analysis of projectile jump: tube #4106	69
21a. Probabilistic analysis of gun jump: tube #4988	71
21b. Probabilistic analysis of projectile jump: tube #4988	72
22a. Probabilistic analysis of gun jump: tube #4990	73
22b. Probabilistic analysis of projectile jump: tube #4990	74
23a. Probabilistic analysis of gun jump: tube #4992	75
23b. Probabilistic analysis of projectile jump: tube #4992	76
24a. Probabilistic analysis of gun jump: tube #4994	77
24b. Probabilistic analysis of projectile jump: tube #4994	78
25a. Probabilistic analysis of gun jump: tube #4996	79
25b. Probabilistic analysis of projectile jump: tube #4996	80
26. Probabilistic analysis: projectile jump averages	82
27. Probabilistic analysis: projectile jump offset	84
28. Probabilistic analysis: calculated centers of impact	85

INTRODUCTION

Conventional tank battles are an important aspect of current and future warfare techniques. A prime example was shown in Operation Desert Storm. After Iraq's reconnaissance capabilities were nullified by massive air strikes, the coalition forces virtually annihilated the enemy by a swift and accurate ground attack spearheaded by relentless tank assaults. The battlefield was a virtual 'junk yard' of Iraqi warfare equipment. However, we should not rest on our laurels by embracing the mindset that the best in tank gun accuracy has been achieved. We can do more!

Consider today's state of affairs regarding the military. Downsizing is the buzzword; not just bodies but also training, equipment, etc, etc. The 'fleet zero' requirement which was introduced a few years ago dovetails nicely into this concept. Basically, it means that zeroing exercises will be conducted for the entire fleet using only a few tanks, therefore, less hands-on firing will be conducted. The contribution of individual tubes to a tank's accuracy is no longer determined. Therefore, for the concept to work, variability in tube-to-tube manufacture (or more importantly the variability that contributes to accuracy) must be minimized. It still remains that a first round kill is paramount in tank battles.

Through the years, the Army Research Laboratory (ARL formerly Ballistic Research Laboratory (BRL)), Benét Laboratories (BL), Tank Automotive Command (TACOM), and various other agencies both domestic and foreign have been and are currently working in the area of simulating weapon dynamics for the express purpose of determining accuracy.

At ARL considerable ongoing research in the area of dynamic simulation, projectile disengagement and flight characteristics, gun mount and support characteristics, gun tube heating and cooling is being conducted (refs 1-12). The list of references is just a small sample of what has been achieved. At BL and Watervliet Arsenal considerable attention is being given to the design and manufacture of gun tubes having consistent characteristics such as straightness, wall variation, and material homogeneity.

In this report a correlation among gun tube, mount, projectile, and ballistic characteristics and their combined effect upon shot accuracy is presented for a set of 120-mm M256 gun tubes used in the dynamic index test (DIT) conducted in the early 1990s. The modelling codes used are the Benét Uniform Segments Gun Vibration Model (USM) that was developed in the late 1980s and the code Simatic's Simulation of Barrel Dynamics (SIMBAD) recently purchased from the United Kingdom. Unfortunately, some of the modelling parameters are quite uncertain but extremely sensitive in gun dynamics models, therefore, these will be used as random input variables and their statistical impact upon model response will be determined. The overall goal is to provide aiming point correction factors based upon system dynamics for a specific tube, mount, projectile, and ballistic pulse. These factors may be included in the current ballistic solution software used in the M1A1 tank.

DYNAMIC INDEXING OF GUN TUBES AND TEST RESULTS

The M256 cannon has characteristics that cause transverse gun vibrations during firing. One of these is due to the offset breech (about 1.25 inches below center line of bore). As the gun recoils, this offset mass produces an inertia couple that transmits a vibration wave along the tube's axis overtaking the projectile and disturbing the muzzle before shot exit. Also, as the projectile travels along the bore, interactive loads develop between the tube and projectile causing additional vibrations of both. Upon exit, the intended direction of the round has been compromised. As ARL suggests (ref 3), the effect could be mitigated by specifying a bore profile containing certain characteristics that minimize this effect. Based upon dynamic analysis results at ARL, a profile could be devised which when excited would vibrate in such a manner as to provide a relatively straight path for the projectile to follow. This would minimize side loadings and projectile vibrations. The profile that minimizes this side loading was termed the 'optimum profile'. The method of implementing this feature is called dynamic indexing of the tube (DIT).

The 'optimum profile' is dependent upon both projectile and charge temperature; the HEAT round has its own 'optimum profile' as well as another for the KE round. Since the KE round is considered critical, the 'optimum profile' is assumed to mean optimum for the KE round. The profile has the following characteristics. In the vertical plane the 'optimum profile' resembles a sine wave having a wavelength about 25 percent greater than the tube length and a magnitude of about 0.015 inch. In the horizontal plane the optimum profile is a negative sine wave of a wavelength equal to the tube length and a magnitude of about 0.002 inch. ARL did not suggest that tubes be manufactured to this profile, but that they be orientated during manufacture such that the top vertical center line of the tube be established so the tube's actual profile best matched the optimums. A least squares technique and a computer algorithm were incorporated into the manufacturing process. Normally, the standard method of tube indexing (STD) is to orient the top vertical center line of the gun such that the plane of greatest bending is vertical and the tube's muzzle points up. This method tends to minimize curvature due to normal gravity droop when cannon is mounted in its vehicle.

Dynamic Indexed Tube Test

In attempted to verify the DIT claim, an extensive test was performed during the early 1990s (ref 13). A considerable number of new M256 gun tubes were specifically manufactured for the test. Of these a number were dynamically indexed, whereas the rest were indexed according to the standard method. The cannons were mounted on M1A1 vehicles and accuracy tests performed. Both HEAT and KE rounds conditioned to various temperatures were used in the test. Each tube fired three rounds using each round type and condition temperature. The centers of impact (COI) and target impact dispersion (TID) were the primary data reported. Reference 13 contains all the data.

For the study to be reported herein, a portion of the unclassified data is used. The goal is not to verify dynamic indexing but rather attempt to establish a relationship between the calculated exit conditions of the projectile from gun vibrations models and the round's impact at the target for a representative sample of M256 gun tubes. It is felt that the profile characteristic of each tube (either indexed to the optimum or standard method) has an effect upon the projectile's 'ride' down the bore and its subsequent jump upon disengagement. One round type

conditioned to ambient temperature was chosen for the modelling. Rounds of this type were fired through ten gun tubes. Five were dynamically indexed, whereas the remaining were standard indexed. Profile data was received from Watervliet Arsenal's Quality Assurance Branch and used to establish the 'best' polynomial fit (ref 14) for each tube. The profile data, calculated fit, and curvature derived from the second derivative of the fit for all ten tubes are shown in Figures 1a to 1j for the vertical plane and in Figures 2a to 2j for the horizontal plane.

In Figures 1a to 1e, the vertical profile data, functional fits, and curvatures for the five DIT tubes are shown. The profile characteristics are quite similar. All five tubes tend to point down at the muzzle. Tube #4098 has the greatest deviation of 0.020 inch occurring over the last 50 inches of travel. Tube #4104 has the same amount of deviation, however, it is spread over 100 inches of travel. The remaining three tubes have deviations of lesser magnitude. The order of fit specified on the graphs represents the order of the approximating polynomial used to determine the continuous function that best represents the profile. The curvature function shown on the lower graphs is derived from the second derivative of the polynomial fit. The curvature is an important factor in dynamic modelling since it is directly proportional to the interactive point load between projectile and tube. Hence, the greater the magnitude of curvature, the greater the transverse load at its point of application. This implies more movement of both tube and projectile. For the DIT tubes, the curvature in the vertical plane tends to decrease towards the muzzle. The magnitudes near the muzzle, however, are somewhat different. For tube #4098, the value is -40 microreciprocal inches, whereas for tube #4106, the muzzle curvature is only 10 microreciprocal inches. The muzzle curvature for the remaining three tubes falls between these values.

The vertical profile data, functional fits, and curvature for the five STD tubes are shown in Figures 1f to 1j. These are similar in that the muzzle end of each points up. Tube #4992 has the greatest profile deviation of -0.024 inch, which occurs over the last 60 inches of travel. The orders of fit range from 3 to 5. Curvature values are somewhat unique. For tubes #4988 and #4996, curvature tends to begin at -40 microreciprocal inches, grows to slightly above 0, and finally ends up at 0 to -5 microreciprocal inches at the muzzle. Tube #4990 has a curvature that is nearly a mirror image of the tubes #4988 and #4996, whereas the curvature for tubes #4992 and #4994 is very close to 0 for the entire length.

Profile data, fits, and curvature values in the horizontal plane for the DIT tubes are shown in Figures 2a through 2e. As indicated on the plots, the orders of fit range from 2 to 5. Tubes #4100 and #4106 possess the greatest deviation of around 0.012 inch midpoint along the tube. Tube #4104 is nearly straight. Curvature signatures have no similarity. Tube #4104 has nearly zero curvature, whereas tube #4106 has a curvature signature that bows down and achieves a value of 40 microreciprocal inches at the muzzle. The curvature for tube #4098 is nearly a mirror image of that of #4106. Curvatures for the remaining tubes in this group are within these bounds.

For the STD tubes, the horizontal profile data, fits, and curvatures are shown in Figures 2f through 2j. Due to the indexing technique used for these tubes, the horizontal plane possesses nearly zero profile deviation. Hence, all tubes with the exception of #4990 contain curvature responses of less than 10 microreciprocal inches. The curvature response for #4990 begins at -30 million reciprocal inches, increases to 0 for about 75 inches, and then increases to 20

120mm M256 ACCURACY STUDY
STATIC PROFILE and CURVATURE of DIT TUBES
STATISTICALLY 'CORRECT' POLYNOMIAL FIT
for PROFILE and CURVATURE

TUBE# 4098

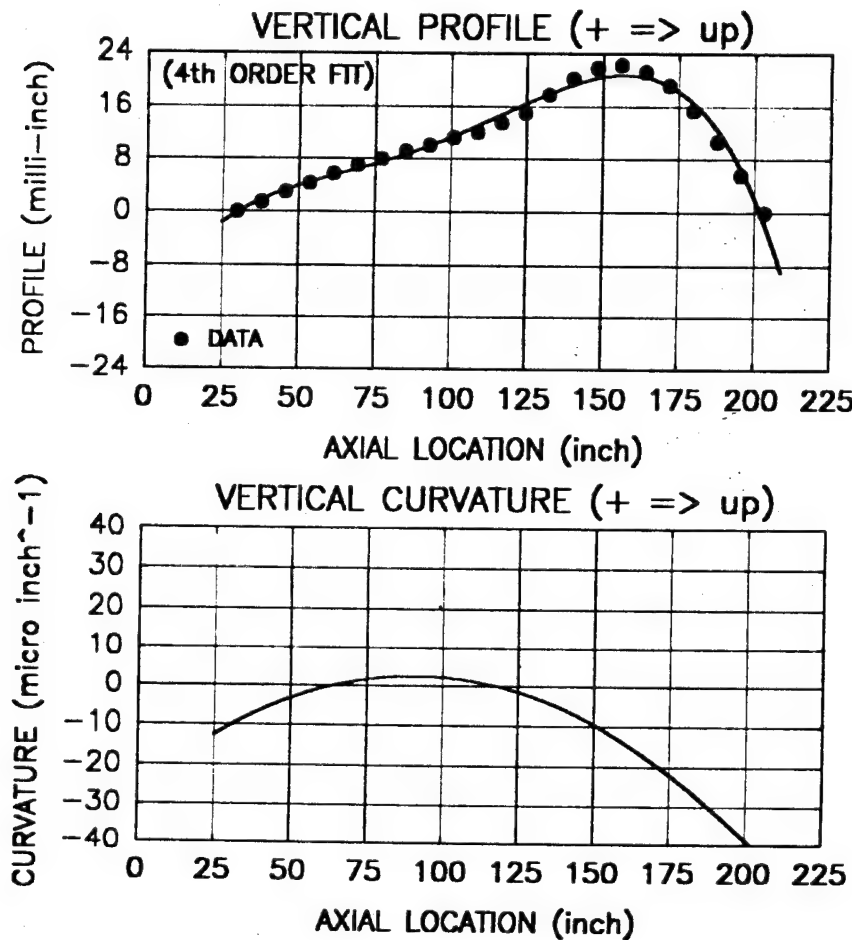


Figure 1a. Profile and curvature vertical plane tube #4098.

120mm M256 ACCURACY STUDY
STATIC PROFILE and CURVATURE of DIT TUBES
STATISTICALLY 'CORRECT' POLYNOMIAL FIT
for PROFILE and CURVATURE

TUBE# 4100

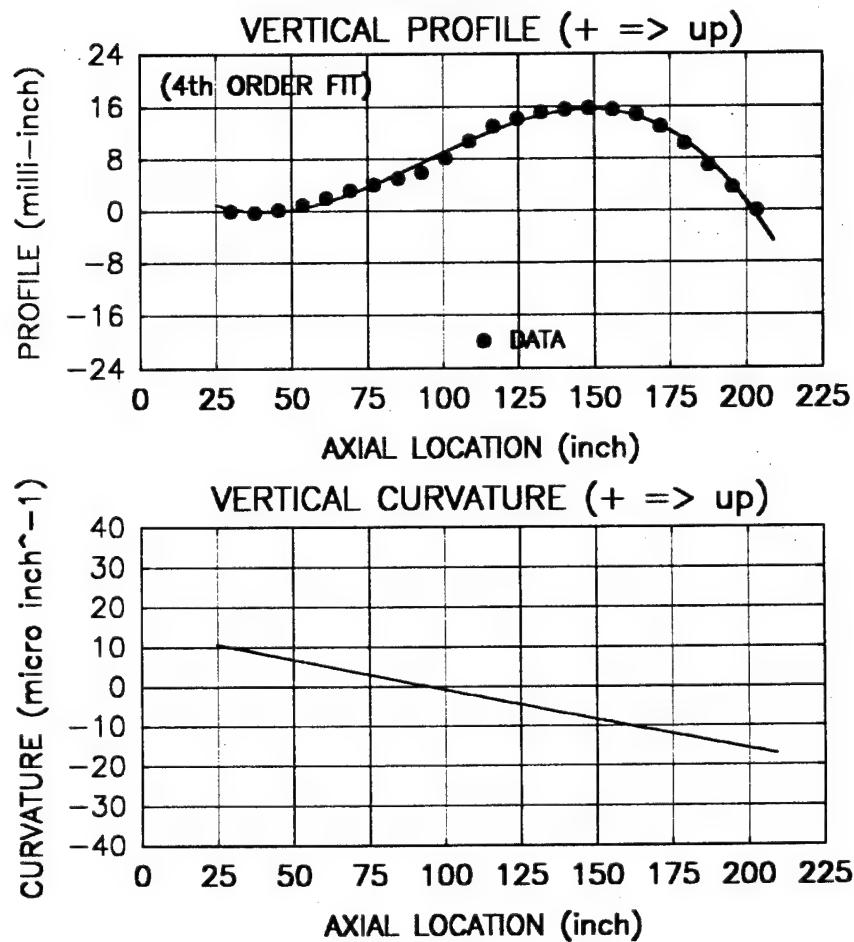


Figure 1b. Profile and curvature vertical plane tube #4100.

120mm M256 ACCURACY STUDY
STATIC PROFILE and CURVATURE of DIT TUBES
STATISTICALLY 'CORRECT' POLYNOMIAL FIT
for PROFILE and CURVATURE

TUBE# 4102

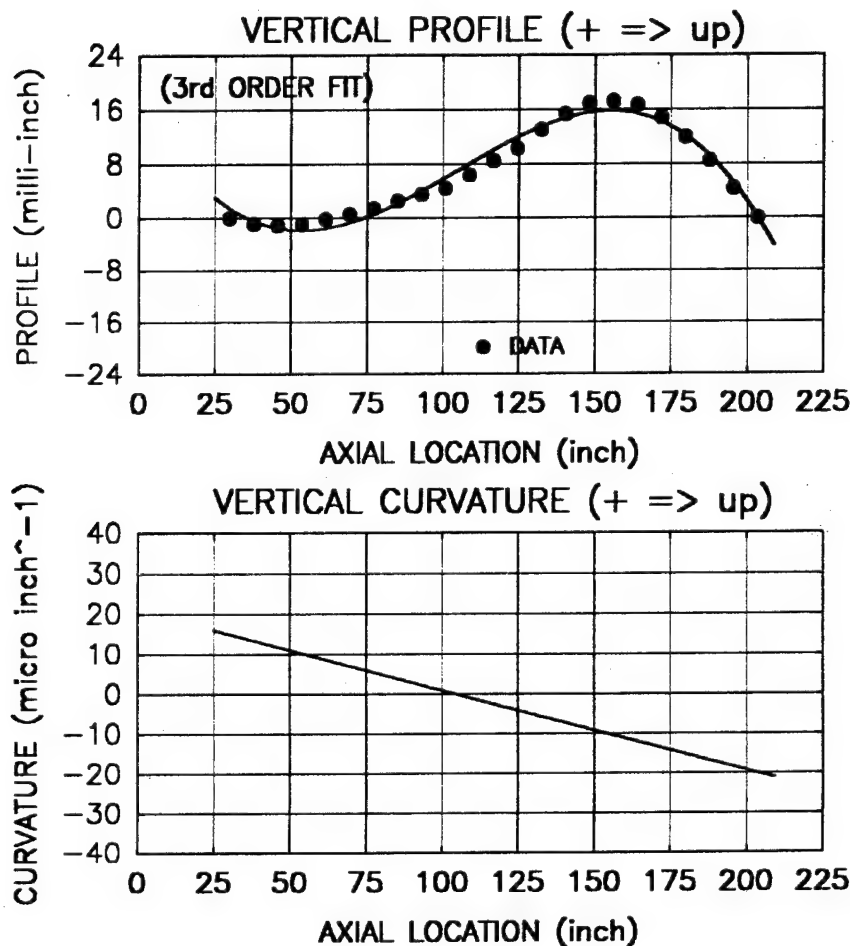


Figure 1c. Profile and curvature vertical plane tube #4102.

**120mm M256 ACCURACY STUDY
STATIC PROFILE and CURVATURE of DIT TUBES
STATISTICALLY 'CORRECT' POLYNOMIAL FIT
for PROFILE and CURVATURE**

TUBE# 4104

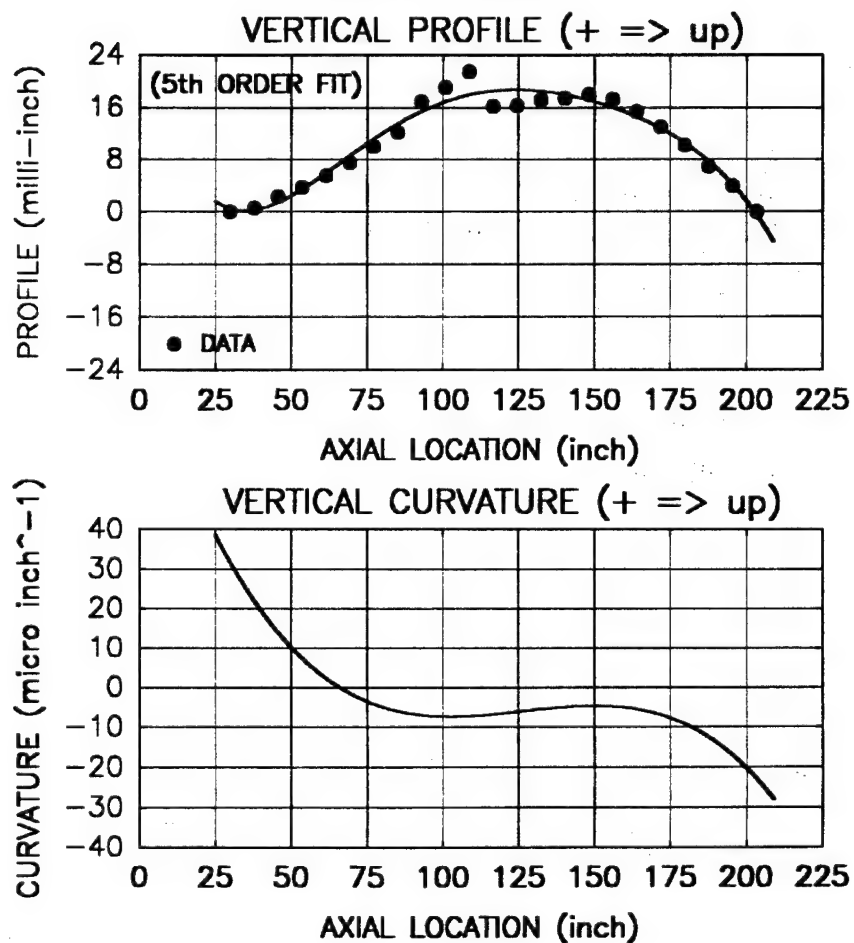


Figure 1d. Profile and curvature vertical plane tube #4104.

120mm M256 ACCURACY STUDY
STATIC PROFILE and CURVATURE of DIT TUBES
STATISTICALLY 'CORRECT' POLYNOMIAL FIT
for PROFILE and CURVATURE

TUBE# 4106

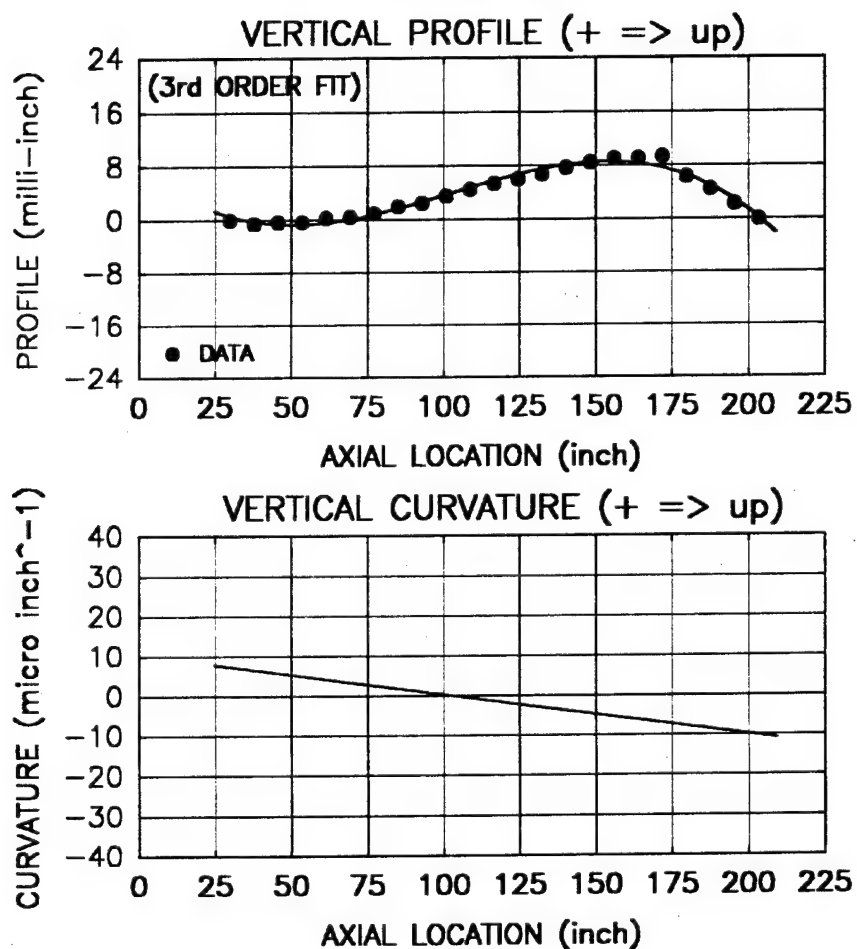


Figure 1e. Profile and curvature vertical plane tube #4106.

**120mm M256 ACCURACY STUDY
STATIC PROFILE and CURVATURE of STD TUBES
STATISTICALLY 'CORRECT' POLYNOMIAL FIT
for PROFILE and CURVATURE**

TUBE# 4988

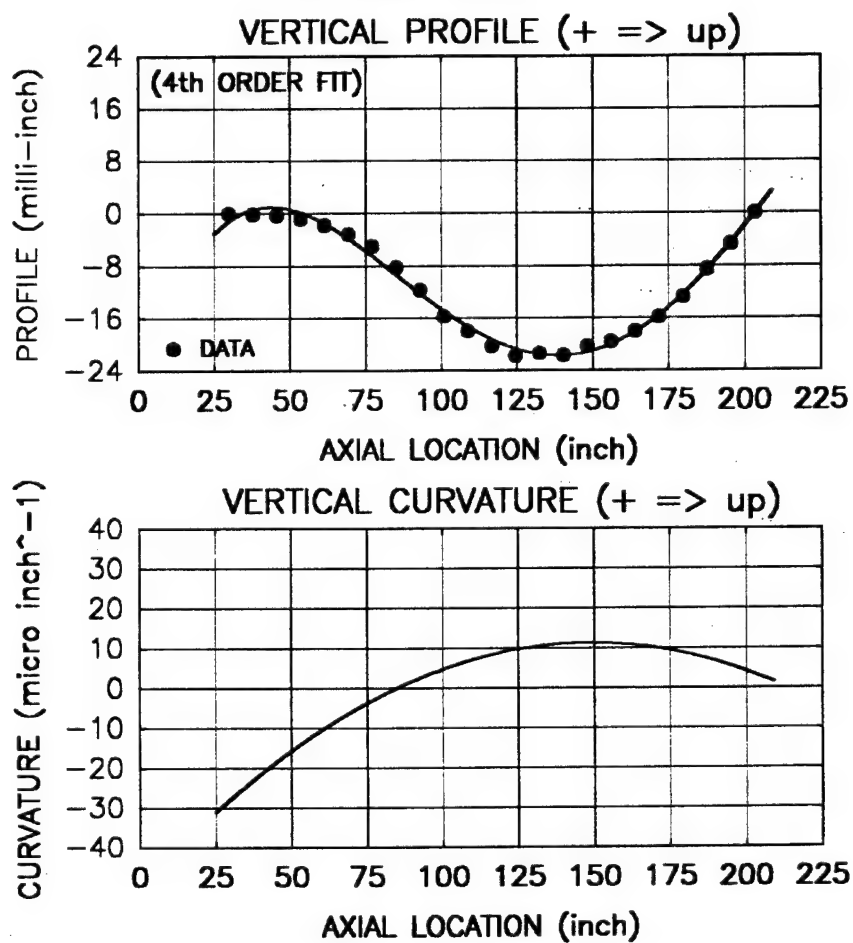


Figure 1f. Profile and curvature vertical plane tube #4988.

120mm M256 ACCURACY STUDY
STATIC PROFILE and CURVATURE of STD TUBES
STATISTICALLY 'CORRECT' POLYNOMIAL FIT
for PROFILE and CURVATURE

TUBE# 4990

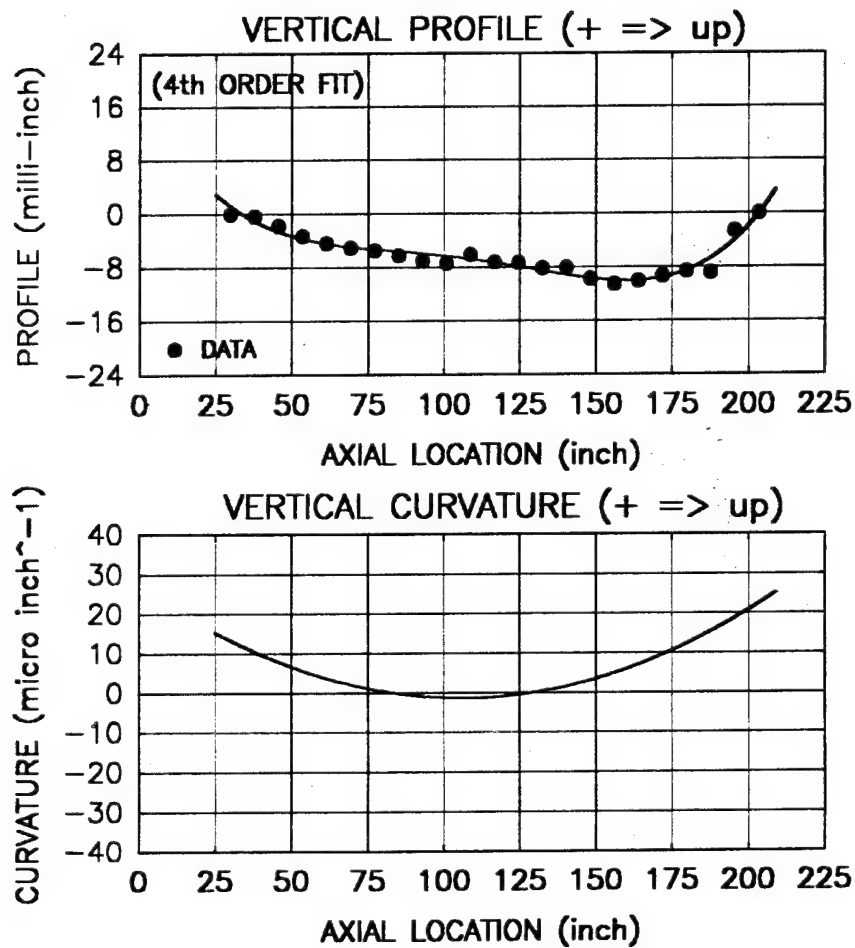


Figure 1g. Profile and curvature vertical plane tube #4990.

120mm M256 ACCURACY STUDY
STATIC PROFILE and CURVATURE of STD TUBES
STATISTICALLY 'CORRECT' POLYNOMIAL FIT
for PROFILE and CURVATURE

TUBE# 4992

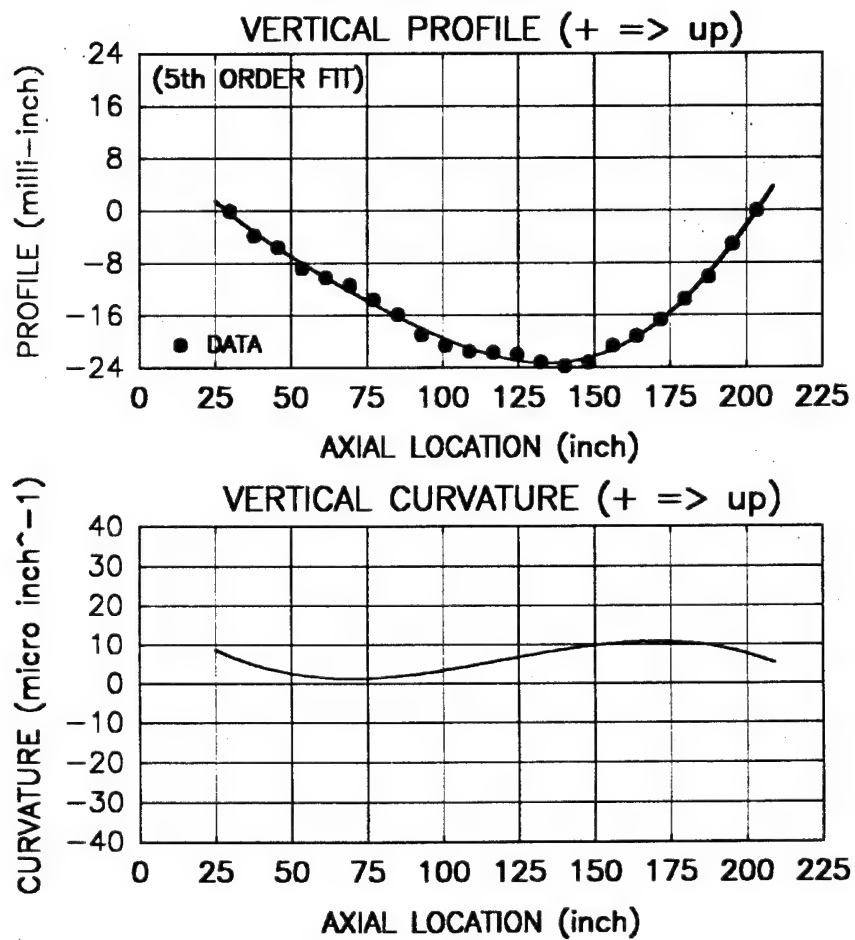


Figure 1h. Profile and curvature vertical plane tube #4992.

120mm M256 ACCURACY STUDY
STATIC PROFILE and CURVATURE of STD TUBES
STATISTICALLY 'CORRECT' POLYNOMIAL FIT
for PROFILE and CURVATURE

TUBE# 4994

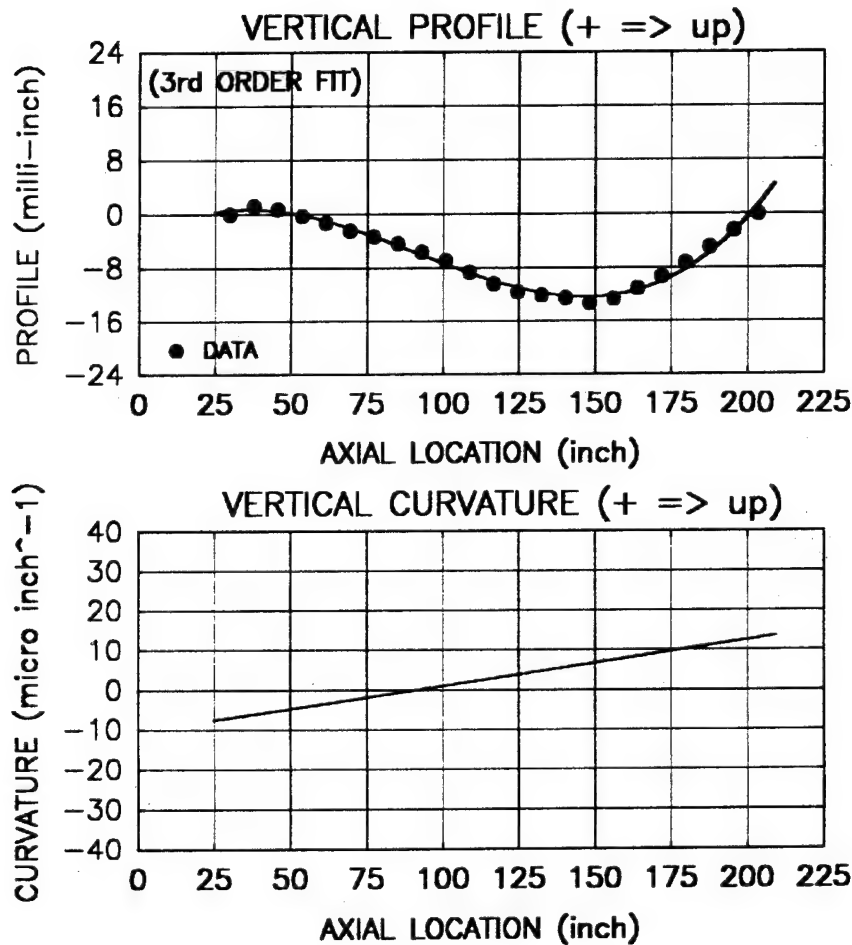


Figure 1i. Profile and curvature vertical plane tube #4994.

120mm M256 ACCURACY STUDY
STATIC PROFILE and CURVATURE of STD TUBES
STATISTICALLY 'CORRECT' POLYNOMIAL FIT
for PROFILE and CURVATURE

TUBE# 4996

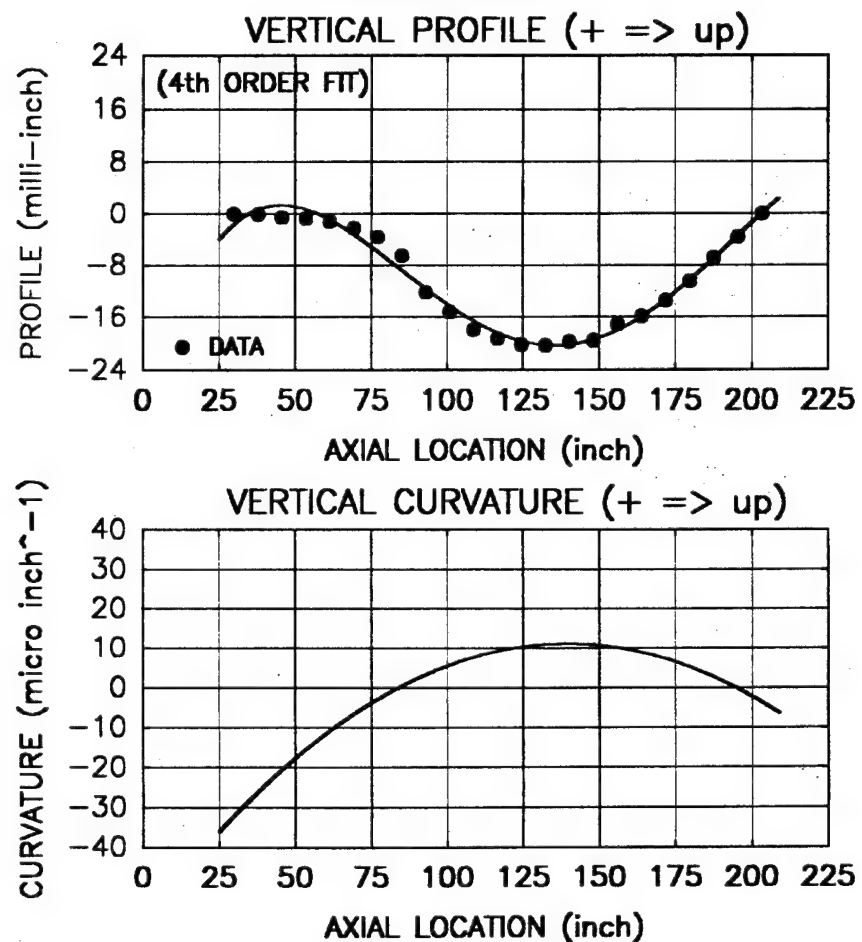
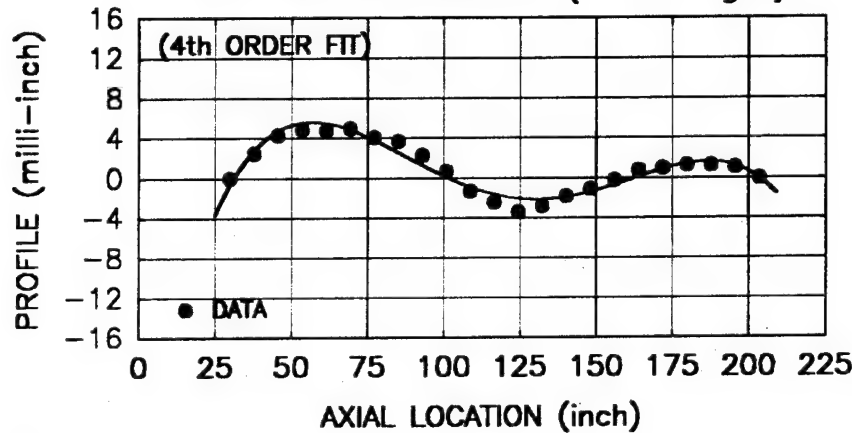


Figure 1j. Profile and curvature vertical plane tube #4996.

120mm M256 ACCURACY STUDY
STATIC PROFILE and CURVATURE of DIT TUBES
STATISTICALLY 'CORRECT' POLYNOMIAL FIT
for PROFILE and CURVATURE

TUBE # 4098

HORIZONTAL PROFILE (+ => right)



HORIZONTAL CURVATURE (+ => right)

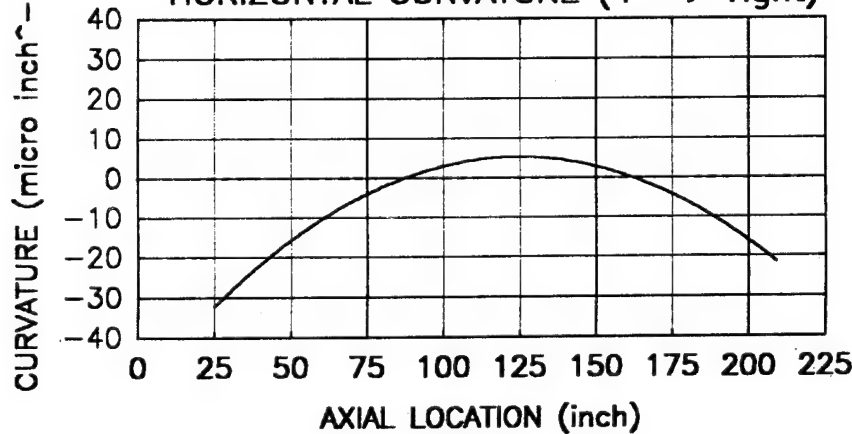
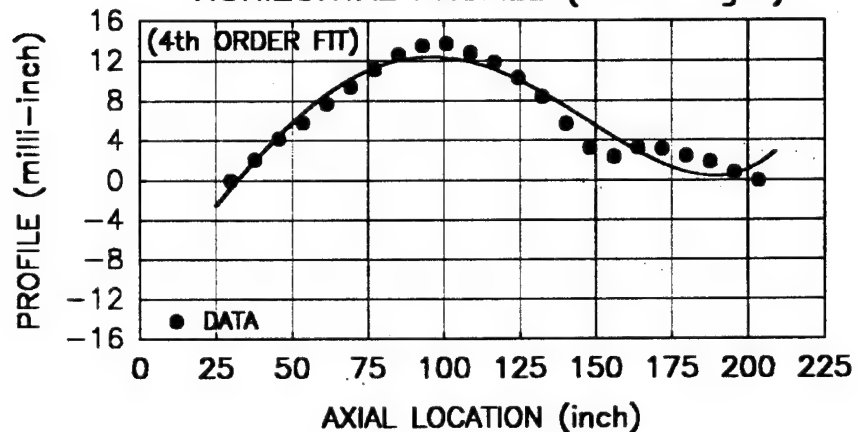


Figure 2a. Profile and curvature horizontal plane tube #4098.

120mm M256 ACCURACY STUDY
STATIC PROFILE and CURVATURE of DIT TUBES
STATISTICALLY 'CORRECT' POLYNOMIAL FIT
for PROFILE and CURVATURE

TUBE# 4100

HORIZONTAL PROFILE (+ => right)



HORIZONTAL CURVATURE (+ => right)

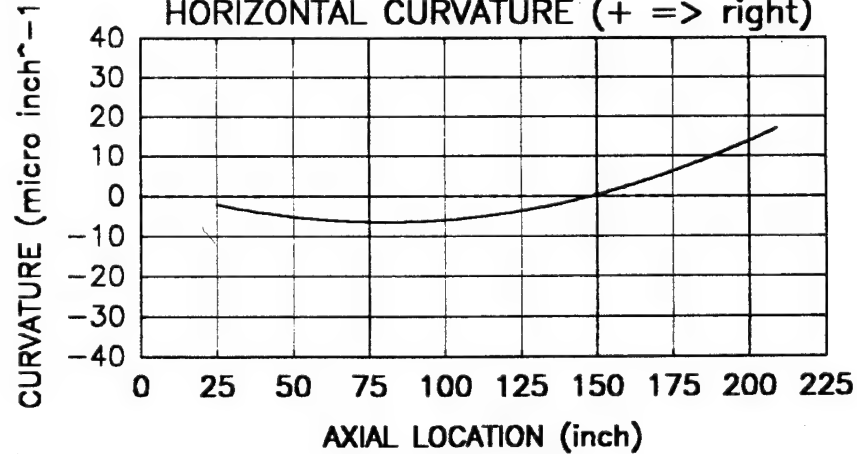
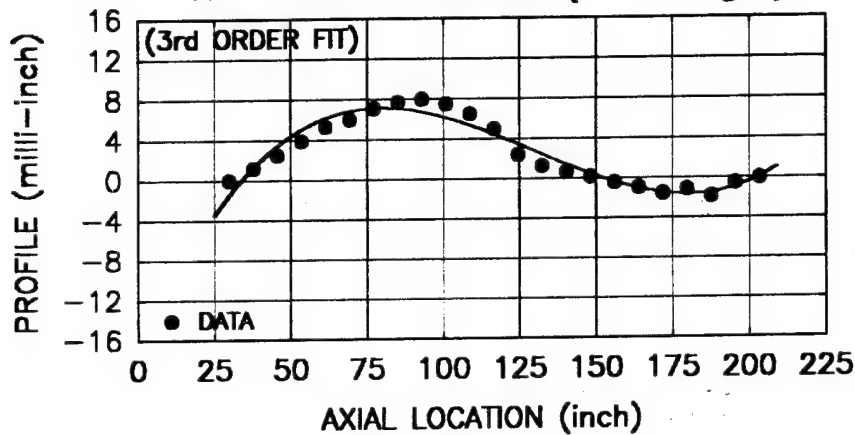


Figure 2b. Profile and curvature horizontal plane tube #4100.

120mm M256 ACCURACY STUDY
STATIC PROFILE and CURVATURE of DIT TUBES,
STATISTICALLY 'CORRECT' POLYNOMIAL FIT
for PROFILE and CURVATURE

TUBE# 4102

HORIZONTAL PROFILE (+ => right)



HORIZONTAL CURVATURE (+ => right)

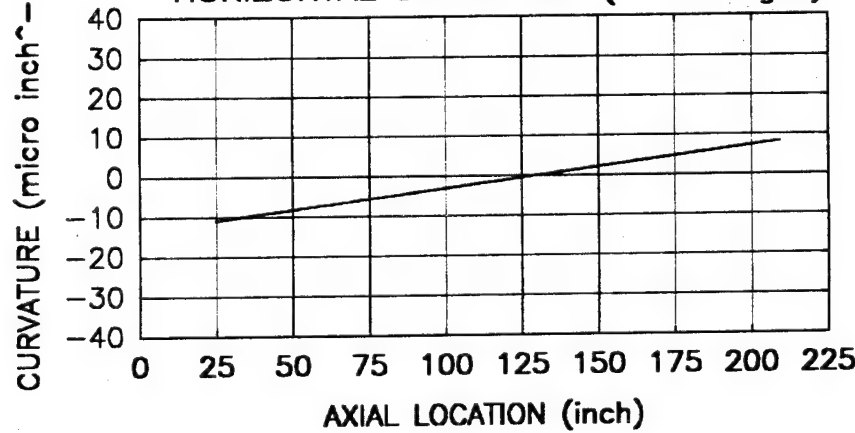
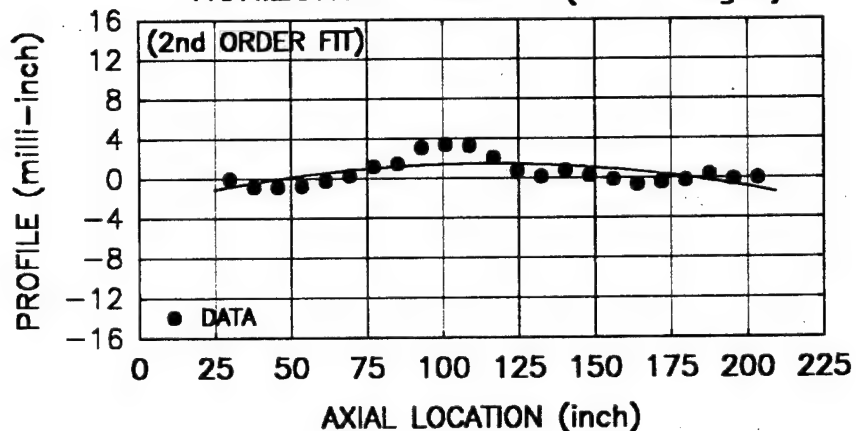


Figure 2c. Profile and curvature horizontal plane tube #4102.

120mm M256 ACCURACY STUDY
STATIC PROFILE and CURVATURE of DIT TUBES
STATISTICALLY 'CORRECT' POLYNOMIAL FIT
for PROFILE and CURVATURE

TUBE# 4104

HORIZONTAL PROFILE (+ => right)



HORIZONTAL CURVATURE (+ => right)

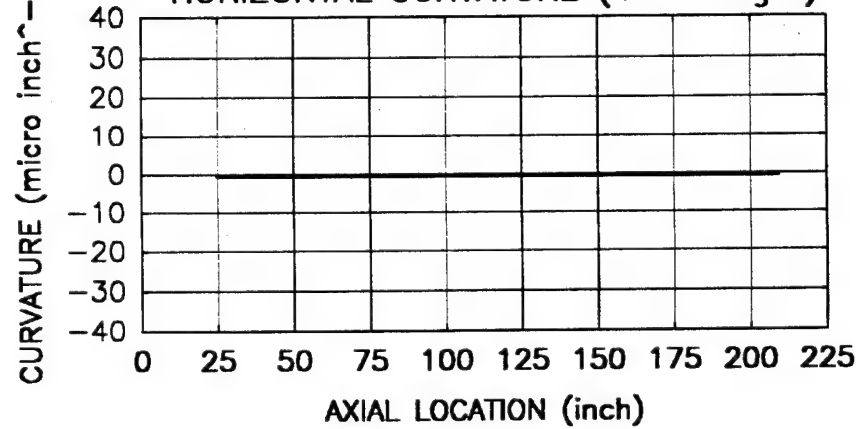
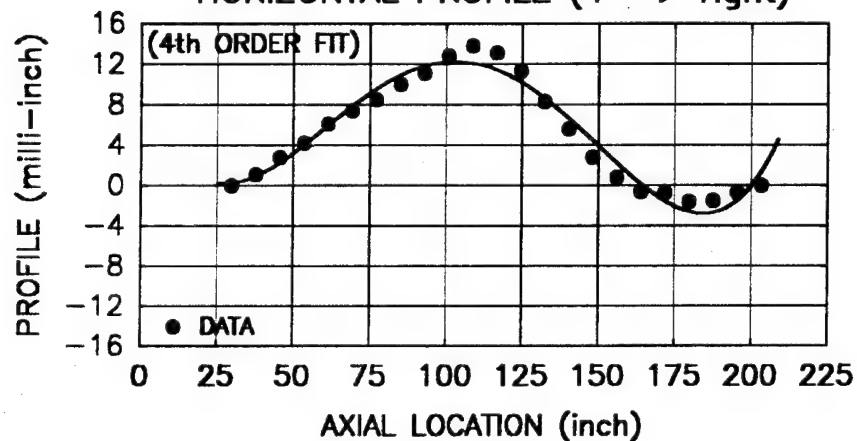


Figure 2d. Profile and curvature horizontal plane tube #4104.

120mm M256 ACCURACY STUDY
STATIC PROFILE and CURVATURE of DIT TUBES
STATISTICALLY 'CORRECT' POLYNOMIAL FIT
for PROFILE and CURVATURE

TUBE# 4106

HORIZONTAL PROFILE (+ => right)



HORIZONTAL CURVATURE (+ => right)

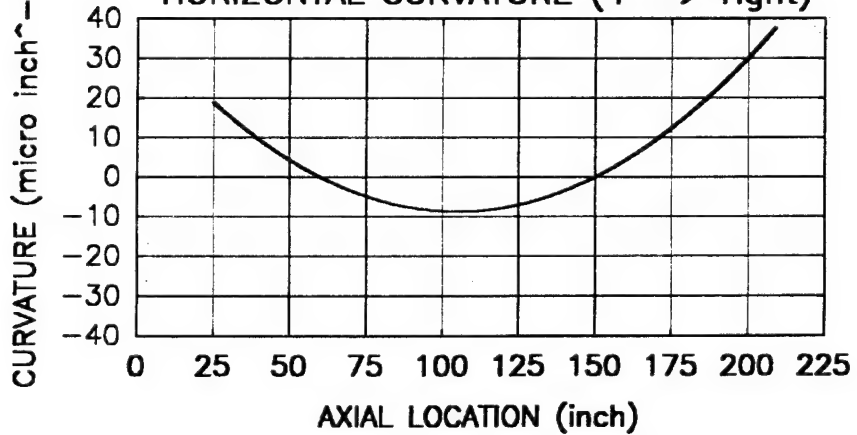
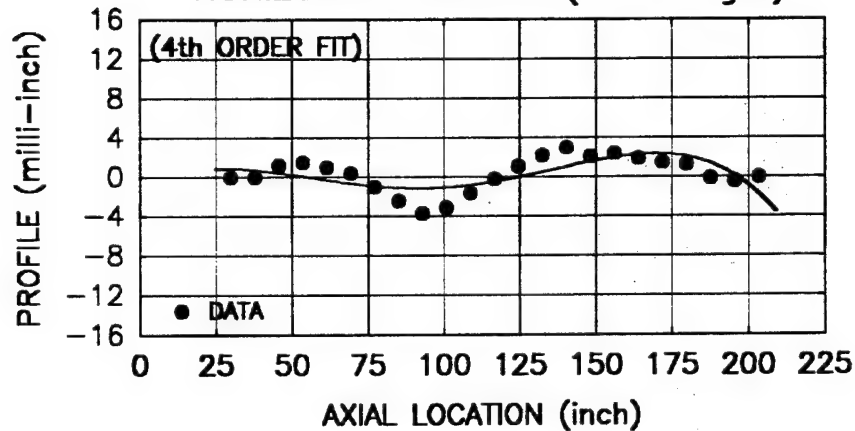


Figure 2e. Profile and curvature horizontal plane tube #4106.

120mm M256 ACCURACY STUDY
STATIC PROFILE and CURVATURE of STD TUBES
STATISTICALLY 'CORRECT' POLYNOMIAL FIT
for PROFILE and CURVATURE

TUBE# 4988

HORIZONTAL PROFILE (+ => right)



HORIZONTAL CURVATURE (+ => right)

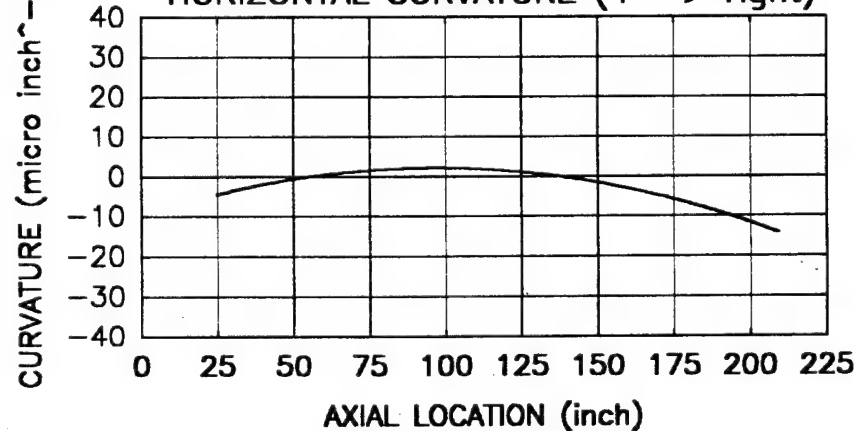
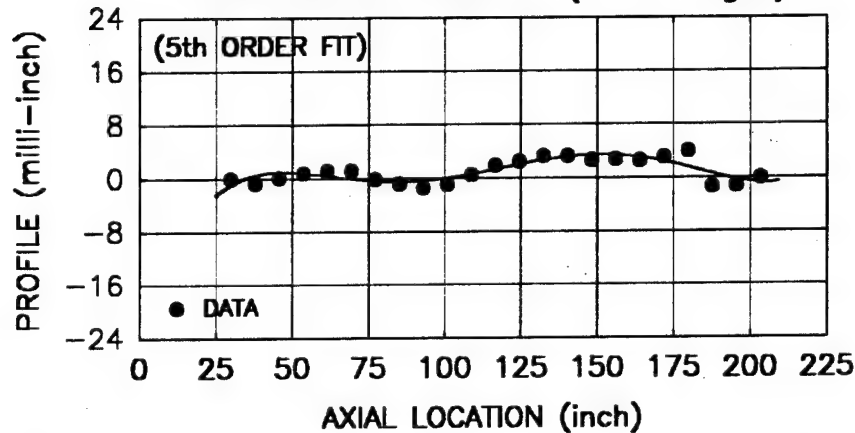


Figure 2f. Profile and curvature horizontal plane tube #4988.

120mm M256 ACCURACY STUDY
STATIC PROFILE and CURVATURE of STD TUBES
STATISTICALLY 'CORRECT' POLYNOMIAL FIT
for PROFILE and CURVATURE

TUBE# 4990

HORIZONTAL PROFILE (+ => right)



HORIZONTAL CURVATURE (+ => right)

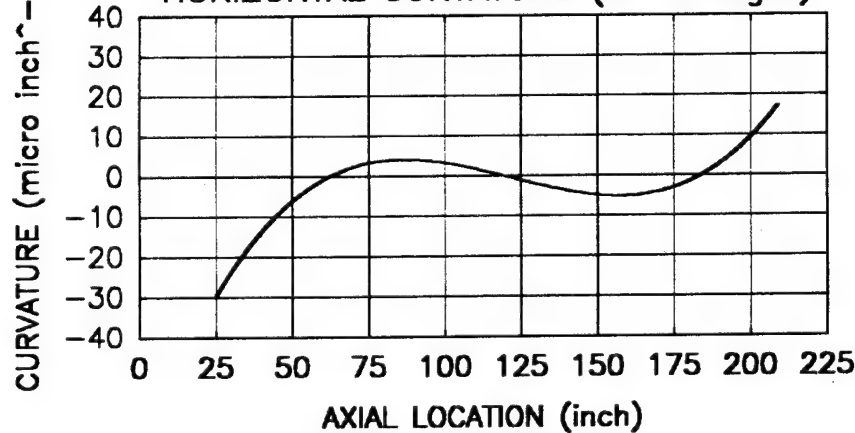
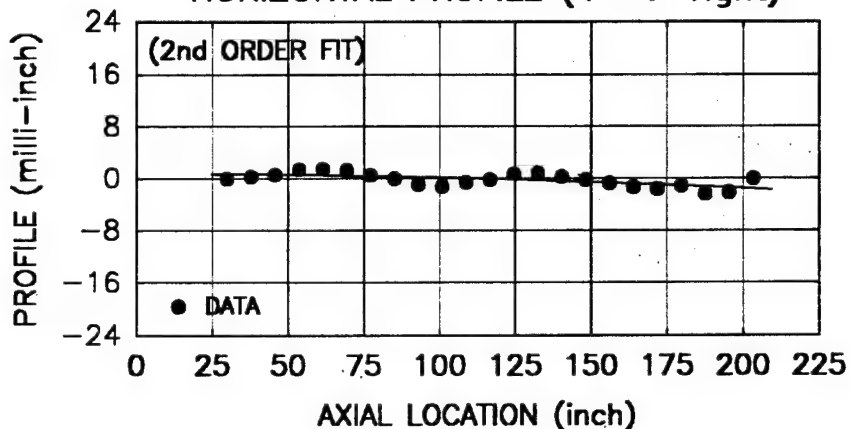


Figure 2g. Profile and curvature horizontal plane tube #4990.

120mm M256 ACCURACY STUDY
STATIC PROFILE and CURVATURE of STD TUBES
STATISTICALLY 'CORRECT' POLYNOMIAL FIT
for PROFILE and CURVATURE

TUBE# 4992

HORIZONTAL PROFILE (+ => right)



HORIZONTAL CURVATURE (+ => right)

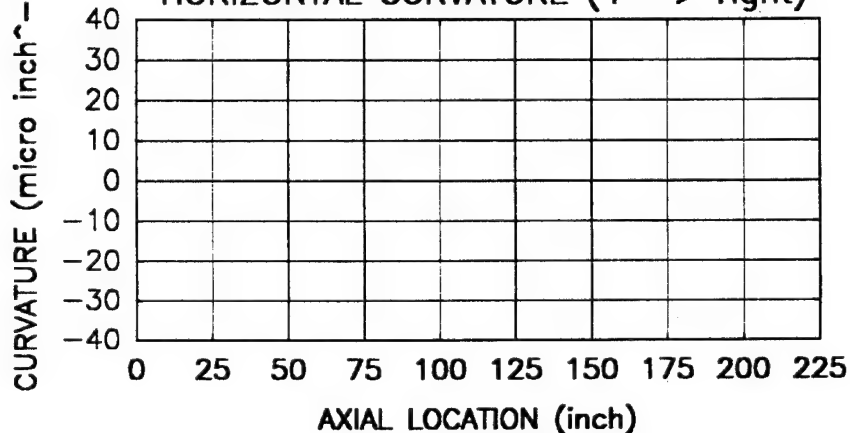
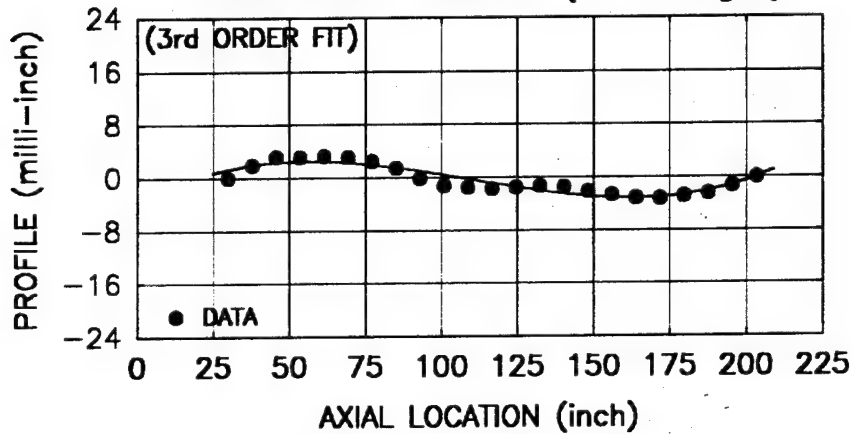


Figure 2h. Profile and curvature horizontal plane tube #4992.

120mm M256 ACCURACY STUDY
STATIC PROFILE and CURVATURE of STD TUBES
STATISTICALLY 'CORRECT' POLYNOMIAL FIT
for PROFILE and CURVATURE

TUBE# 4994

HORIZONTAL PROFILE (+ => right)



HORIZONTAL CURVATURE (+ => right)

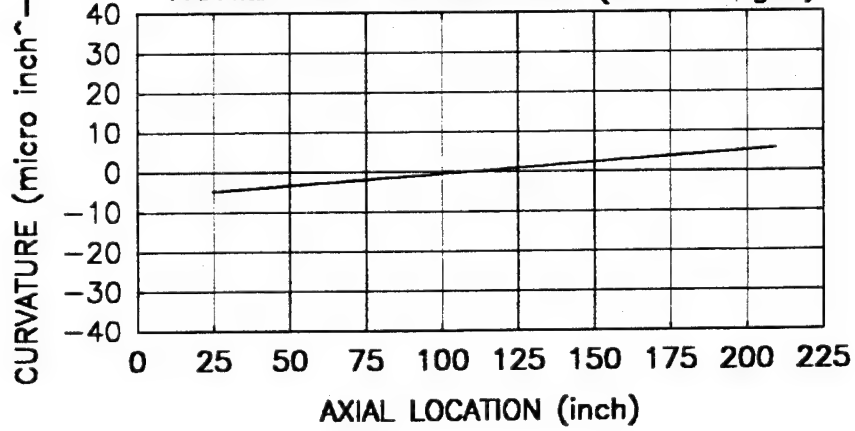


Figure 2i. Profile and curvature horizontal plane tube #4994.

120mm M256 ACCURACY STUDY
STATIC PROFILE and CURVATURE of STD TUBES
STATISTICALLY 'CORRECT' POLYNOMIAL FIT
for PROFILE and CURVATURE

TUBE# 4996

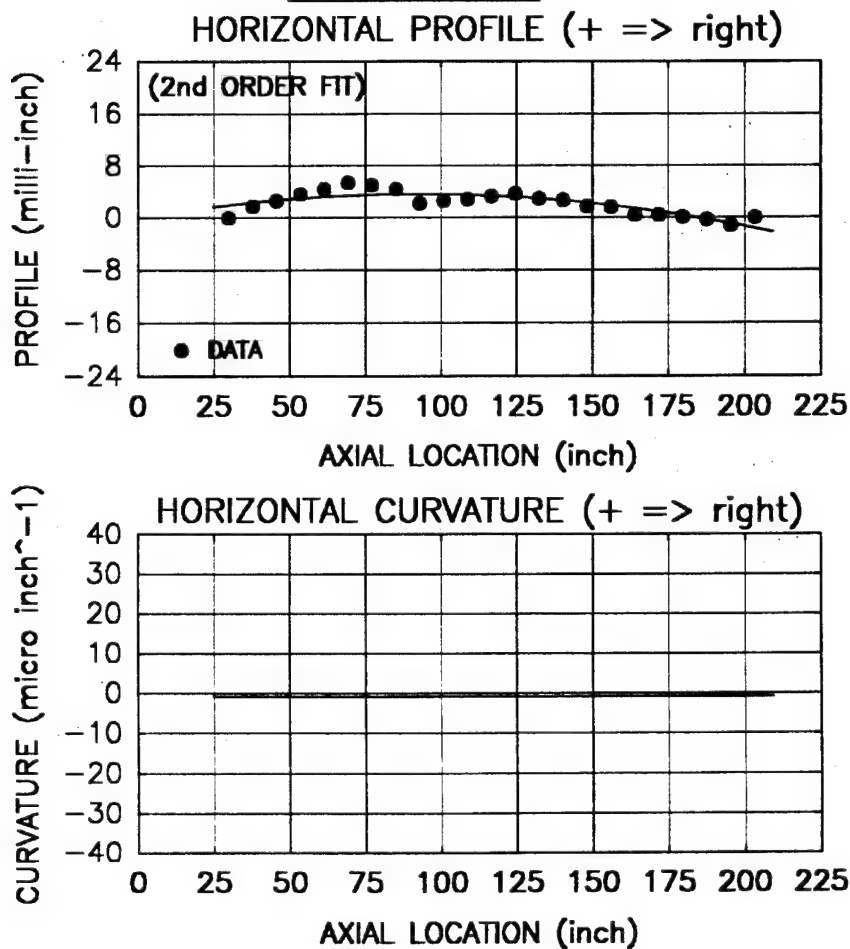


Figure 2j. Profile and curvature horizontal plane tube #4996.

microreciprocal inches at the muzzle. It is anticipated that very little projectile/tube interaction will occur for these tubes.

In Figure 3 the average COI values for the ten tubes are presented. On the chart the closed triangle symbol refers to a DIT tube and the open triangle refers to an STD tube. With the exception of one flier for the DIT group, the remaining four responses seem to reside at a definite location on the plot, whereas the five from the STD group reside at a different location. The basic idea of dynamic indexing is to reduce the tube-to-tube variation in impact location and dispersion. But as is concluded in the report (ref 13), neither dispersion has been significantly reduced, nor has the impact location remained constant. However, as the COI data indicates, the DIT tubes brought the impact points closer to the point of aim, which is at the crosshairs. Additionally, the DIT tubes were not manufactured to the 'optimum profile', but rather the tubes' natural profile was best aligned to the optimum. (There is also some controversy as to the processing sequence after the index plane was found.)

The idea of dynamic indexing versus standard indexing, profile samples, and partial results of a DIT test has been presented in this section. In the next and subsequent sections various gun dynamics models and results pertaining to estimating shot accuracy are discussed.

DYNAMIC MODELLING AND ACCURACY

For the last 15 to 20 years the use of dynamic modelling of a firing weapon has increased substantially (refs 1,4,7,8,15,16). Through the symbiotic relationship between analysis and experimentation, a number of dedicated computer codes written for the express use in gun dynamic studies have evolved. These models have proven track records in their gun motion predictive capabilities. To name a few, RASCAL, DYNA-3D, and SHOGUN are used at ARL, and SIMBAD and USM are used at Benét Laboratories. The underlying principle governing the use of these models is to predict the accuracy of projectile flight subsequent to exit from the gun. The models themselves only produce the dynamic state of the gun and projectile up to the point of exit. The models, therefore, predict the initial conditions for the projectile's free flight towards the target. A number of other factors such as sabot discard, projectile disengagement, and aerodynamic jump contribute heavily to the free flight trajectory of a round. In this study both SIMBAD and the USM are used in an attempt to establish relationships between a gun system's characteristics (i.e. tube, mount, projectile, and ballistics) and the impact at the target through the use of dynamic modelling.

Simulation of Barrel Dynamics (SIMBAD) Vibration Model

The SIMBAD model developed in Great Britain (ref 17) and recently purchased by Benét Laboratories is a quick running finite element code (fem) that employs two-dimensional beam elements for the gun tube and a variety of options for modelling the projectile, mount, and cradle. Regarding the tube, either the Euler-Bernoulli or Timoshenko formulation may be used. The projectile may have its own fem representation or simply a solid shot coupled to the tube through elastic driving bands. The mount and cradle may also have their own fem or simply a lumped spring and mass representation. A direct fixed time step integration method is employed to solve the system of differential equations.

120mm M256 ACCURACY STUDY
CENTERS of IMPACT DATA at 800 MILS
DYNAMIC INDEX TUBE TEST APG 1992

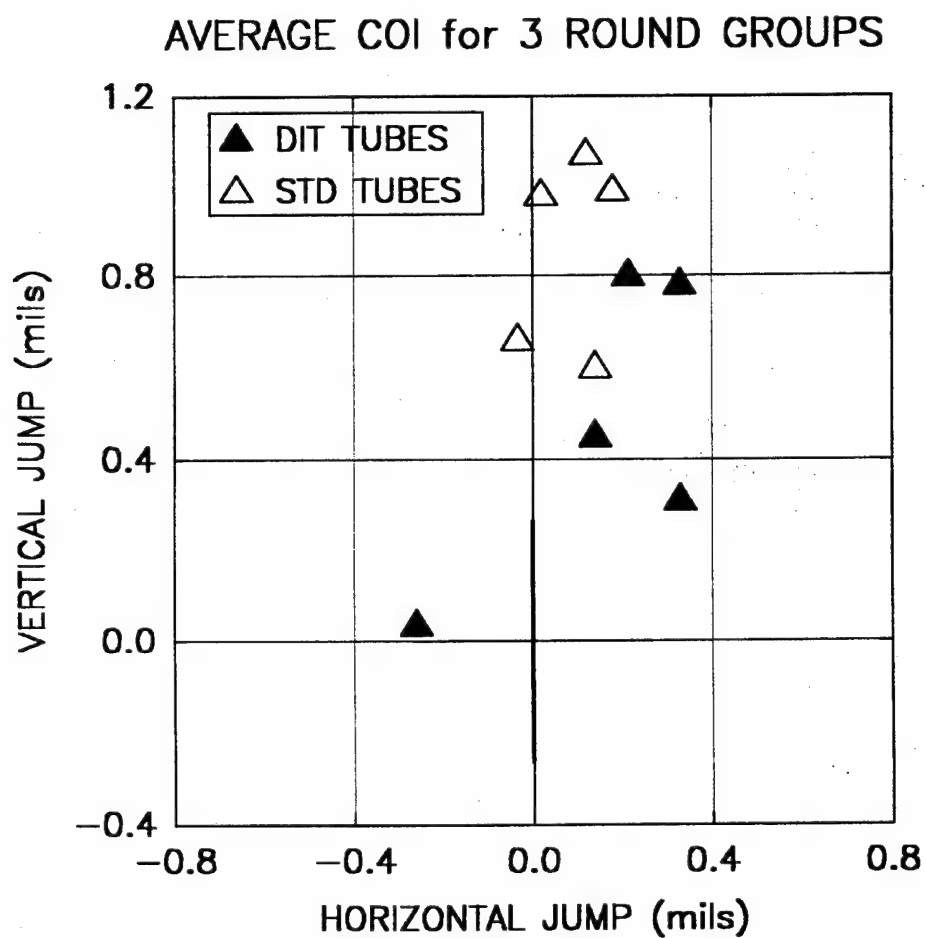


Figure 3. Centers of impact (COI) for DIT test.

The program runs interactively through user defined inputs. For the study conducted herein, the tube employs a 40-element Euler beam model, the mount is simulated using non-linear elastic supports to ground, and the projectile is a solid shot with elastic centering and rear bands. A cradle was not used. This is probably the minimum amount of information needed to provide reasonable run times and accurate results for tube and projectile dynamics. An 8.0 millisecond (msec) simulation runs in slightly less than one minute real time.

Uniform Segments Method (USM) Vibrations Model

The USM (ref 18) employs a modal analysis technique divided into three distinct modules. In the first, the gun-beam is axially segmented into a number of prismatic sections. The Euler-Bernoulli partial differential equation for a uniform beam employing free-free boundary conditions is applied locally to each segment, resulting in an ordinary differential equation (ODE) involving functions in the spatial domain. The equation that solves this ODE is a four-term function containing trigonometric and hyperbolic terms with unspecified coefficients. Across segment boundaries, continuity of displacement, slope, moment, and shear are invoked. The resulting system of equations are globally written in matrix form with the term coefficients as the unknown vector. When solved using appropriate numerical techniques, each requested frequency is determined and mode shape coefficients at this frequency are calculated. The number of mode shapes needed for a convergent solution is usually around eight (which includes two rigid body modes).

The second portion of the solution involves the application of the gun's initial conditions. In this step the bore profile and/or wall thickness variation (e.g. due to manufacturing anomalies) is defined. Any additional masses such as breech, bore evacuator, thermal shroud, and/or muzzle brake are added, the cannon support is defined, and (if the solution is in the vertical plane) gravity droop is included.

In the final step, the dynamic response is determined by the application of the appropriate load functions. Since the mode shapes are orthogonal, the transient solution leads to a system of coupled second order differential equations. Standard numerical techniques are used to solve this system, and the integrations are performed by a predictor-corrector technique employing adaptive time stepping, if required. The code is adapted to perform multiple runs in which both the initial conditions, the load, and many other model parameters may be changed between runs.

The model used in this study employs a five-segment eight-mode shapes depiction for the tube, and a breech and muzzle reference system mass both of which are offset with respect to the bore. The gun supports are non-linear springs with clearance. The shot model in the USM is a solid mass on hard supports, therefore, band stiffness is not modelled. Projectile eccentricity, however, may be applied. It is modelled as a travelling couple the magnitude of which is proportional to the round's acceleration and the amount of eccentricity assumed for the shot. For the USM, an 8.0-ms simulation runs in less than one-half minute, making it about twice as fast as SIMBAD.

PARAMETERS OF THE ACCURACY STUDY

The ultimate goal of this study is to determine whether or not the dynamic response of the gun system can be used for predicting accuracy. The means by which this relationship may be established is to model the test conditions of the individual shots and relate the dynamic response at exit to the impact location of the round. To accomplish this, the values of many system parameters are required as input to the models. With the exception of the relevant dimensions of the gun tubes used in the test, many of remaining parameters were neither measured nor recorded.

To deal with this problem, parametric methods are used, whereas the model is run using ranges of values (within reasonable tolerances) for those unknown input parameters to determine whether or not a sensitivity exists regarding its effect upon the exit conditions. If the parameter is non-sensitive, then it is set to its nominal value throughout the remaining portion of the study. If not, then a statistical approach is employed for selecting appropriate values and the responses are reported by their mean and standard deviation values.

Gun Mount Specifications

The most elusive modelling parameter in this gun system is the determination of the stiffness and clearances between the recoiling and vibrating cannon and its stationary mount. In both SIMBAD and USM the mount is characterized by non-linear spring elements applied at the gun's mounting locations. The function representing this relationship need be neither linear nor continuous.

A schematic of the major components involved in the mounting of the gun are shown in Figure 4. Points A and B are seal locations between which the recoil fluid resides. These are also considered the cannon's mounting points for vibrational analysis. The spring located in this chamber compresses between the piston head and rear surface of the cradle during recoil. It provides the necessary energy to return the cannon to its in-battery position. All components except the cradle are subject to recoil motion and the major level of transverse vibration. The adaptor, which has an internal profile closely matching the gun tube's outer profile, is held in place by the bearing that drives the adaptor inward thus engaging the tube's outer surface. The king nut, which is threaded to the outer surface of the tube, provides the clamping force to maintain the bearing/adaptor assembly to the tube. The thrust nut is the link that marries together all of the recoiling components. It has an internal thread that engages a mating thread on the outer diameter of the bearing. When tightened, the load pulls the cannon and piston forward through the bearing, king nut, tube, and breech threads. The cradle is assumed to be grounded along the face at the shoulder located just forward of the fluid and spring chamber. Examine feature C in the figure. This represents the forward end of the rotor and is considered to be ground with respect to the vibrating cannon.

By examining the relevant component drawings, the range of clearances between recoiling and stationary components has been determined. At point A (rear support), the clearance range is 0.005 to 0.010 inch. At the forward support (point B), the clearance range is 0.001 to 0.011 inch. When the cannon is within the clearance, its transverse motion is unopposed by any external loads except its own inertia. To determine the structural resistance during contact, a

120mm M256 CANNON and MOUNT

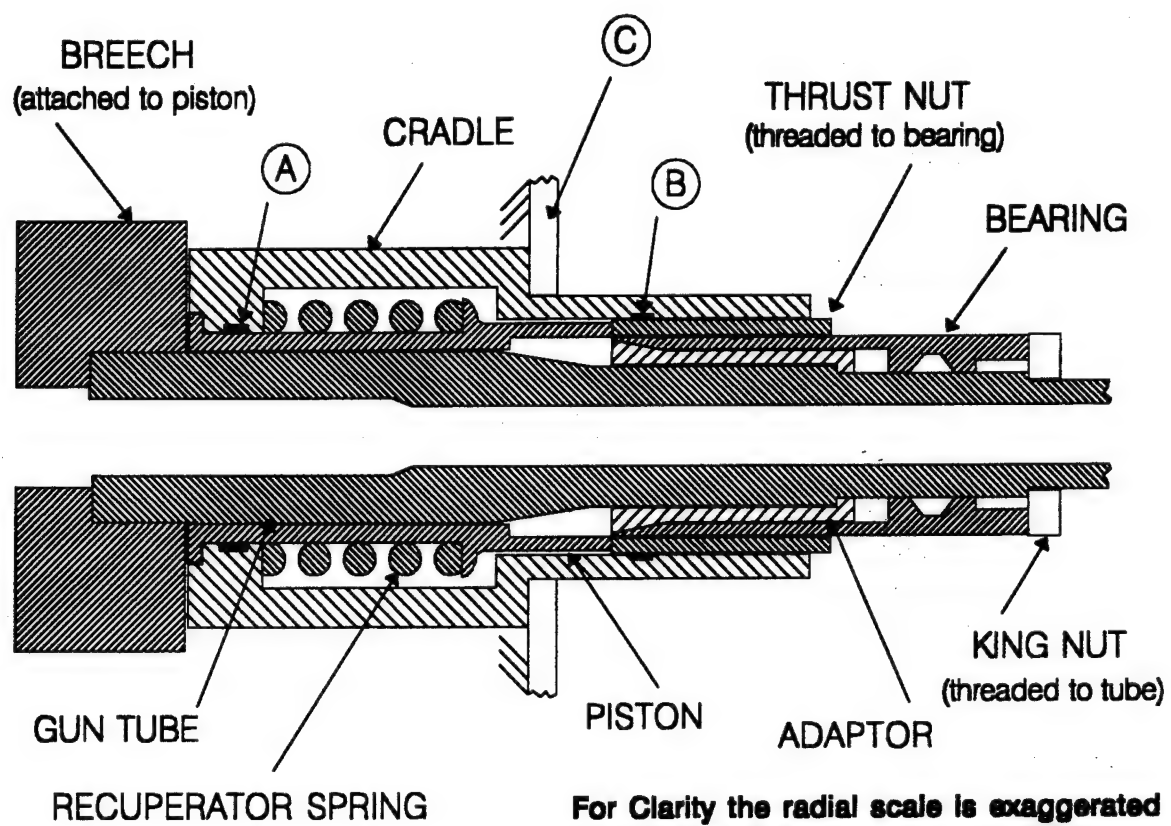


Figure 4. 120-mm M256 cannon and mount.

twofold approach was employed. Since the cradle is assumed to be 'grounded' along its midaxial location (see feature C in Figure 4), both the breech and the muzzle end resemble short cantilever beams. Stiffness values for this type of structure is well documented in textbooks on deformable materials. For the dimensions of the mount in question, cradle stiffness values based upon the described beam model are on the order of 40 million pounds per inch. By using linear stiffness values of this magnitude, the interface loads will most likely be grossly inaccurate. Therefore, a second type of response, namely Hertzian contact, was applied in series with the beam model. Hertzian contact is a microscopic model in which the local deformations and contact stresses between elastic components of various geometries are determined. Unlike the beam model whose stiffness is constant regardless of the level of deformation, the interface stiffness in the Hertz model begins at zero and rapidly rises in a non-linear fashion for increasing penetration between materials. The geometry of the interface components has a direct influence upon the load-deflection response for the Hertz model. By employing these two models in series, a slightly non-linear load-deflection response occurs that is more realistic than using either as a sole resistive load.

Projectile Stiffness Specifications

Projectile flexibility is included in the SIMBAD model only. Its most basic implementation is to consider a solid projectile body coupled to the tube through two elastic elements at the projectile's bore riding locations. For the DIT data being modelled, the round type contains a semi-rigid sabot constructed of aluminum and nylon. See Figure 5 for schematic details of the round. Lyon (ref 11) tested this round and provided experimental data for stiffness at both the front and rear bore riders. As indicated in his report, the stiffness for both is non-linear. The material resistance is small during initial sabot deflection, then gradually increases as deflection becomes greater. This, of course, is quite understandable since the interaction between the sabot and tube is like a Hertzian contact situation. Resistance is light during initial penetration and builds rapidly thereafter. A second characteristic of this round is that due to its construction (three symmetrical petals of 120-degree included angle), the assembly stiffness is a function of the location around the sabot's periphery. For example, if the projectile is oriented such that the load is applied to the circumferential center of a petal, its stiffness is different than if the load were applied at the joint between two petals. The stiffness range around the periphery varies from 5 to 45 percent of the maximum stiffness value. In Table 1, values for stiffness and their applicable deflection ranges are given.

120mm GENERIC KINETIC ENERGY ROUND

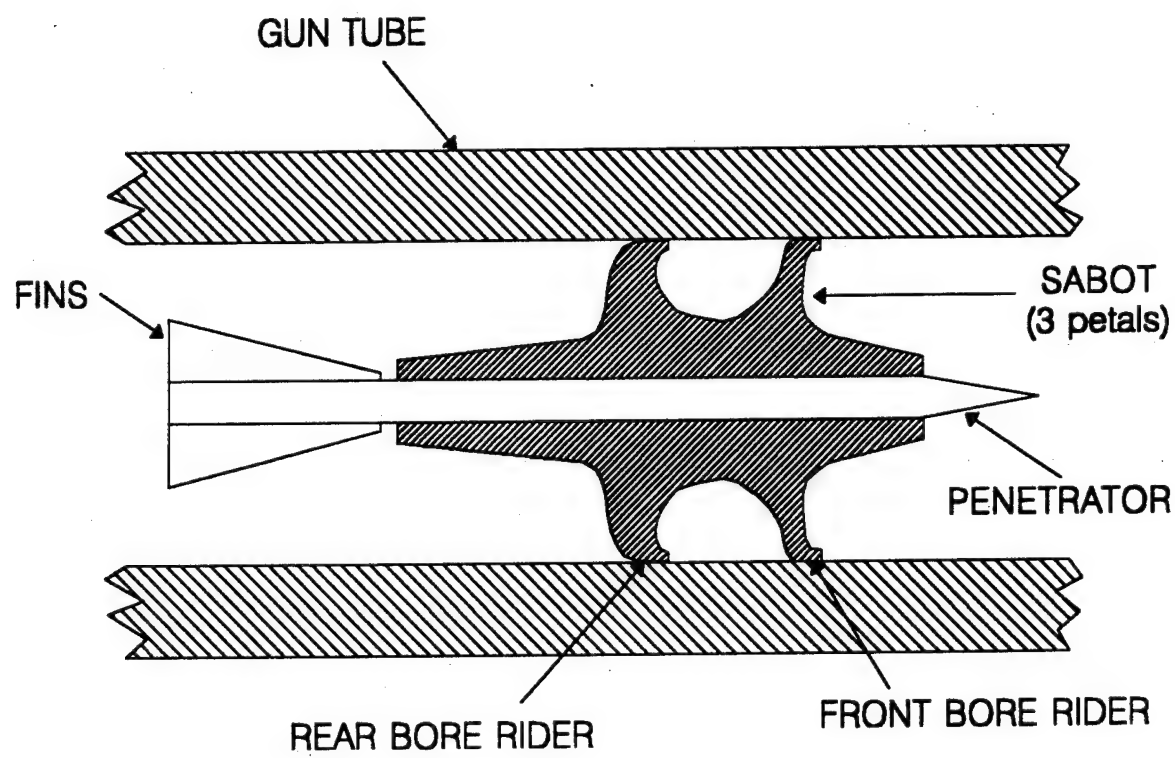


Figure 5. 120-mm generic kinetic energy round.

Table 1. Sabot Stiffness For Generic Kinetic Energy Round

Bore Rider Axial Location	Location on Petal	Deflection Range (milli-in.)	Stiffness Value (M-lbs/in.)	Deflection Range (milli-in.)	Stiffness Value (M-lbs/in.)
Front	Edge	0-6.0	0.267	6.0-16.0	0.447
	Center	0-7.0	0.204	7.0-15.0	0.425
Rear	Edge	0-2.0	0.952	2.0-4.0	2.80
	Center	0-4.0	0.513	4.0-6.0	2.32

To determine the sensitivity of the projectile response to stiffness, various values within the ranges listed in the above table will be used in the SIMBAD model.

Projectile Eccentricity Specifications

Projectile eccentricity values in the radial coordinate may be used in both SIMBAD and USM models. To determine a representative range for this parameter, engineering drawings of the subject round were studied. This method yielded very sketchy results. Eccentricity tolerance is not explicitly called out on either component or assembly drawings. Concentricity features of the projectile components were used to determine valid ranges for eccentricity values. This method yielded a maximum value of up to 0.05 inch of round eccentricity. The upper bound of 0.05 inch is used in the parametric study to follow.

Ballistic Uncertainties

Tolerances on ballistic performance are usually determined by examining variations in projectile velocities from shot-to-shot at a specific propellant-conditioning temperature. This information has not been retained for the subject test, therefore, a nominal tolerance of ± 5 percent is assumed for the parametric study. This value is slightly larger than normally found in previous tests, however, results for this level of uncertainty will be interesting to study.

SENSITIVITY TO VARIATION IN SYSTEM PARAMETERS

The conduction and results of parameter sensitivity analysis are presented and discussed in this section. The purpose of this study is twofold. First, we must identify the sensitivity of unknown test parameters so that appropriate allowances can be made during subsequent analyses. Second, since we are using two widely different approaches for simulation, the comparisons between results from both allows us to quickly spot anomalies in either or both models and to make an educated decision in selecting the model of choice for future studies.

Both models provide a myriad of point and transient graphical output. We focus on two point values, only: namely, (1) muzzle jump and (2) projectile jump at projectile exit. Jump values are estimates of the deviation in the exit direction of the projectile with respect to the initial aiming direction at the onset of firing. Since both muzzle and/or projectile jump at exit are related to the initial values for the projectile's in-flight condition, their values may be proportional to the impact location at the target.

Parameter Values

In the last section the focus was on possible ranges for unknown parameters. In the following paragraphs nominal and range values for these parameters are presented.

1. Tube profile. The nominal values for tube profile for the ten tubes in the test are calculated as previously described. Ranges of values are not used for this parameter.
2. Mount specifications. The nominal clearance value for the rear support is 0.005 inch. No range is used for this parameter. For the front support, the nominal value is again 0.005 inch, with a range of 0.001 to 0.011 inch in five increments. Stiffness values are calculated based upon clearance and the contact/beam approach previously cited. The nominal value for the modulus of elasticity is 30.0 Mpsi with no tolerance used.
3. Ballistic specifications. A nominal set of pressure, acceleration, velocity, and travel curves has been generated using a standard ballistics modelling code. To allow for a range of values, scale factors from 0.95 to 1.05 inch in four increments were used to simulate variances in ballistic response.
4. Projectile bore rider stiffness. For the muzzle jump calculations, an extremely stiff set of riding bands is used for the SIMBAD model. For the USM model, the projectile is considered solid. For the projectile jump calculations in the SIMBAD model, the nominal stiffness of the rear bore rider is 14.0 million pounds per inch (M-lb/inch) with a range of 6.0 to 22.0 M-lb/inch in eight increments. For the front bore rider, the nominal value is 4.5 M-lb/inch with a range of 2.3 to 6.9 M-lb/inch.
5. Projectile eccentricity. For both models, the nominal value for eccentricity is zero with a range of 0.05 inch in two increments at four orthogonal circumferential locations.

Response Presentation

The muzzle and projectile jump values for each parameter are plotted on two-dimensional target-type graphs in cartesian coordinates that include the actual shotfall data at 800 mils for the corresponding shots. There are two charts per gun tube: one for gun jump and one for projectile jump. For example, suppose we wish to represent the muzzle jump sensitivity to mount clearance for tube #4100. While setting all other parameters equal to their nominal values (i.e., ballistics, eccentricity, etc.), a series of runs using each model is conducted while the mount clearance parameter is incremented through its expected range of values. The muzzle jump (both vertical and horizontal) for each run is plotted on its target graph along with the actual data for the corresponding shot. By presenting the sensitivity results in this manner, a model/model and model/test comparison can be shown. As a result of this exercise, follow-up studies are anticipated.

Graphical presentations of these results are found in Figures 6a and 6b through Figures 15a and 15b. The figure number delineates the results by tube number. Results for the DIT tubes are shown in Figures 6 through 10 and for the STD tubes in Figures 11 through 15. Figure letter 'a' presents calculated muzzle jump values (both models) for a solid projectile, and figure letter 'b' presents projectile jump values (SIMBAD model) for a flexible band projectile. On chart 'a' three graphs are shown: namely, the muzzle jump responses for the mount, ballistic, and eccentricity parameters. On chart 'b' four graphs are shown: namely, the projectile jump values for the mount, ballistic, eccentricity, and projectile stiffness parameters.

Response Discussion

Group 1. DIT tubes; muzzle jump; solid shot; Figures 6a,7a,...,10a

In viewing the overall results for this group, the vertical response due to the mount parameter indicates the greatest variation. The vertical response range for the USM is about 0.80 mils, whereas for the SIMBAD model the range is slightly less. In the horizontal plane little sensitivity (0.10 mils maximum) is indicated in either model. The absolute location for the mount response is very close to the origin of the target for both models. Tube-to-tube sensitivities appear to be minimal. Regarding the ballistic parameter, the responses for both models are insignificant when compared to the responses due to the mount. The vertical range for the USM is 0.20 mils with very little sensitivity in the horizontal plane. For SIMBAD the vertical response is about half that of the USM, however, for tubes #4098 and #4106 some deviation exists in the horizontal plane. The nominal value for the center of each group is slightly below the horizontal axis and to the left or right of the vertical axis depending upon the tube. Muzzle jump response to the projectile eccentricity parameter is quite excessive in both planes for both models. Each eccentricity value was orthogonally located beginning at 45 degrees from the horizontal line through the diameter of the gun and ending at 315 degrees. The responses are symmetric for both models and for all tubes in the group. The range envelope for the USM response is 0.50 mils considering an eccentricity value of 0.05 inch, whereas the SIMBAD response is about half this value. The variation between models may be due to the estimated projectile stiffness used in SIMBAD. This stiffness that simulated a solid shot was chosen such that the time step needed for convergence was reasonable in regard to calculation time. The value chosen may have understated physical reality. For both models the range of

response values is the same regardless of the tube. It may be concluded that tube profile and projectile eccentricity are independent drivers of muzzle jump.

In regard to the model's predictive capabilities, the exception seems to be tube #4098. The shotfall patterns for the all other tubes are quite similar. All lie in the first quadrant of the target within the rectangular envelope of 0.2 to 0.3-mils horizontal and 0.4 to 0.8-mils vertical. Shotfall for tube #4098 straddles the second and third quadrants. If we exclude the shotfall results for this tube, the following may be speculated. Owing to the uncertainty in the dimensions of the mount components, it is quite conceivable to select a clearance value such that the predicted vertical muzzle jump of the modelling results approach the vertical jump component of the firing data. By selecting the mount clearance in the 0.007 to 0.009-inch range, the predicted vertical jump values for both USM and SIMBAD lie between 0.40 to 0.50 mils, which is close to the test results. In the horizontal direction the mount parameter has little effect, however, by varying the projectile eccentricity (probably a random variable), both the vertical and horizontal components of predicted muzzle jump are affected. The ballistic parameter has little effect on predicting shotfall patterns.

Group 2. DIT tubes; projectile jump; flexible shot; Figures 6b,7b,..,10b

The projectile jump response in the vertical direction is again most sensitive to mount clearance. For all tubes the vertical jump response range lies between 0.25 and 0.45 mils. The horizontal component is nearly zero. In comparing the muzzle jump values for a solid round to the projectile jump values for the flexible round as a function of mount clearance, the mean for the flexible round is 0.20 mils greater with a range about one-half that of the solid round. The response range due to the ballistic parameter is like its muzzle jump counterpart--small in the vertical direction and practically nil in the horizontal direction. Projectile jump shows no sensitivity to eccentricity. As indicated on the graphs, all eight cases for this parameter are nearly superimposed. On the other hand, projectile stiffness affects the jump response in both the vertical and horizontal directions. In addition there appears to be a tube dependency since the results for all tubes in this group have their own characteristic patterns. In Table 2 the extreme locations for the response due to projectile stiffness are reported by tube number.

Table 2. Projectile Jump Extremes, Flexible Round, DIT Tubes

Tube Number	Horizontal Bounds	Vertical Bounds
4098	-0.05 to 0.20	0.10 to 0.40
4100	-0.20 to 0.05	-0.05 to 0.35
4102	-0.10 to 0.10	0.00 to 0.35
4104	0.00 to 0.00	0.20 to 0.50
4106	-0.30 to 0.00	-0.05 to 0.35

120mm M256 ACCURACY STUDY

COI DATA vs GUN JUMP
for VARIOUS SYSTEM PARAMETERS
TUBE #4098 (DIT INDEX)

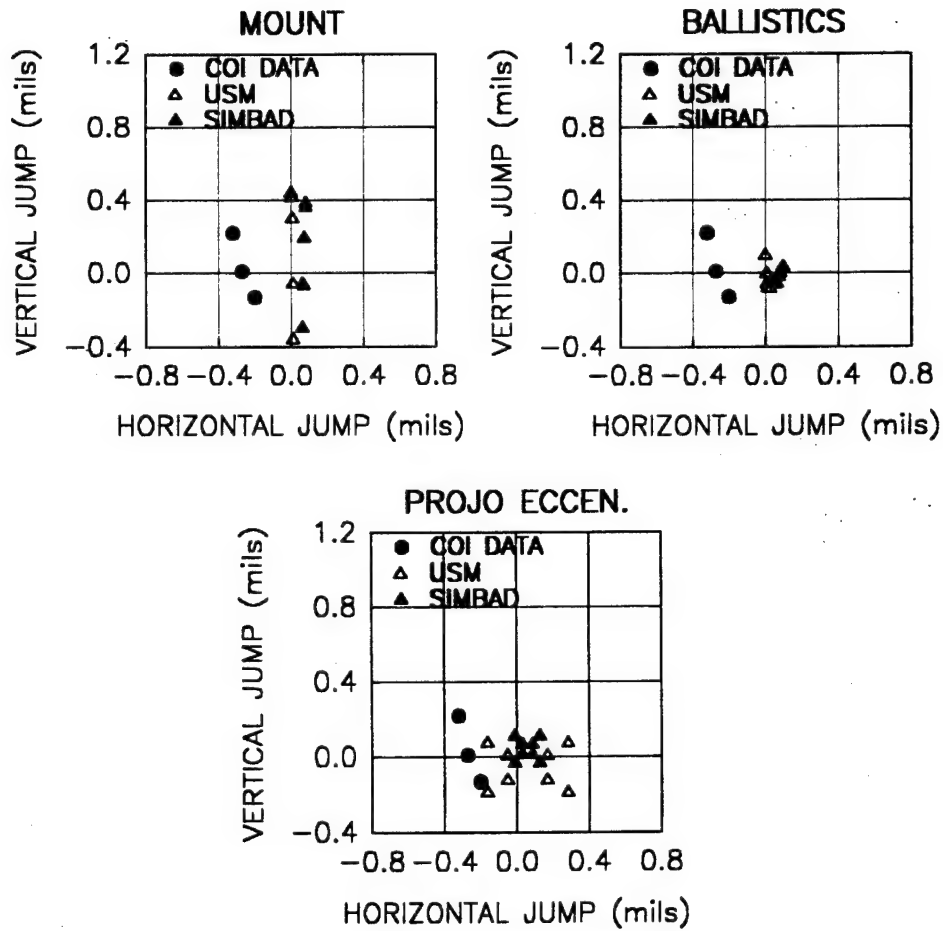


Figure 6a. COI data and calculated gun jump: tube #4098.

120mm M256 ACCURACY STUDY

COI DATA vs PROJECTILE JUMP
for VARIOUS SYSTEM PARAMETERS
TUBE #4098 (DIT INDEX)

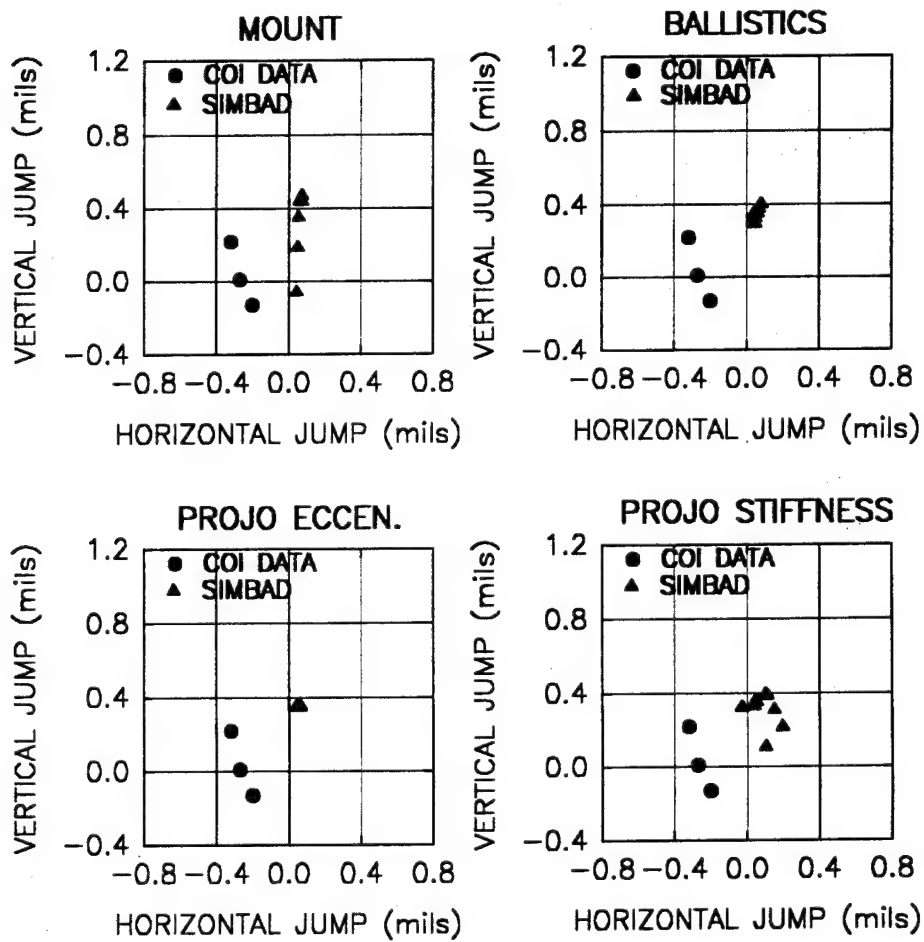


Figure 6b. COI data and calculated projectile jump: tube #4098.

120mm M256 ACCURACY STUDY

COI DATA vs GUN JUMP
for VARIOUS SYSTEM PARAMETERS
TUBE #4100 (DIT INDEX)

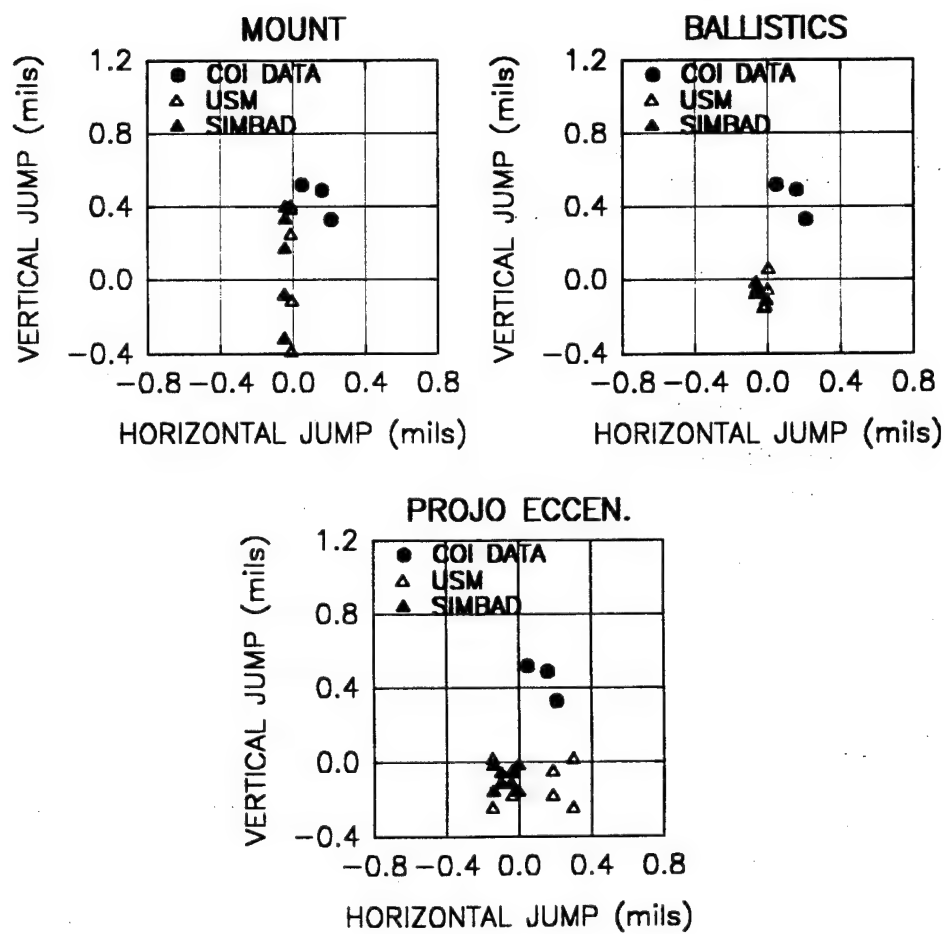


Figure 7a. COI data and calculated gun jump: tube #4100.

120mm M256 ACCURACY STUDY
COI DATA vs PROJECTILE JUMP
for VARIOUS SYSTEM PARAMETERS
TUBE #4100 (DIT INDEX)

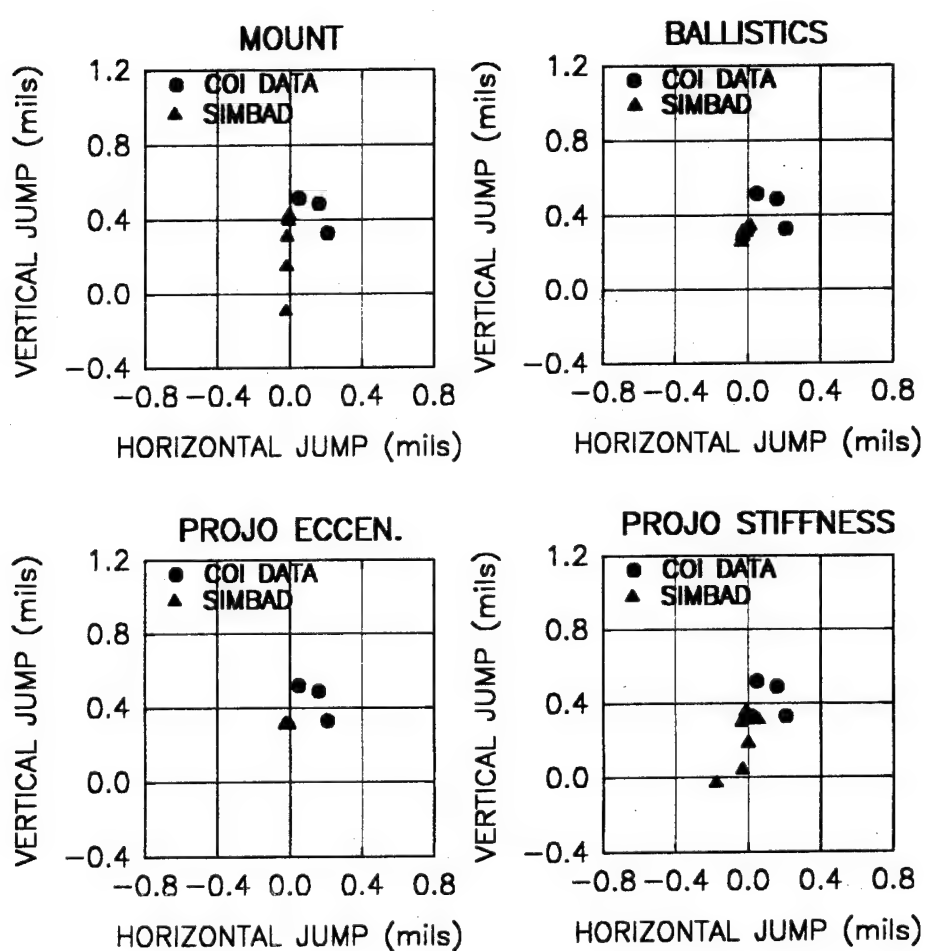


Figure 7b. COI data and calculated projectile jump: tube #4100.

120mm M256 ACCURACY STUDY

COI DATA vs GUN JUMP
for VARIOUS SYSTEM PARAMETERS
TUBE #4102 (DIT INDEX)

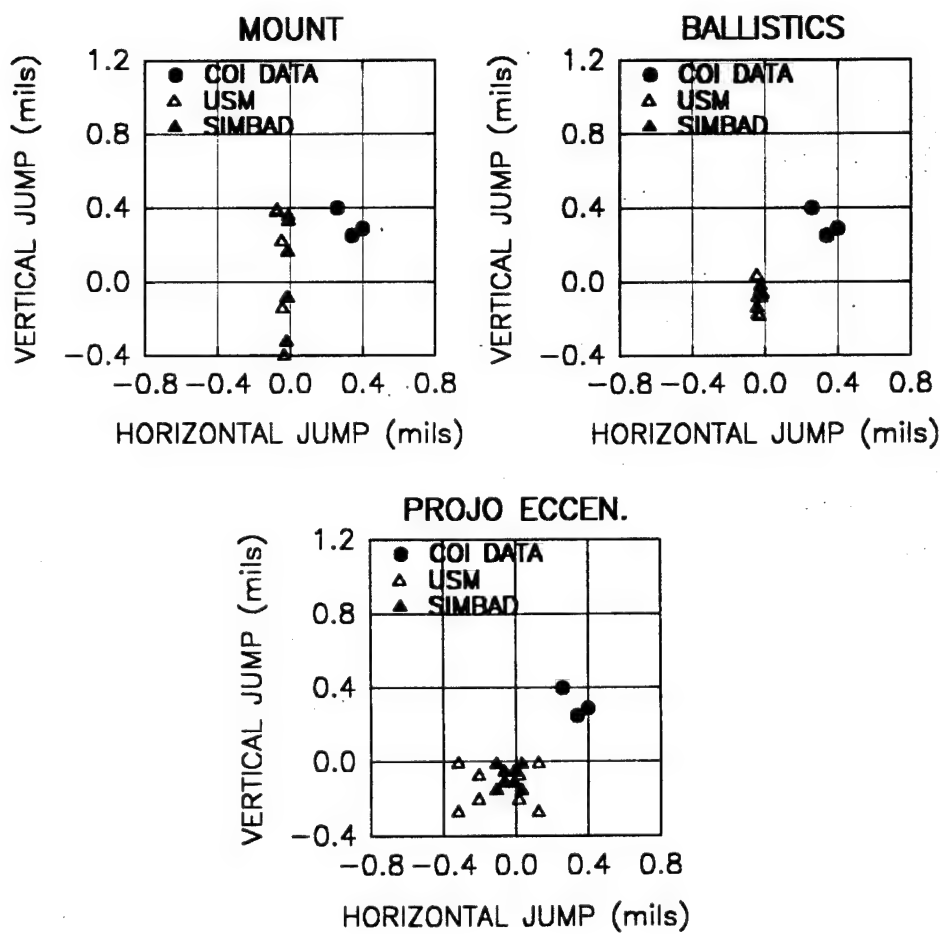


Figure 8a. COI data and calculated gun jump: tube #4102.

120mm M256 ACCURACY STUDY

COI DATA vs PROJECTILE JUMP
for VARIOUS SYSTEM PARAMETERS
TUBE #4102 (DIT INDEX)

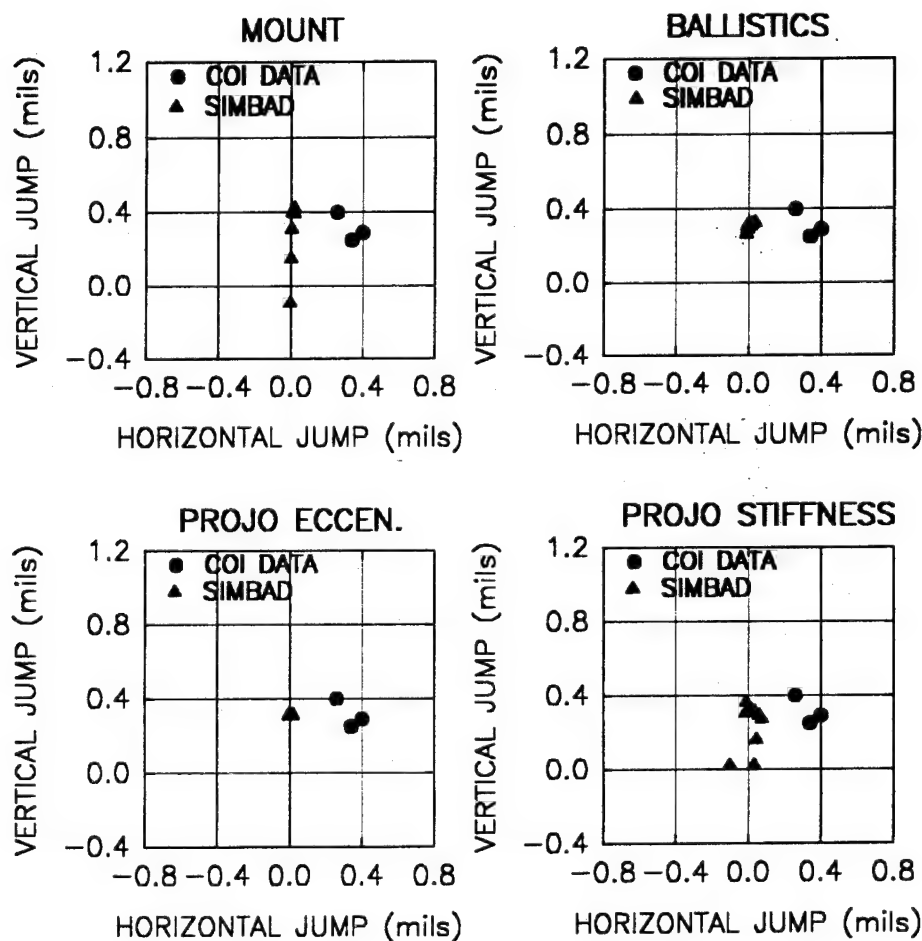


Figure 8b. COI data and calculated projectile jump: tube #4102.

120mm M256 ACCURACY STUDY

COI DATA vs GUN JUMP
for VARIOUS SYSTEM PARAMETERS
TUBE #4104 (DIT INDEX)

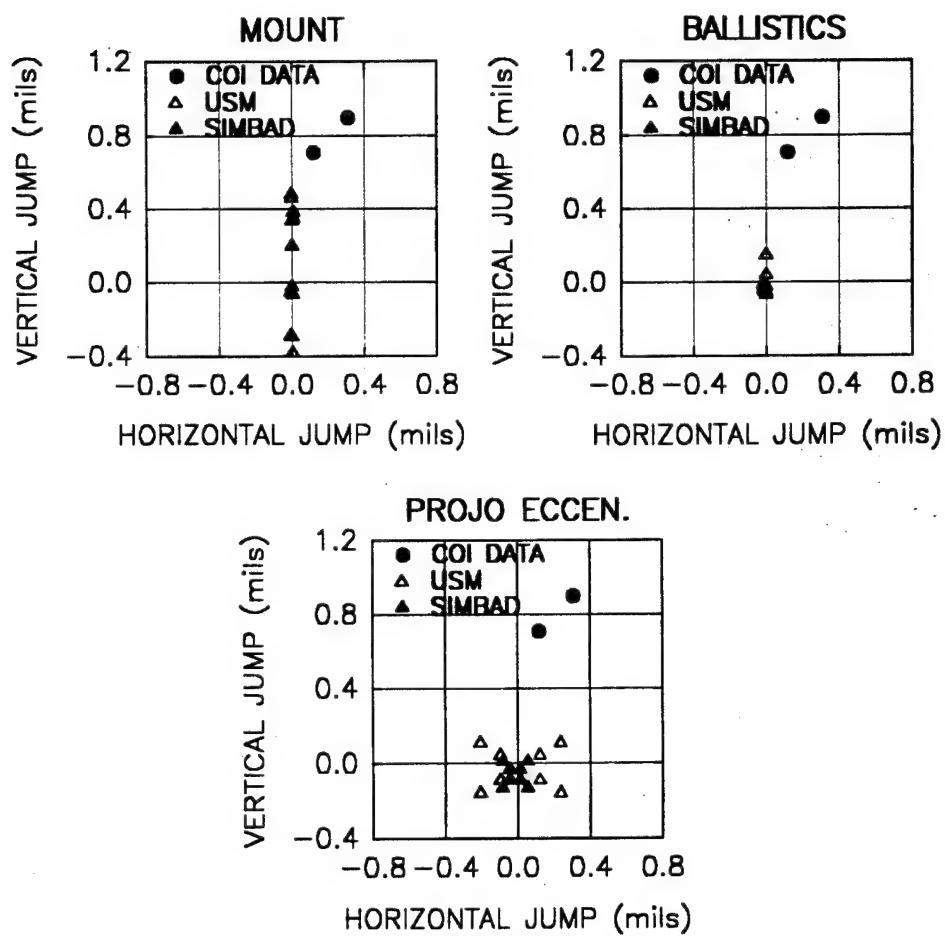


Figure 9a. COI data and calculated gun jump: tube #4104.

120mm M256 ACCURACY STUDY
COI DATA vs PROJECTILE JUMP
for VARIOUS SYSTEM PARAMETERS
TUBE #4104 (DIT INDEX)

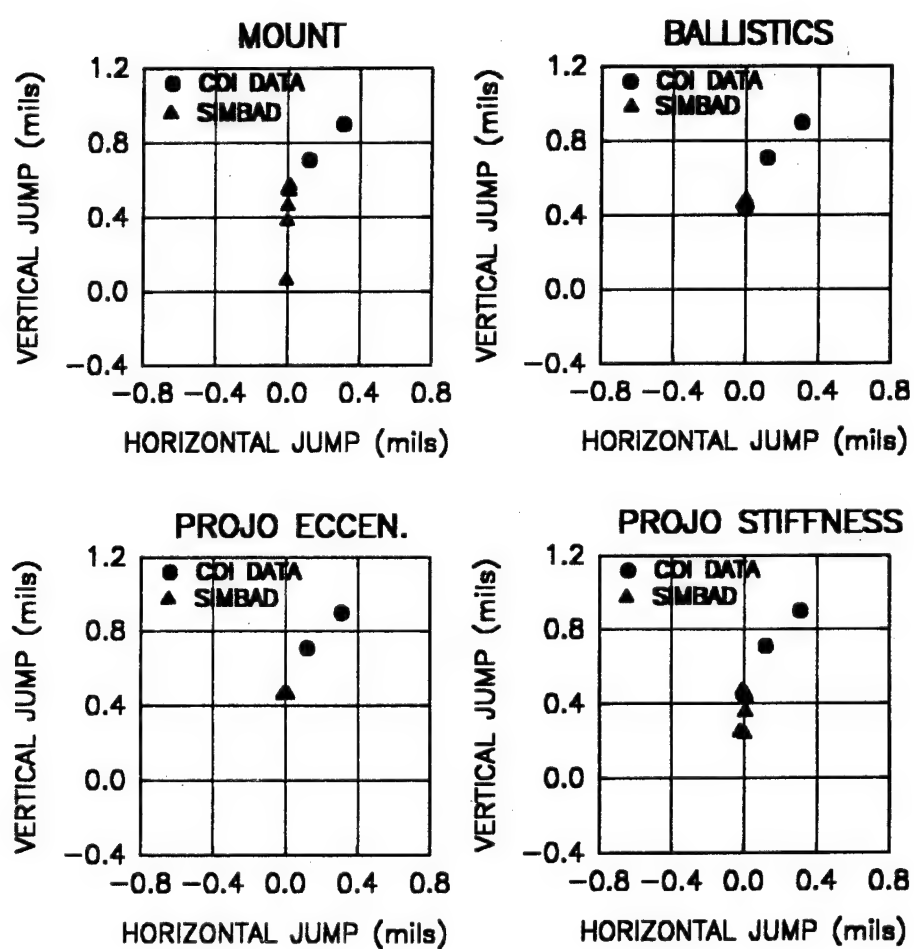


Figure 9b. COI data and calculated projectile jump: tube #4104.

120mm M256 ACCURACY STUDY

COI DATA vs GUN JUMP
for VARIOUS SYSTEM PARAMETERS
TUBE #4106 (DIT INDEX)

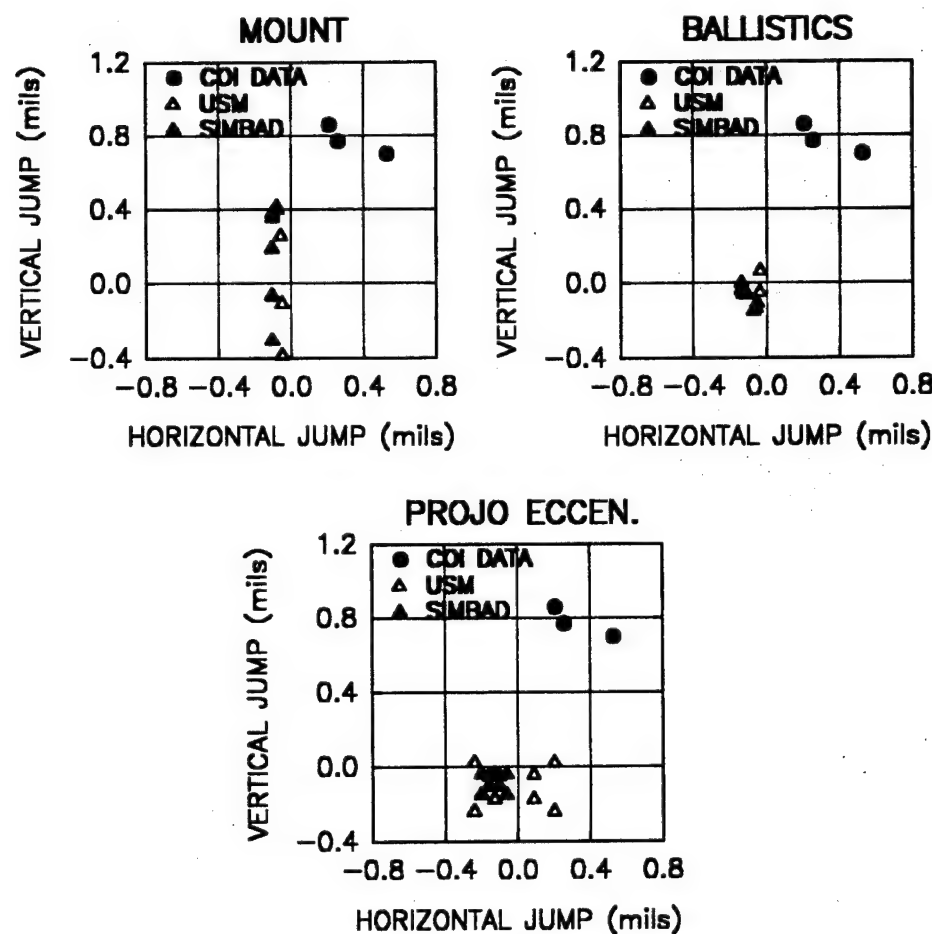


Figure 10a. COI data and calculated gun jump: tube #4106.

120mm M256 ACCURACY STUDY
COI DATA vs PROJECTILE JUMP
for VARIOUS SYSTEM PARAMETERS
TUBE #4106 (DIT INDEX)

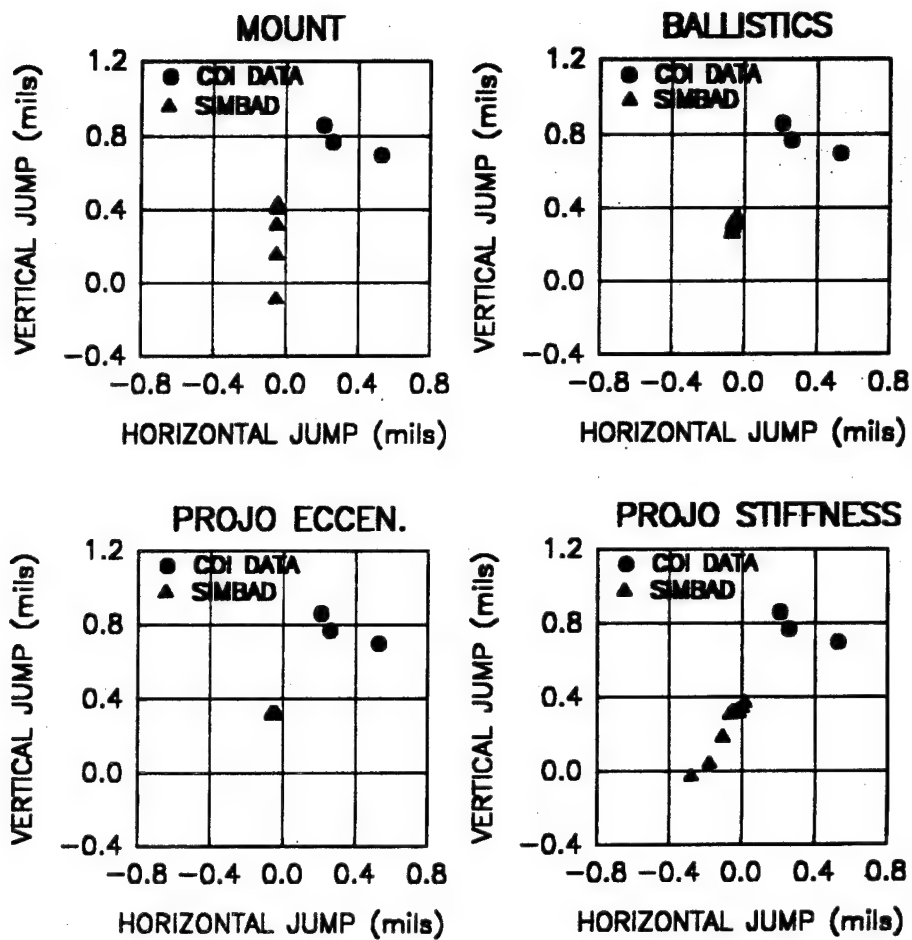


Figure 10b. COI data and calculated projectile jump: tube #4106.

In regard to using projectile jump to predict shotfall, many of the same conclusions for using muzzle jump as a predictor may be drawn. For example, if tube #4098 is excluded, the mount clearance that best allows the projectile jump calculations in the vertical direction to approach the firing data is 0.009 inch. In addition, for a specified mount clearance, the projectile jump values in the vertical direction are about 0.20 mils greater than their muzzle jump counterparts for the solid shot. Since the vertical component of the shot data is greater than either projectile or muzzle jump, this slight increase realized by using projectile jump means that the calculations are producing results that are closer to the actual data. Neither ballistic deviations nor projectile eccentricity drive the response towards the data, however, projectile stiffness holds some promise. The fact that this parameter, which in itself is a random variable, drives the response in both directions makes it quite attractive for use in a simulation study using statistical methods for parameter selection.

Group 3. STD tubes; muzzle jump; solid shot; Figures 11a,12a,...,15a

The groupings for the muzzle jump responses for the STD tubes show many of the same tendencies that the DIT tubes possess. Mount clearance is the most sensitive parameter, driving vertical jump values through a range of 0.90 mils for the USM and 0.70 mils for SIMBAD. The mean values are between 0.10 and 0.25 mils for both models. The horizontal response range is nearly 0 for the USM and 0.15 for SIMBAD. Muzzle jump due to ballistic deviation and projectile eccentricity behave similarly to that of the DIT tubes. The typical vertical jump range as a function of ballistic deviations is 0.20 mils for the USM and 0.12 mils for SIMBAD. Muzzle jump due to projectile eccentricity indicates considerable activity in both planes for both models. However, the response range is independent of the tube. As before, the USM response range is twice that of SIMBAD.

All shotfall patterns tend to reside in the first quadrant and just to the right of the vertical axis. Vertical shotfall is greater for this group than for the DIT tubes. Vertical range is between 0.6 and 1.0 mils, while the horizontal range is between 0 and 0.2 mils. Much like its DIT counterpart, using a mount clearance value of 0.009 inch allows the vertical jump calculations to approach the firing data.

Group 4. STD tubes; muzzle jump; flexible shot; Figures 11b,12b,...,15b

The projectile jump tendency for this group is very similar to that of the previous group. The range in vertical jump values is around 0.50 mils, whereas the horizontal jump is less than 0.10 mils. The vertical response range due to ballistic variations is within 0.20 mils and the horizontal range is less than 0.05 mils. Sensitivity to projectile eccentricity is non-existent. For tubes #4992, #4994, and #4996, the response to projectile stiffness lies mostly in the vertical plane, while the remaining two tubes show sensitivities in both planes. This response is again dependent upon the tube. In Table 3 the actual range boundaries for the jump response due to projectile stiffness is shown by tube number.

Table 3. Projectile Jump Extremes, Flexible Round, STD Tubes

Tube Number	Horizontal Bounds	Vertical Bounds
4988	-0.01 to 0.80	0.00 to 0.46
4990	-0.39 to -0.10	-0.16 to 0.42
4992	-0.01 to 0.01	0.11 to 0.47
4994	-0.03 to 0.02	-0.09 to 0.41
4996	0.0 to 0.01	0.03 to 0.48

In regard to predicting shotfall, the comments made for the DIT tubes apply equally as well for the tubes in this group.

The results presented in this section indicate that many of the unknown or unmeasured system parameters influence shot dynamics. Under these circumstances, it is quite difficult to predict shotfall locations. In the next section an attempt to resolve this shortcoming through the use of probabilistic design theory is presented. Basically, statistical distributions of the unknown parameters are chosen as model inputs. The resulting response values are reported as statistical distributions as well.

120mm M256 ACCURACY STUDY

COI DATA vs GUN JUMP
for VARIOUS SYSTEM PARAMETERS
TUBE #4988 (STD INDEX)

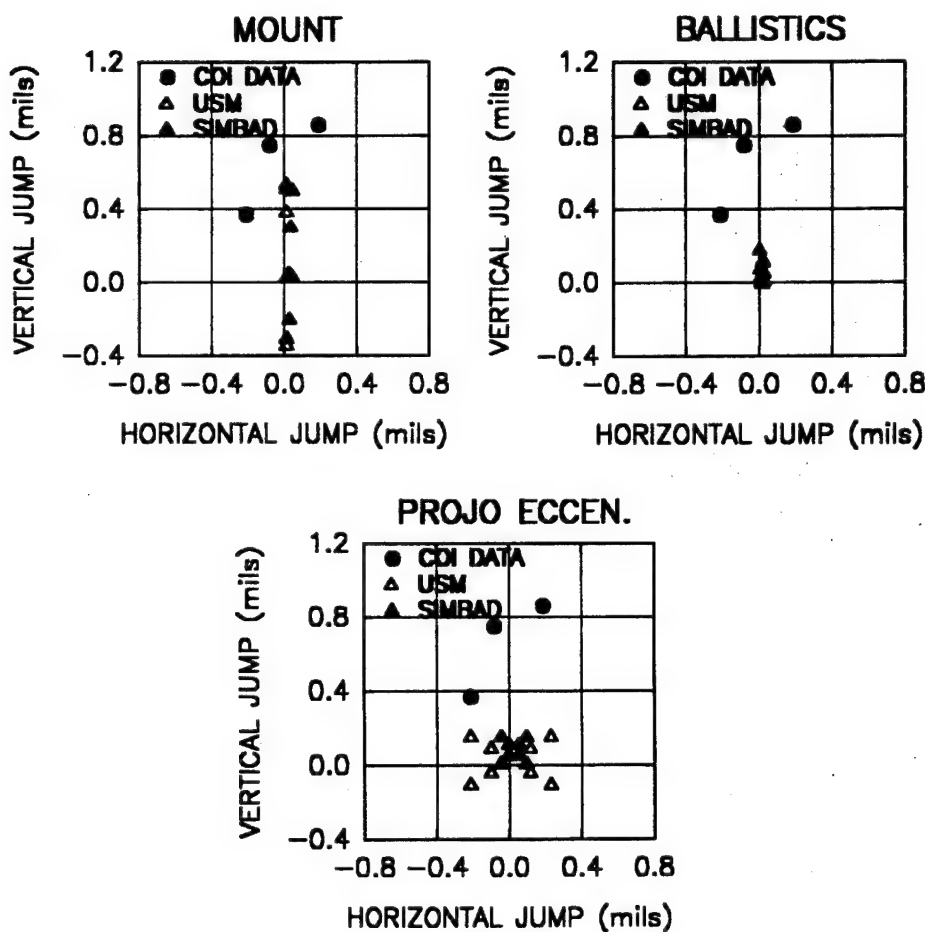


Figure 11a. COI data and calculated gun jump: tube #4988.

120mm M256 ACCURACY STUDY
COI DATA vs PROJECTILE JUMP
for VARIOUS SYSTEM PARAMETERS
TUBE #4988 (STD INDEX)

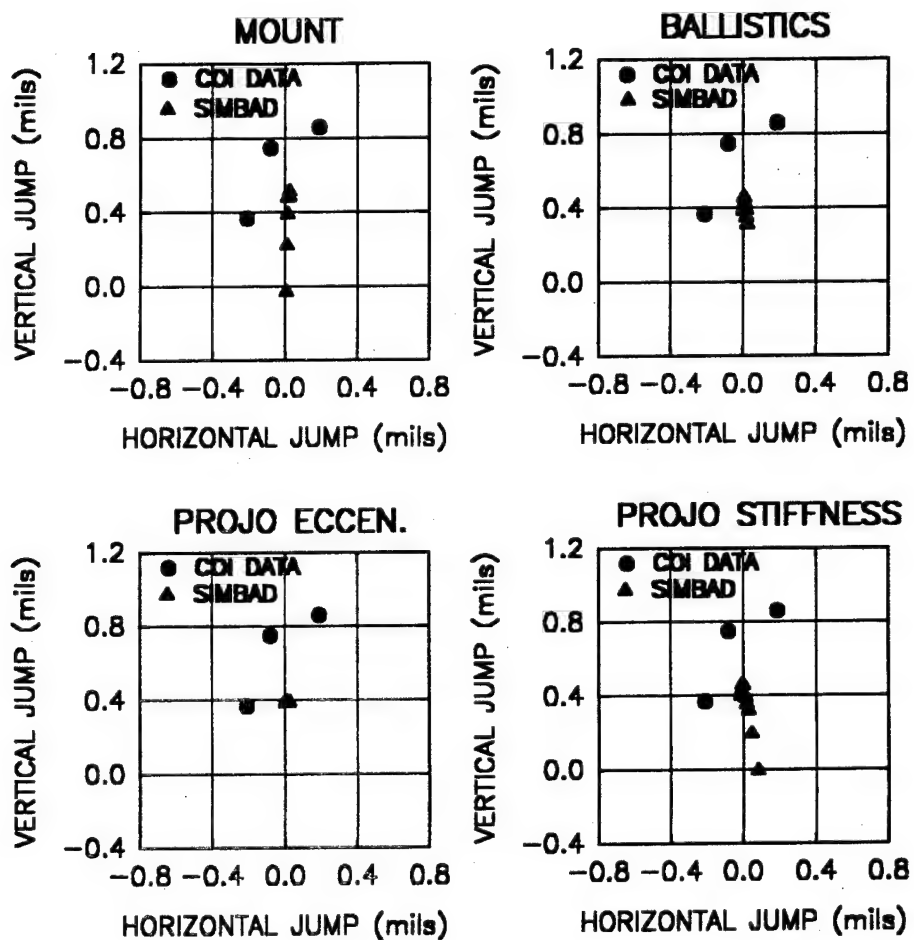


Figure 11b. COI data and calculated projectile jump: tube #4988.

120mm M256 ACCURACY STUDY

COI DATA vs GUN JUMP
for VARIOUS SYSTEM PARAMETERS
TUBE #4990 (STD INDEX)

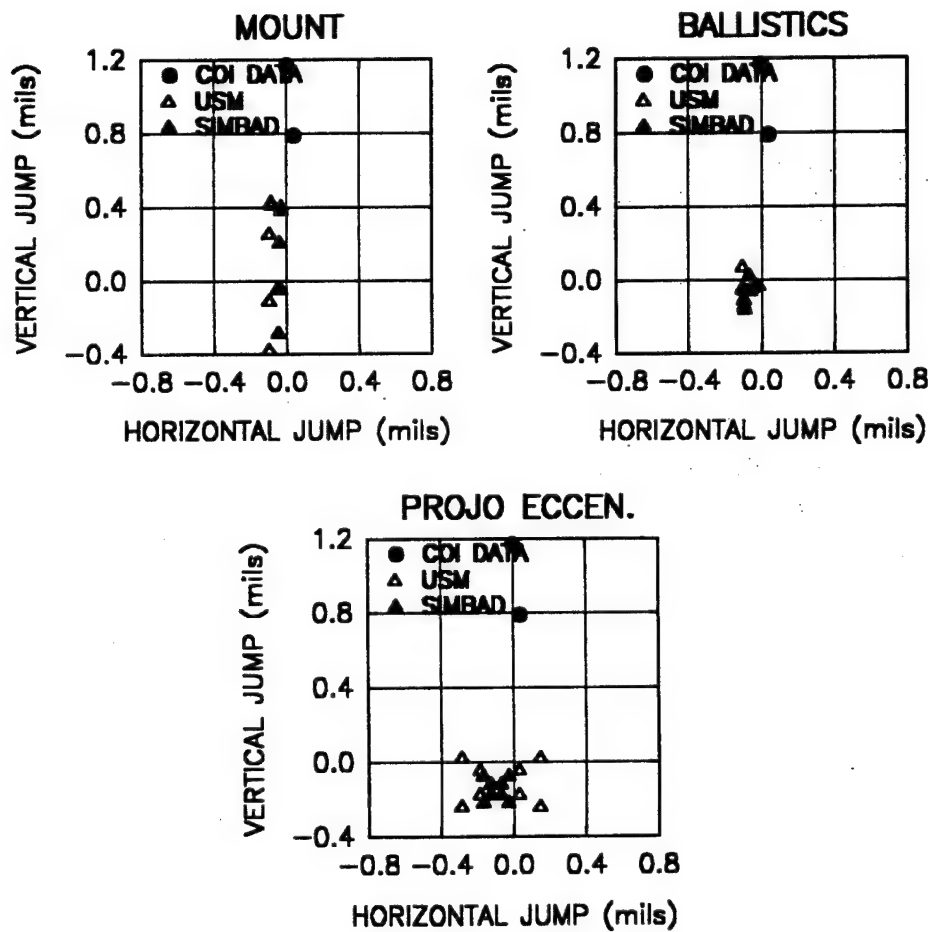


Figure 12a. COI data and calculated gun jump: tube #4990.

120mm M256 ACCURACY STUDY
COI DATA vs PROJECTILE JUMP
for VARIOUS SYSTEM PARAMETERS
TUBE #4990 (STD INDEX)

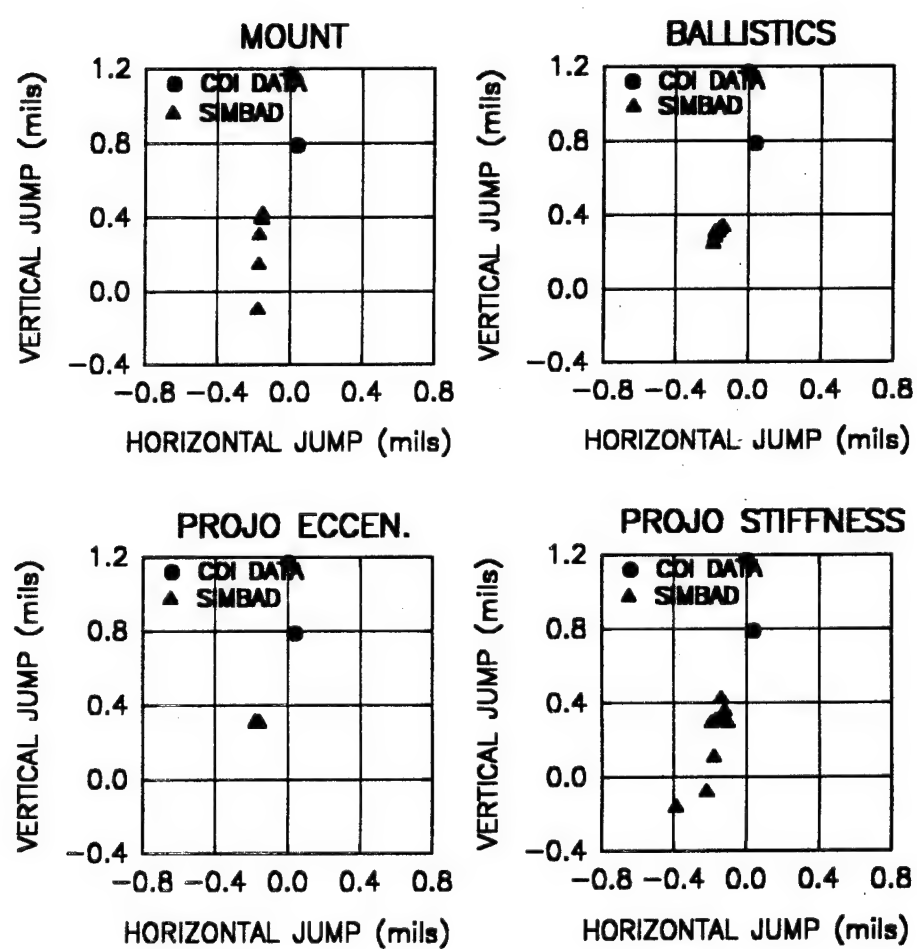


Figure 12b. COI data and calculated projectile jump: tube #4990.

120mm M256 ACCURACY STUDY

**COI DATA vs GUN JUMP
for VARIOUS SYSTEM PARAMETERS
TUBE #4992 (STD INDEX)**

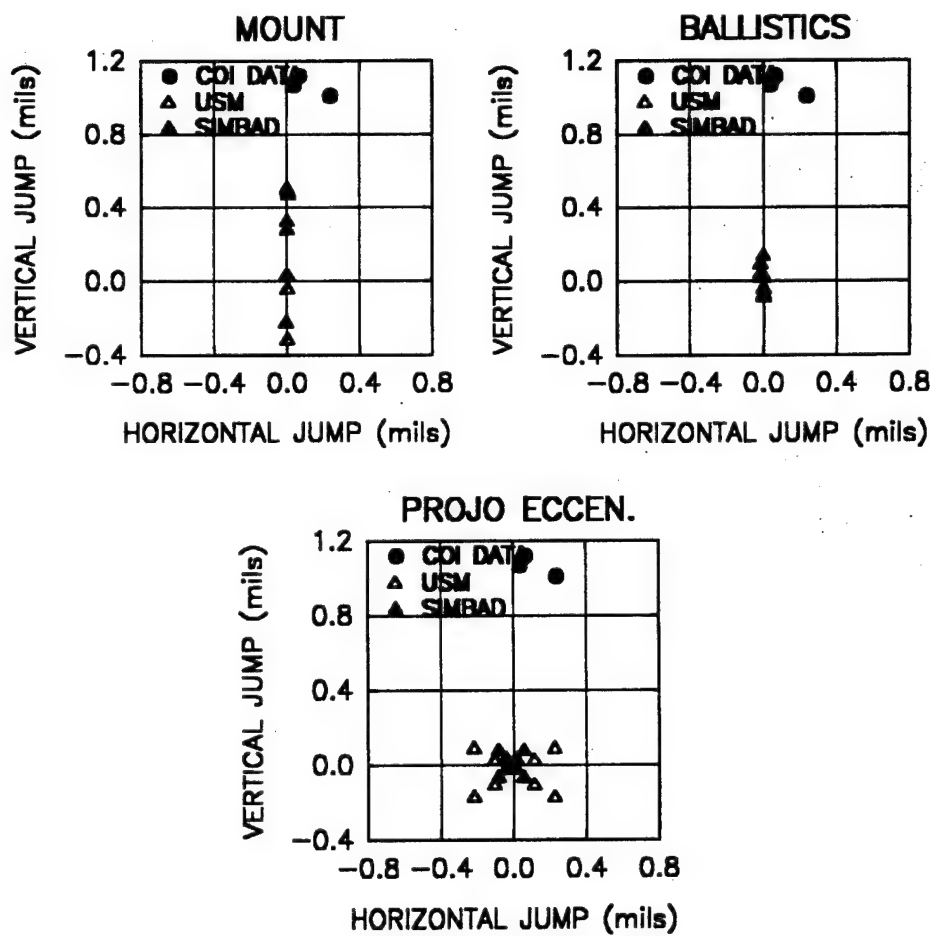


Figure 13a. COI data and calculated gun jump: tube #4992.

120mm M256 ACCURACY STUDY

COI DATA vs PROJECTILE JUMP
for VARIOUS SYSTEM PARAMETERS
TUBE #4992 (STD INDEX)

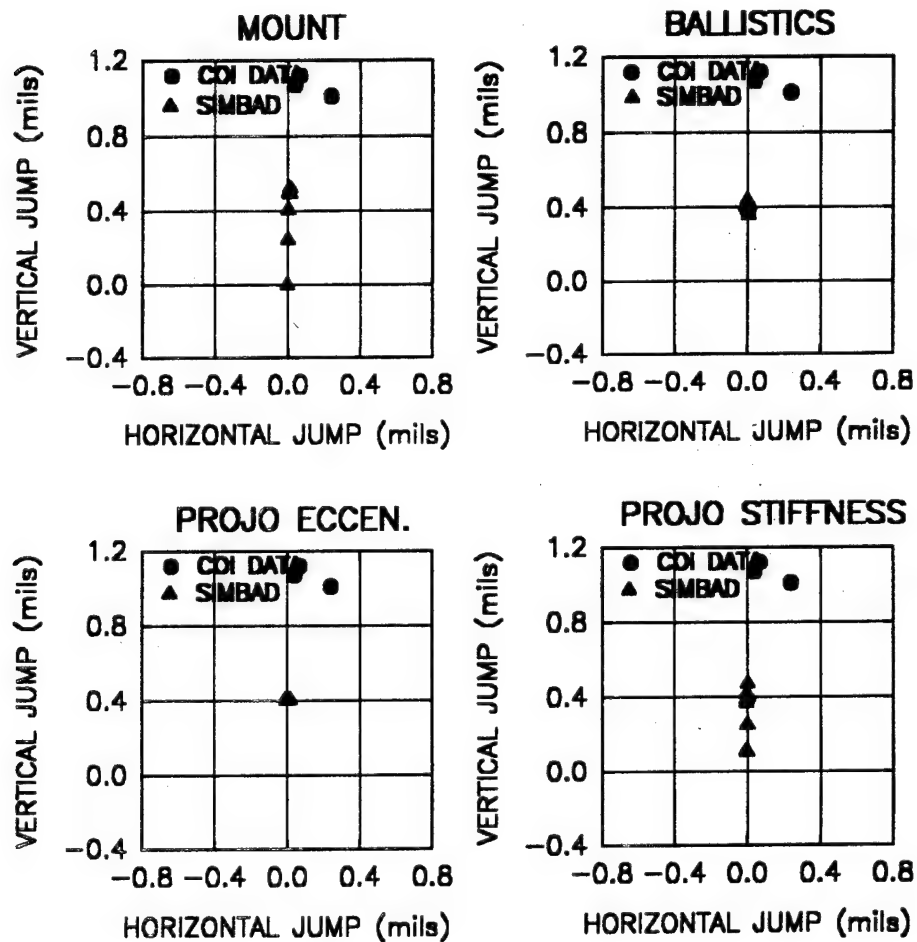


Figure 13b. COI data and calculated projectile jump: tube #4992.

120mm M256 ACCURACY STUDY

COI DATA vs GUN JUMP
for VARIOUS SYSTEM PARAMETERS
TUBE #4994 (STD INDEX)

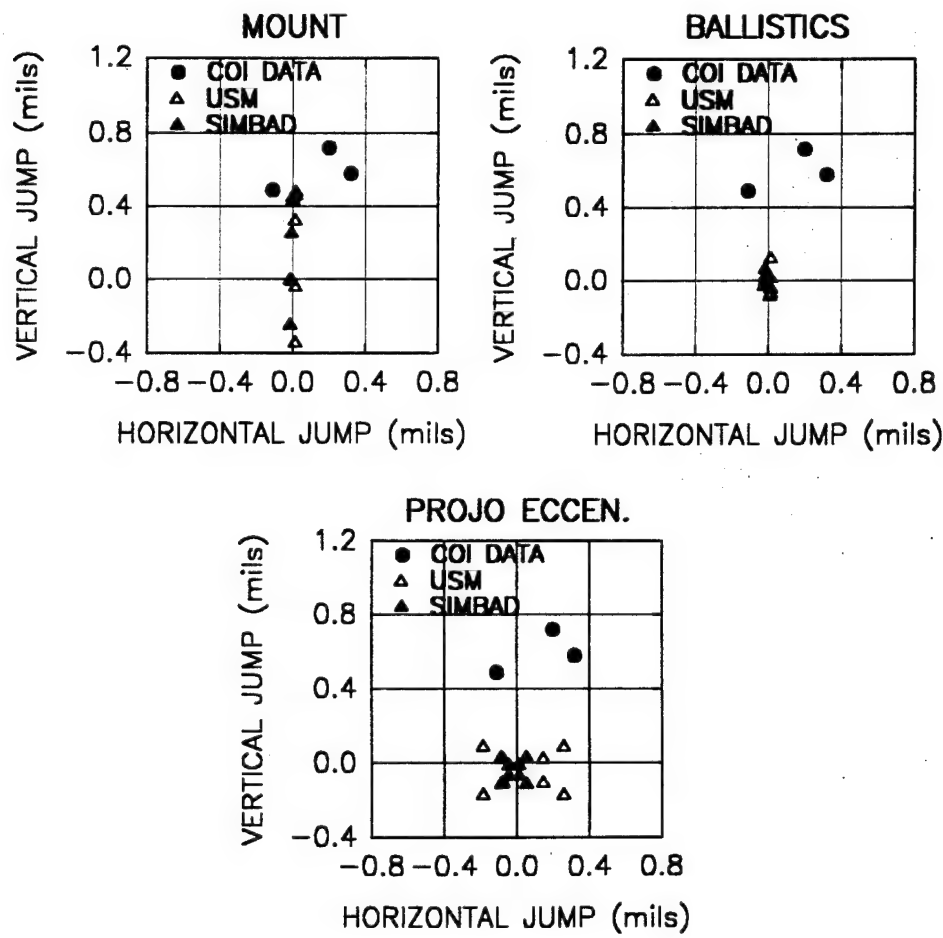


Figure 14a. COI data and calculated gun jump: tube #4994.

120mm M256 ACCURACY STUDY

COI DATA vs PROJECTILE JUMP
for VARIOUS SYSTEM PARAMETERS
TUBE #4994 (STD INDEX)

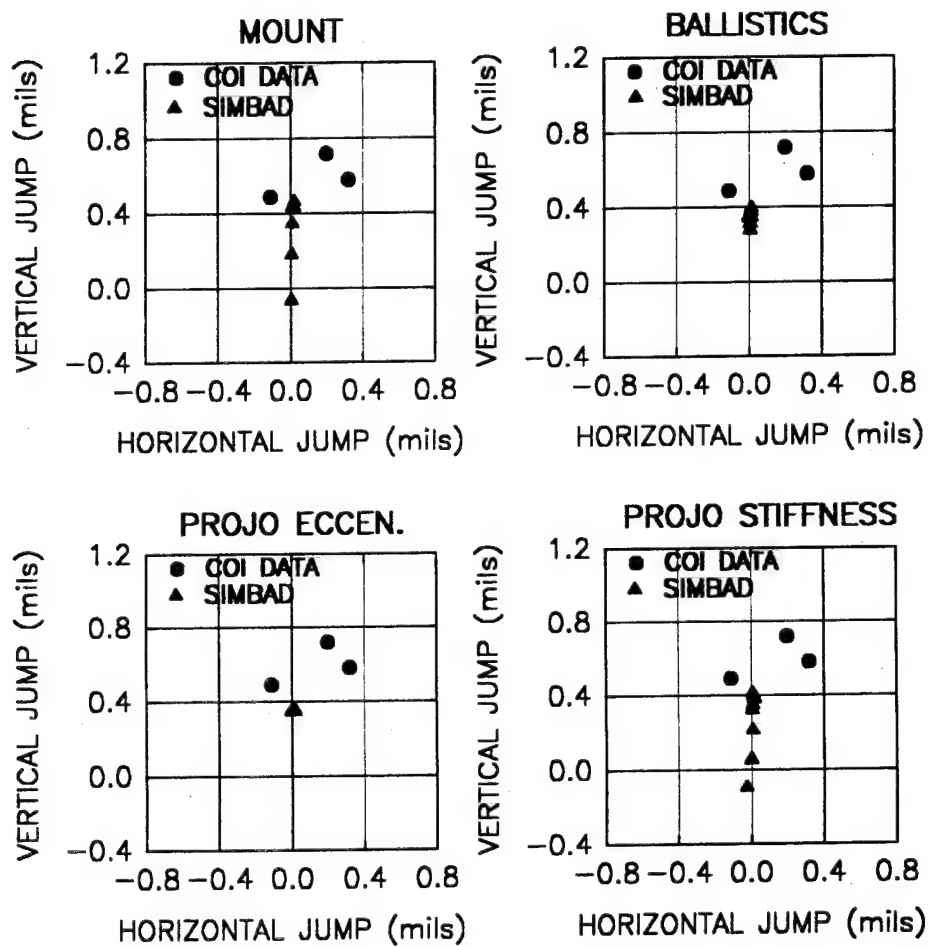


Figure 14b. COI data and calculated projectile jump: tube #4994.

120mm M256 ACCURACY STUDY

COI DATA vs GUN JUMP
for VARIOUS SYSTEM PARAMETERS
TUBE #4996 (STD INDEX)

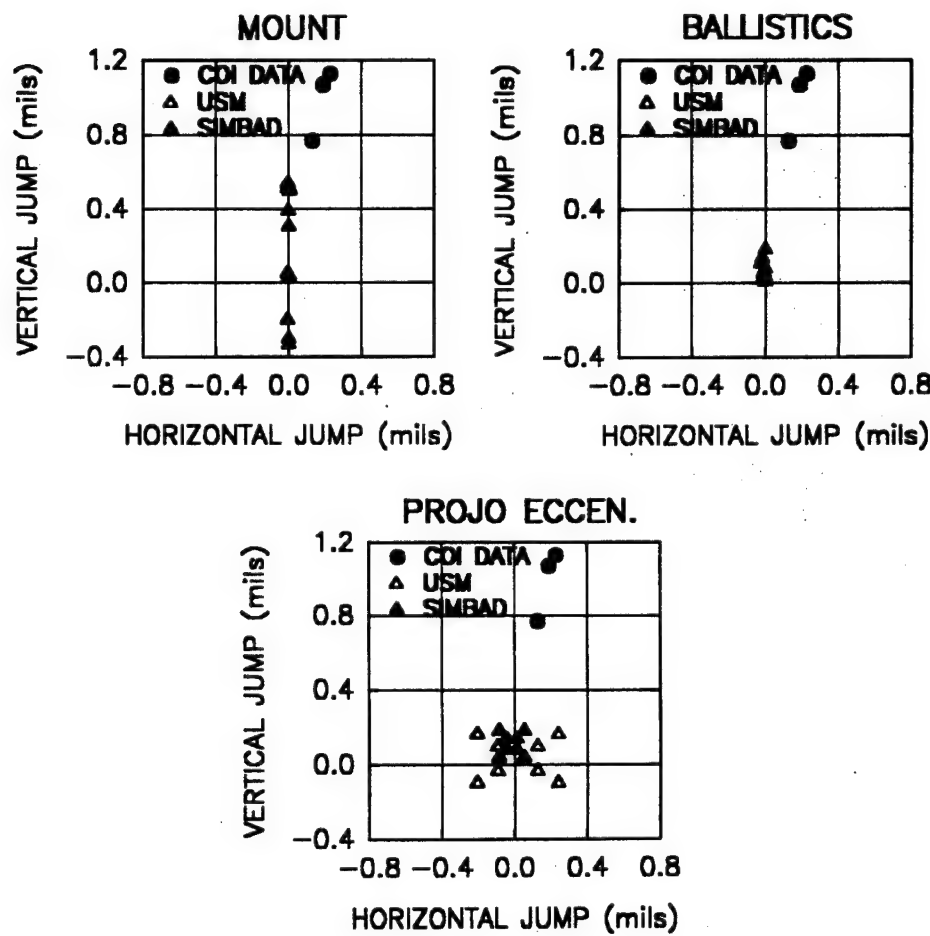


Figure 15a. COI data and calculated gun jump: tube #4996.

120mm M256 ACCURACY STUDY
COI DATA vs PROJECTILE JUMP
for VARIOUS SYSTEM PARAMETERS
TUBE #4996 (STD INDEX)

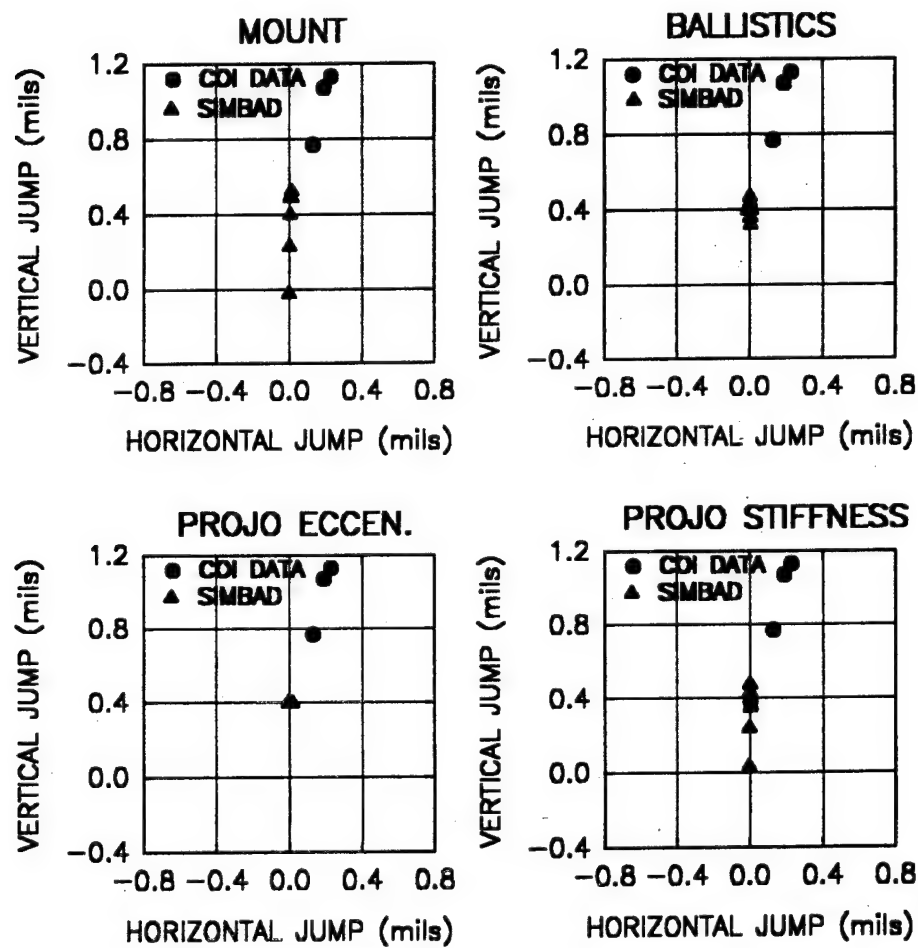


Figure 15b. COI data and calculated projectile jump: tube #4996.

PROBABILISTIC ANALYSIS AND ITS RELATIONSHIP TO ACCURACY

From the results presented in the last section it appears that the use of a purely deterministic analysis model to predict shot accuracy as a function of exit conditions will fail. The values of critical system parameters are problematic. The results from the sensitivity study indicate that both muzzle and projectile jump at shot exit are quite sensitive to a number of the defining parameters in both models. To reiterate mount clearance, tube profile/curvature, projectile eccentricity, bore rider stiffness, and to a lesser degree the shot-to-shot variations in ballistics have an effect on the kinematic conditions at projectile exit. To conclude this study and hopefully generate meaningful results, probabilistic methods are implemented. The model's parameters are defined as random variables using the appropriate statistical distributions selected by interpretation of engineering drawings or experimental data.

Parameter Statistics and Distributions

As previously indicated, the most sensitive parameter is the physical dimensions of the gun mount components and their combined contribution to clearance between the recoiling parts and the cradle. Given that we possess no knowledge of these dimensions for the test components, we may conjecture as to their values by employing the results of the sensitivity study. Since it may be assumed that the same mount was used throughout the test, clearances between components should have been consistent from tube to tube. For all but one case (tube #4098), by setting the clearance value to 0.009 inch for both models, the predicted vertical jump for the tube and projectile closely match the actual values from the test. For this reason the clearance value of 0.009 inch is chosen for the remainder of this study. Since reasonable ballistic deviations at the given temperature of the propellant had little effect upon the exit conditions for either model, randomness in the ballistic parameter is not considered. Rather, nominal values as calculated by internal ballistic routines are used to drive the dynamics. (Note: if the propellant temperature changed from shot-to-shot, a different table of values for the ballistic load and projectile kinematics would be needed.)

The two remaining parameters, both of which are related to the projectile, are bore rider stiffness and mass eccentricity. The experimental values generated by Lyon (ref 11) are the basis for setting the probabilistic bounds on the stiffness parameter, whereas the engineering specifications regarding projectile concentricity are used to define eccentricity bounds. In his experimental work Lyon found that the range in radial stiffness for the rear bore rider was from 0.50 to 2.80 million pounds per inch (M-lbs/in.) depending upon the orientation of the sabot parting lines and the depth of penetration into the material. For the front bore rider the range is 0.20 to 0.48 M-lbs/in. given similar stipulations. The analysis uses three normally distributed random value levels of stiffness each having its own mean and standard deviation. Ten shots are 'fired' in SIMBAD for each tube and stiffness distribution. Terminology and distribution statistics are shown in Table 4.

Table 4. Probabilistic Distribution of Bore Rider Stiffness

Identification	Location	Mean	Std Deviation
Flexible Bands	Rear	0.75 M-lb/in.	0.25 M-lb/in.
	Front	0.25 M-lb/in.	0.05 M-lb/in.
Normal Bands	Rear	1.75 M-lb/in.	0.50 M-lb/in.
	Front	0.35 M-lb/in.	0.10 M-lb/in.
Stiff Bands	Rear	2.50 M-lb/in.	0.75 M-lb/in.
	Front	0.45 M-lb/in.	0.20 M-lb/in.

To assess the effect of projectile eccentricity, the USM is used. Eccentricity data on the round used in the test is unavailable, therefore, we must rely upon estimates from the dimensions, tolerances, and concentricity notes on the projectile's engineering drawings. From a cursory look at the specifications, it appears that a reasonable upper bound for mass eccentricity is 0.05 inch. Therefore, in a manner similar to the treatment of stiffness, three levels of eccentricity are chosen and random samples from a normally distributed set are input to the model. As with SIMBAD, ten shots are 'fired' and the muzzle jump at exit is studied. Terminology and distribution statistics are shown in Table 5.

Table 5. Probabilistic Distribution of Projectile Imbalance

Identification	Mean	Std Deviation
Mostly concentric	0.000 inch	0.005 inch
Mildly eccentric	0.025 inch	0.010 inch
Heavily eccentric	0.050 inch	0.025 inch

The angular locations of these eccentricities around the o'clock positions in the bore are randomly selected from a uniform distribution. The results are plotted on target graphs similar to those illustrated in the previous section.

Response Discussion

The muzzle and projectile jump values (triangle data symbols) for each parameter distribution are plotted on two-dimensional target-type graphs that include the actual shotfall data at 800 mils (circle data symbols) for the corresponding shots. There are two charts per gun tube: one for gun jump and one for projectile jump. Each chart contains three graphs highlighting the response for the random distributions of the test parameter. Each graph contains the results of ten independent runs.

The results for this study are found in Figures 16a and 16b through Figures 25a and 25b. The figure number delineates the results by tube number. Results for the DIT tubes are shown in Figures 16 through 20 and for the STD tubes in Figures 21 through 25. Figure letter 'a' presents calculated muzzle jump values for a solid projectile at various eccentricity distributions using the USM, and figure letter 'b' presents projectile jump values for a flexible projectile at various band stiffness distributions using SIMBAD.

Group 1. DIT tubes; muzzle jump response; solid shot at various eccentricity distributions; Figures 16a,17a,...20a

An assessment of the overall response for this group of tubes indicates that there is a subtle tube dependence on the location of the mean values (filled triangles) of the muzzle jump for the various eccentricity distributions. All of these values are located within a 0.05-mils radius of the point 0.00-mils horizontal and 0.40-mils vertical. As should be expected, the spread among the individual responses increases as the distributions progress from 'mostly concentric' to 'heavily eccentric'. The mean value, however, shows little sensitivity to the distribution. Another interesting point is that the spread in response values is not a function of the tube. Note that each of the individual response patterns with respect to its mean value for a given eccentricity distribution are the same regardless of the tube. This indicates that the muzzle jump response due to eccentricity is strongly a function of projectile eccentricity distribution, but it is independent of tube profile/curvature. With the exception of tube #4100 for mildly and heavily eccentric projectiles, the correlation with the shot data does not exist.

Group 2. DIT tubes; projectile jump response; flexible shot at various band stiffness distributions; Figures 16b,17b,...20b

For this group, the tube-to-tube response definitely indicates a dependence on bore profile. For a given stiffness distribution, the mean value and its spread is markedly different for each tube. For example, the response for 'flexible bands' in tube #4098 (Figure 16b) resides above and to the right of the 0.00-mils horizontal and 0.40-mils vertical location, whereas for tube #4106 (Figure 20b) the response for the same distribution resides below and to the left of this point. In general, for a given tube the response due to 'flexible bands' has the greatest spread of the three, whereas the response to 'normal' and 'stiff bands' is comparable. In addition, as the stiffness distribution increases, the jump response in the vertical direction tends to increase. The same cannot be said for the horizontal response. With the exception of tube #4104 (Figure 19b), the response values are distributed along both horizontal and vertical directions. Since the DIT tubes usually possess more horizontal curvature than the STD tubes, this type of response further confirms the correlated dependence of tube profile and stiffness upon projectile exit. The only responses that tend to match the shotfall patterns are the responses for tube #4100 (Figure 17b). Individual response values and shot data nearly overlap for all stiffness distributions.

120mm M256 ACCURACY STUDY PROBABILISTIC ANALYSIS

COI TEST DATA vs CALCULATED GUN JUMP
for PROJECTILE ECCENTRICITY DISTRIBUTIONS
TUBE #4098 (DIT INDEX)

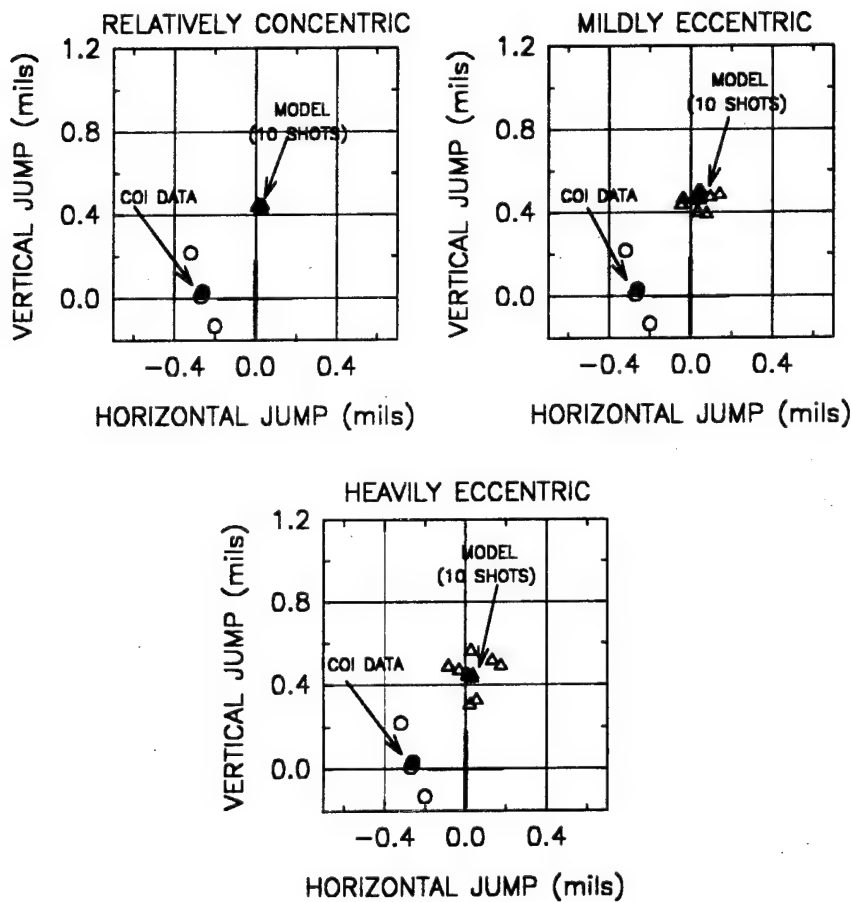


Figure 16a. Probabilistic analysis of gun jump: tube #4098.

120mm M256 ACCURACY STUDY PROBABILISTIC ANALYSIS

COI TEST DATA vs CALCULATED PROJO JUMP
for PROJECTILE STIFFNESS DISTRIBUTIONS
TUBE #4098 (DIT INDEX)

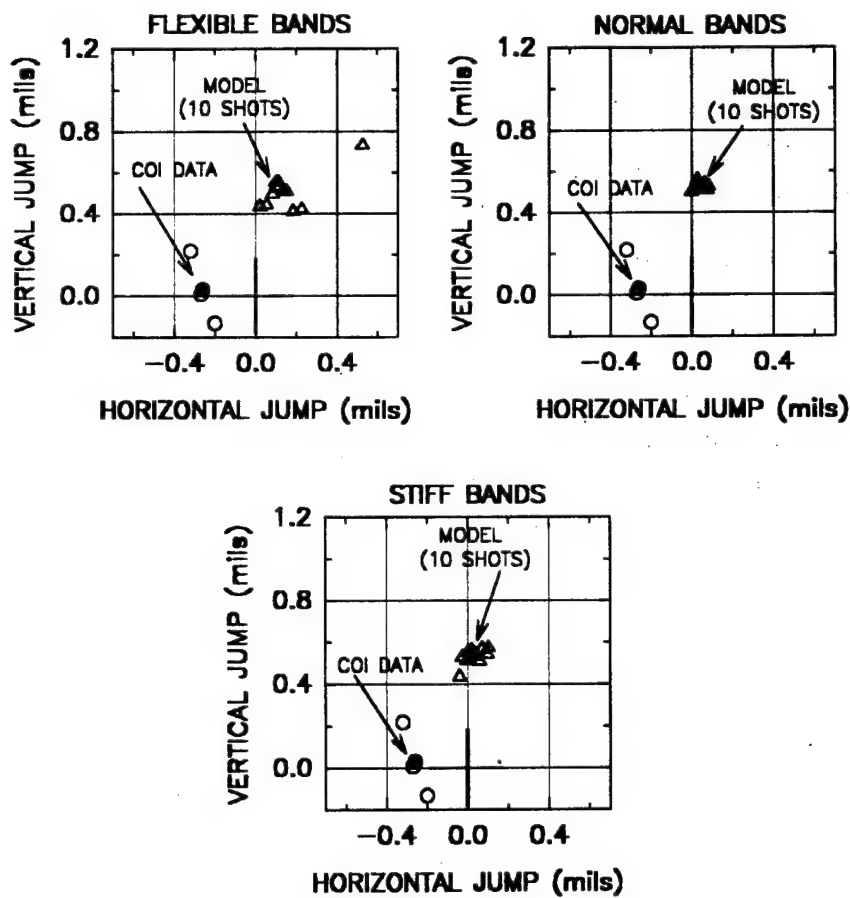


Figure 16b. Probabilistic analysis of projectile jump: tube #4098.

120mm M256 ACCURACY STUDY PROBABILISTIC ANALYSIS

COI TEST DATA vs CALCULATED GUN JUMP
for PROJECTILE ECCENTRICITY DISTRIBUTIONS
TUBE #4100 (DIT INDEX)

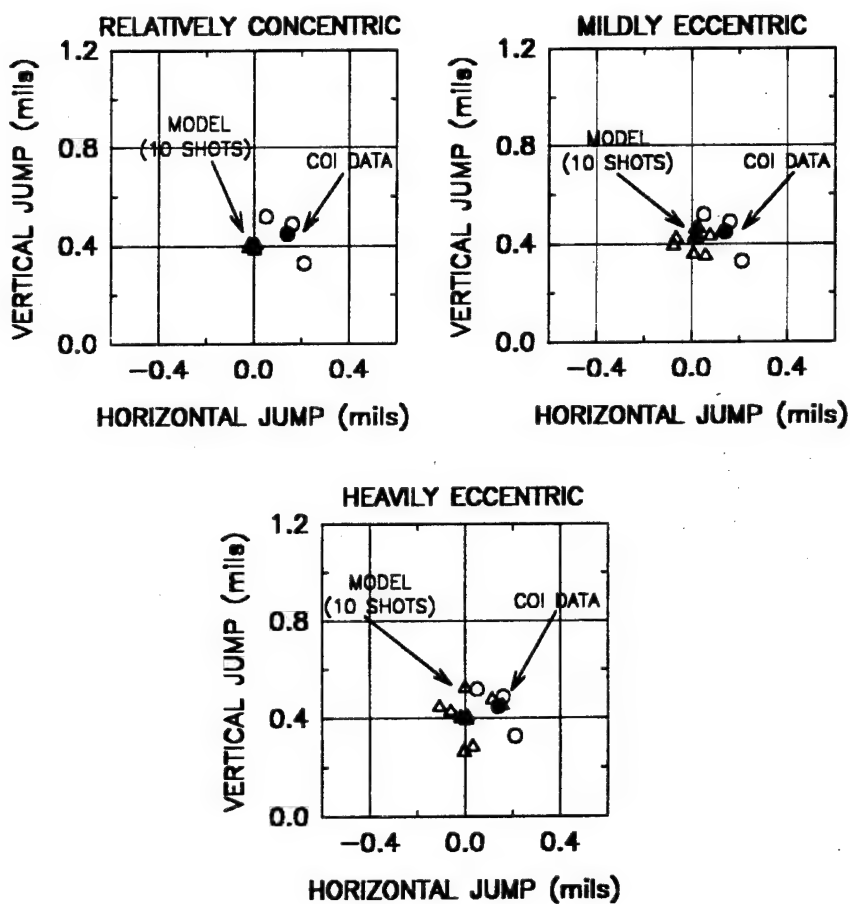


Figure 17a. Probabilistic analysis of gun jump: tube #4100.

120mm M256 ACCURACY STUDY PROBABILISTIC ANALYSIS

COI TEST DATA vs CALCULATED PROJO JUMP
for PROJECTILE STIFFNESS DISTRIBUTIONS
TUBE #4100 (DIT INDEX)

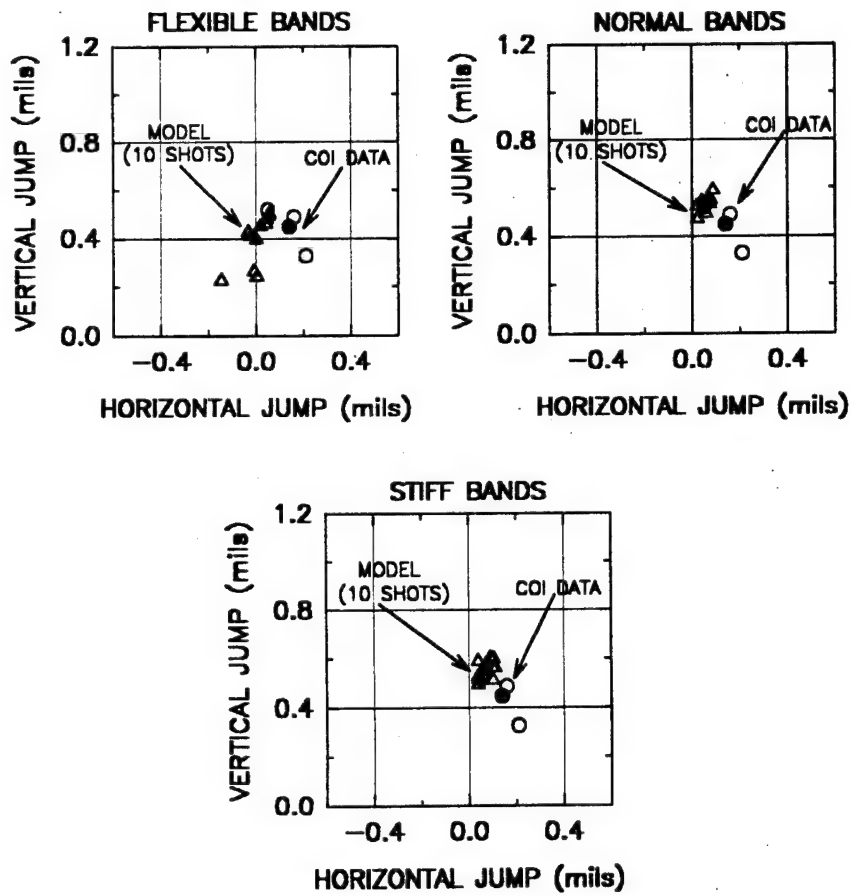


Figure 17b. Probabilistic analysis of projectile jump: tube #4100.

120mm M256 ACCURACY STUDY PROBABILISTIC ANALYSIS

COI TEST DATA vs CALCULATED GUN JUMP
for PROJECTILE ECCENTRICITY DISTRIBUTIONS
TUBE #4102 (DIT INDEX)

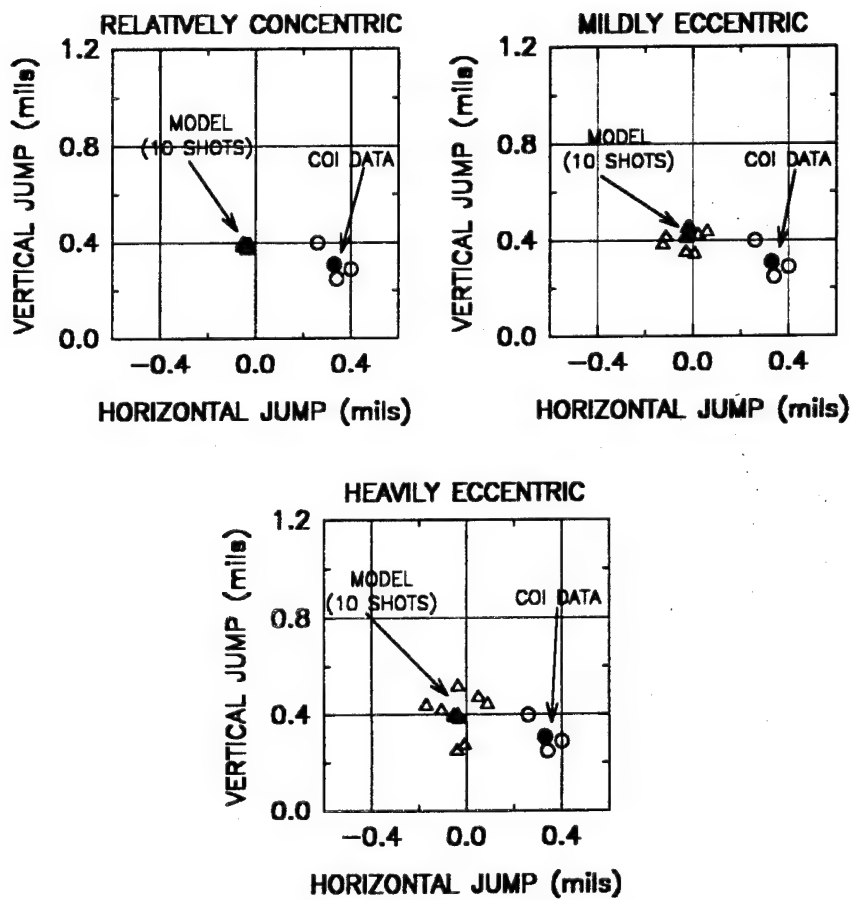


Figure 18a. Probabilistic analysis of gun jump: tube #4102.

120mm M256 ACCURACY STUDY PROBABILISTIC ANALYSIS

COI TEST DATA vs CALCULATED PROJO JUMP
for PROJECTILE STIFFNESS DISTRIBUTIONS
TUBE #4102 (DIT INDEX)

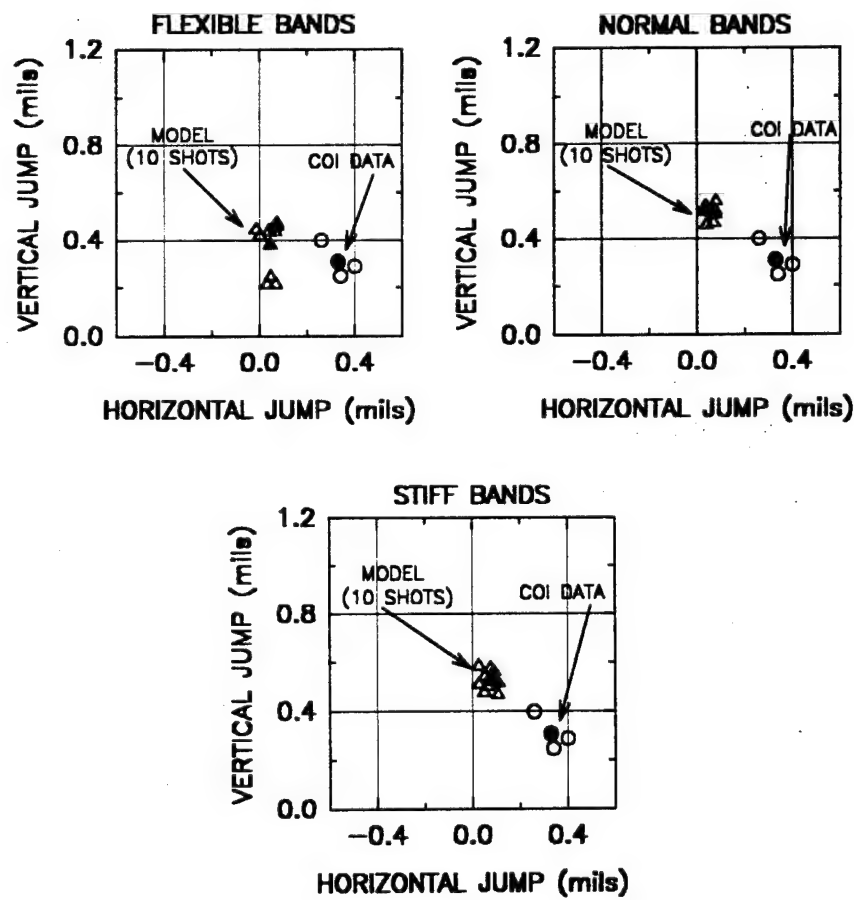


Figure 18b. Probabilistic analysis of projectile jump: tube #4102.

120mm M256 ACCURACY STUDY PROBABILISTIC ANALYSIS

COI TEST DATA vs CALCULATED GUN JUMP
for PROJECTILE ECCENTRICITY DISTRIBUTIONS
TUBE #4104 (DIT INDEX)

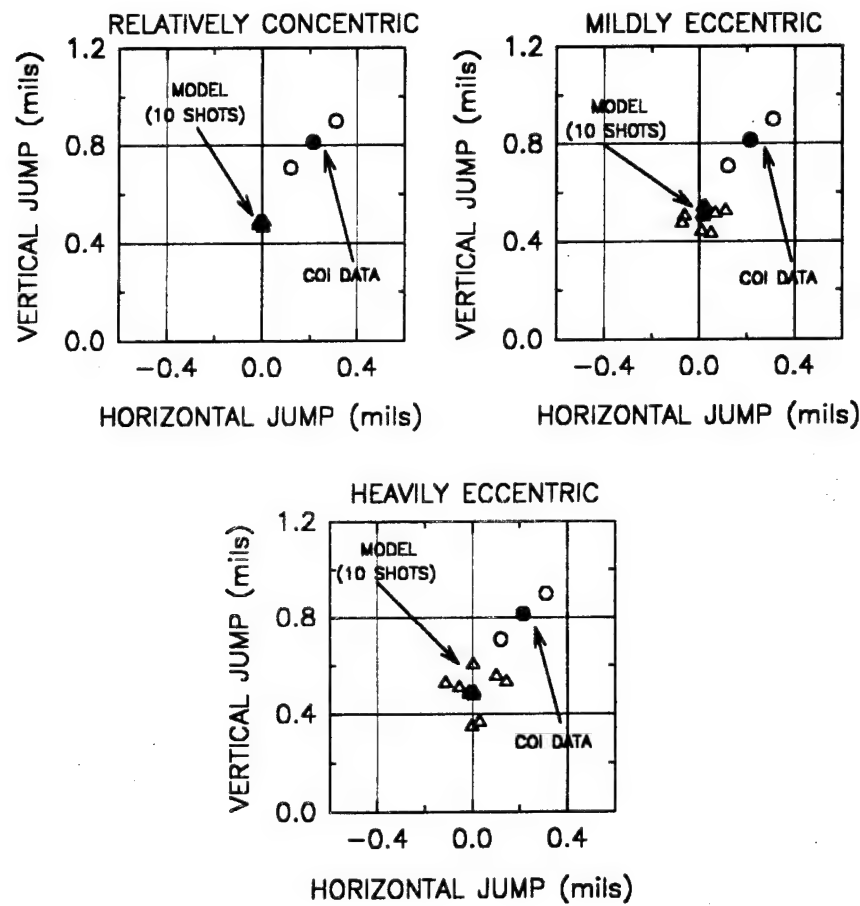


Figure 19a. Probabilistic analysis of gun jump: tube #4104.

120mm M256 ACCURACY STUDY PROBABILISTIC ANALYSIS

COI TEST DATA vs CALCULATED PROJO JUMP
for PROJECTILE STIFFNESS DISTRIBUTIONS
TUBE #4104 (DIT INDEX)

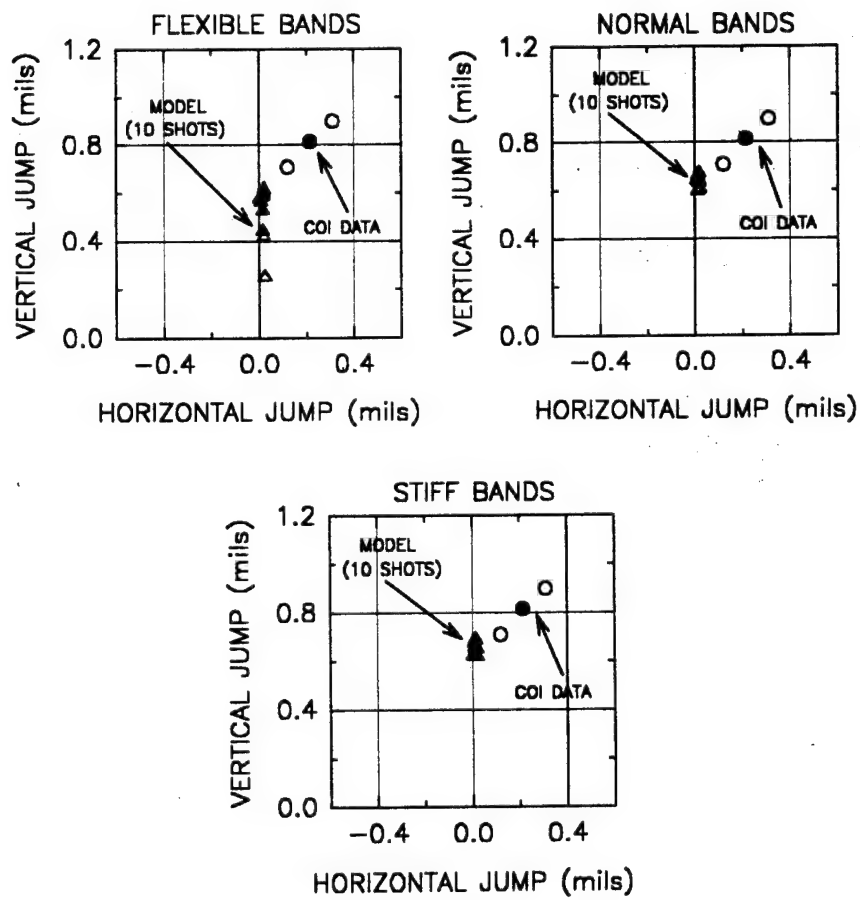


Figure 19b. Probabilistic analysis of projectile jump: tube #4104.

120mm M256 ACCURACY STUDY PROBABILISTIC ANALYSIS

COI TEST DATA vs CALCULATED GUN JUMP
for PROJECTILE ECCENTRICITY DISTRIBUTIONS
TUBE #4106 (DIT INDEX)

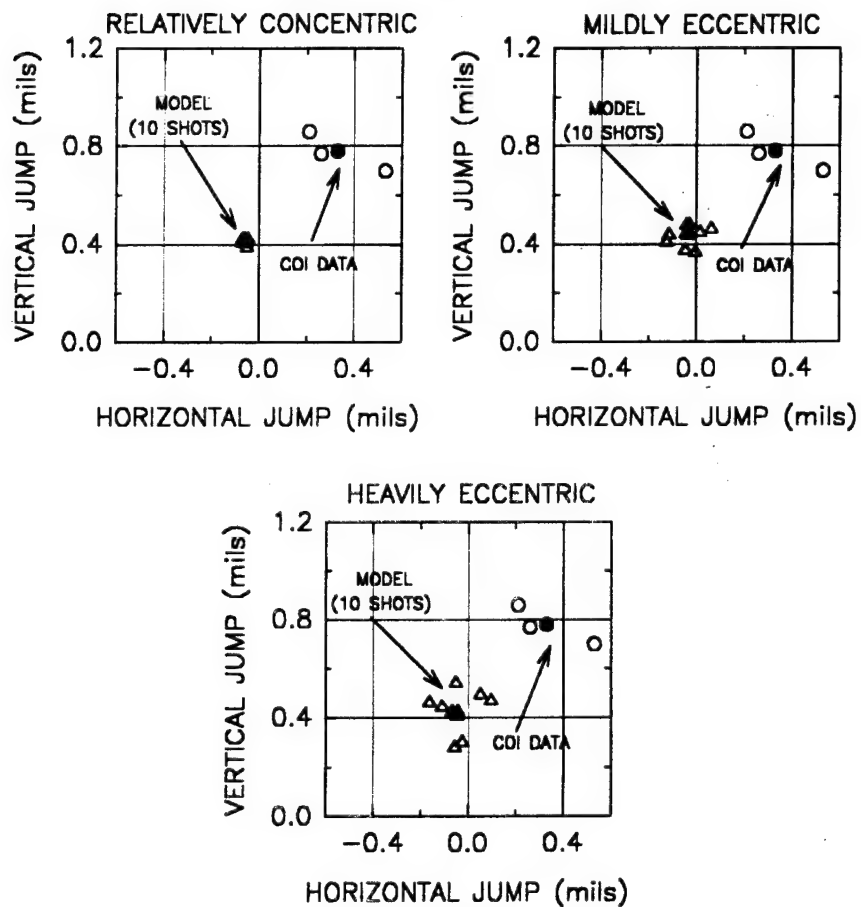


Figure 20a. Probabilistic analysis of gun jump: tube #4106.

120mm M256 ACCURACY STUDY PROBABILISTIC ANALYSIS

COI TEST DATA vs CALCULATED PROJO JUMP
for PROJECTILE STIFFNESS DISTRIBUTIONS
TUBE #4106 (DIT INDEX)

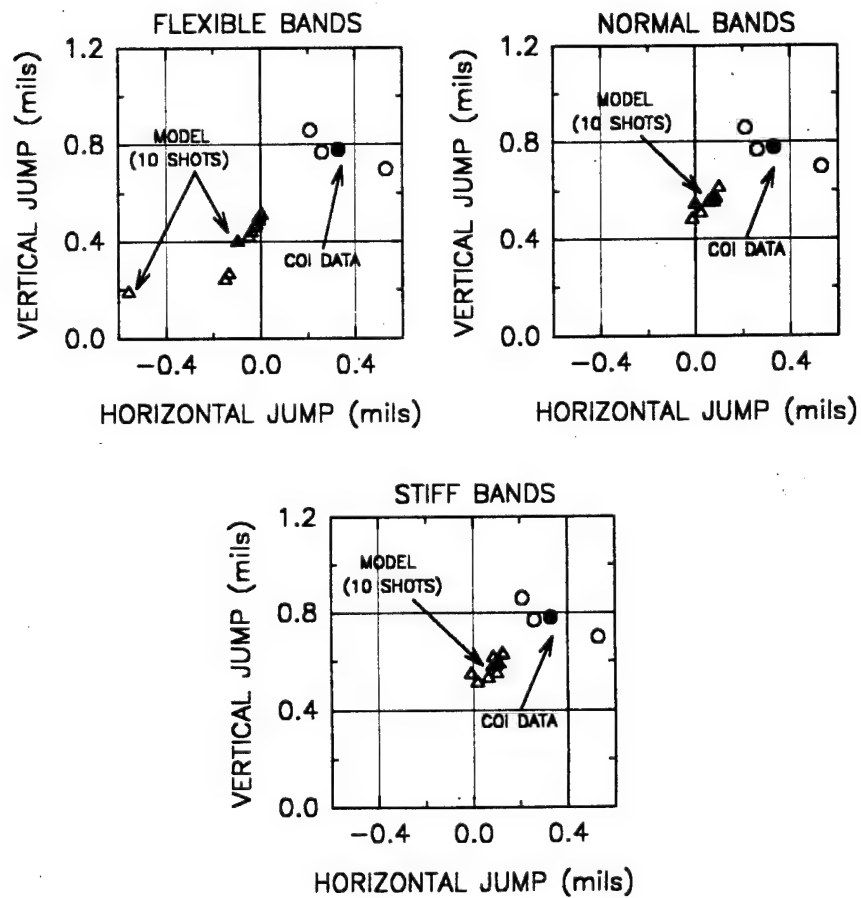


Figure 20b. Probabilistic analysis of projectile jump: tube #4106.

Group 3. STD tubes; muzzle jump response; solid shot at various eccentricity distributions; Figures 21a,22a,...25a

The comments made for group 1 apply to this group as well. For any tube the mean value of the response is not a function of distribution, and the spread around the mean is the same regardless of tube. Correlation exists for tubes #4988 (Figure 21a) and #4994 (Figure 24a) in that the response spread for 'mildly' and 'heavily eccentric' projectiles overlaps the COI distribution.

Group 4. STD tubes; projectile jump response; flexible shot at various band stiffness distributions; Figures 21b,22b,...25b;

In a manner similar to that of group 2, the overall response for this group is dependent upon tube profile and level of projectile band flexibility. The greatest spread in response occurs for the 'flexible band' distribution, whereas for the 'normal' and 'stiff bands' the spread in response is comparable. With the exception of tubes #4988 and #4990 (Figures 21b and 22b), the response spread is in the vertical direction only. The most probable cause lies in the nature of the STD indexing. Recalling the procedure, all tubes in this group have their plane of maximum curvature oriented in the vertical direction with the muzzle pointed up. Therefore, very little if any curvature exists in the horizontal plane. Hence dynamic response to bore profile is absent in this plane. Also, as the band stiffness distribution increases in mean value, the jump response increases in the vertical direction much the same as that for group 2. Again horizontal jump shows no sensitivity to increase in stiffness. Regarding correlation to test data, the response values for tube #4988 (Figure 21b) at 'normal' and 'stiff bands' overlap the shotfall mean value. Tube #4994 (Figure 22b) has reasonably good correlation in the vertical direction at 'normal' and 'stiff bands', whereas the remaining tubes predict vertical exits that are at least 0.50 mils less than the test data. Horizontal correlation for this subset is poor.

120mm M256 ACCURACY STUDY PROBABILISTIC ANALYSIS

COI TEST DATA vs CALCULATED GUN JUMP
for PROJECTILE ECCENTRICITY DISTRIBUTIONS
TUBE #4988 (STD INDEX)

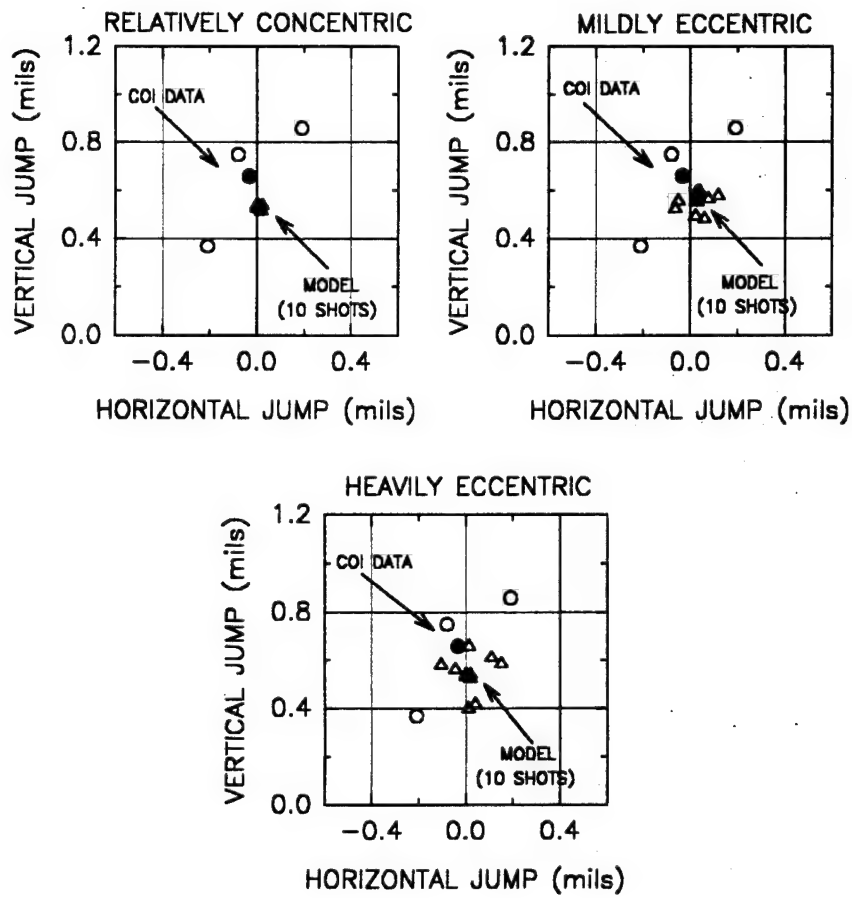


Figure 21a. Probabilistic analysis of gun jump: tube #4988.

120mm M256 ACCURACY STUDY PROBABILISTIC ANALYSIS

COI TEST DATA vs CALCULATED PROJO JUMP
for PROJECTILE STIFFNESS DISTRIBUTIONS
TUBE #4988 (STD INDEX)

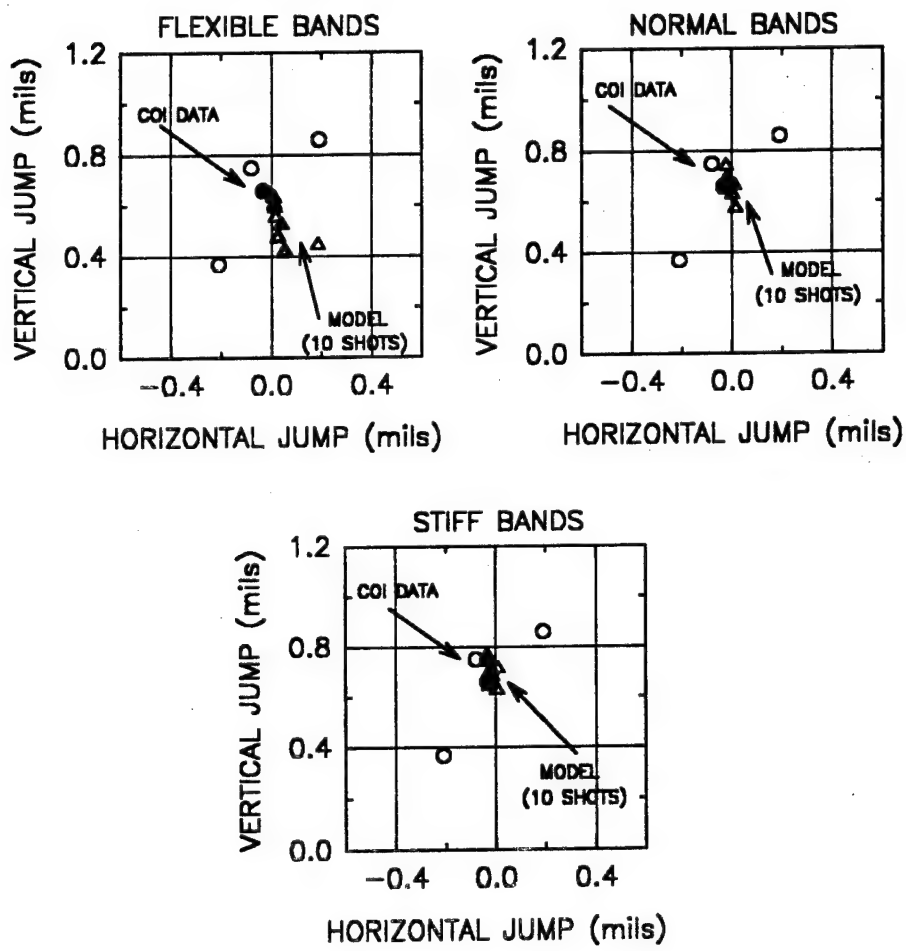


Figure 21b. Probabilistic analysis of projectile jump: tube #4988.

120mm M256 ACCURACY STUDY PROBABILISTIC ANALYSIS

COI TEST DATA vs CALCULATED GUN JUMP
for PROJECTILE ECCENTRICITY DISTRIBUTIONS
TUBE #4990 (STD INDEX)

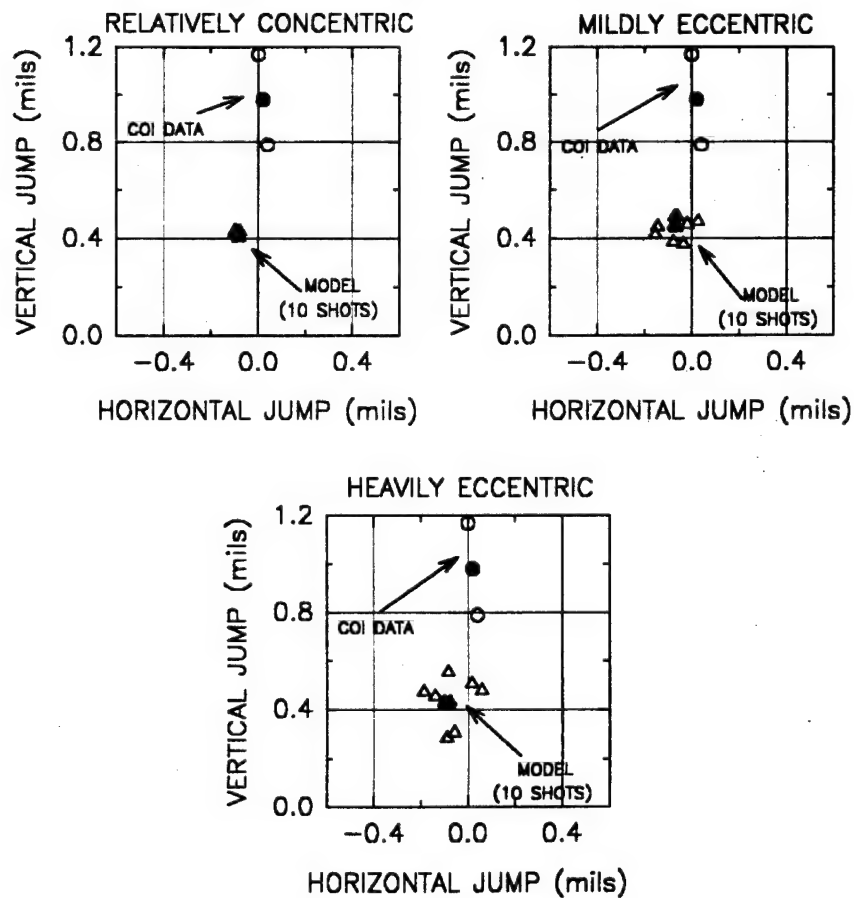


Figure 22a. Probabilistic analysis of gun jump: tube #4990.

120mm M256 ACCURACY STUDY PROBABILISTIC ANALYSIS

COI TEST DATA vs CALCULATED PROJO JUMP
for PROJECTILE STIFFNESS DISTRIBUTIONS
TUBE #4990 (STD INDEX)

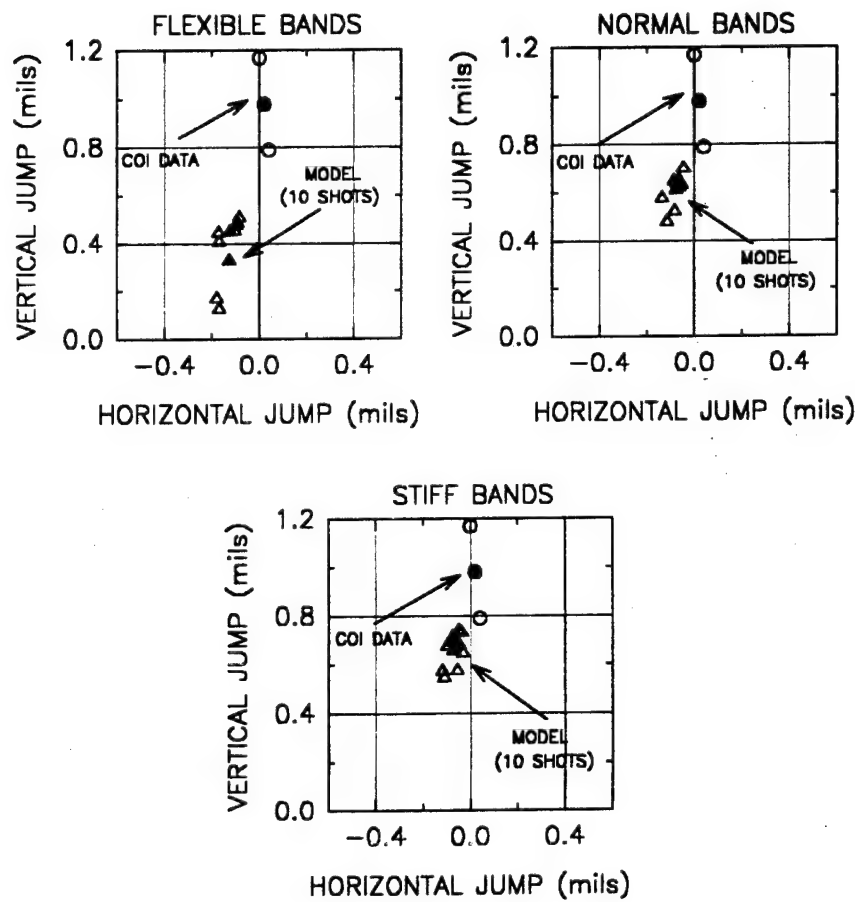


Figure 22b. Probabilistic analysis of projectile jump: tube #4990.

120mm M256 ACCURACY STUDY PROBABILISTIC ANALYSIS

COI TEST DATA vs CALCULATED GUN JUMP
for PROJECTILE ECCENTRICITY DISTRIBUTIONS
TUBE #4992 (STD INDEX)

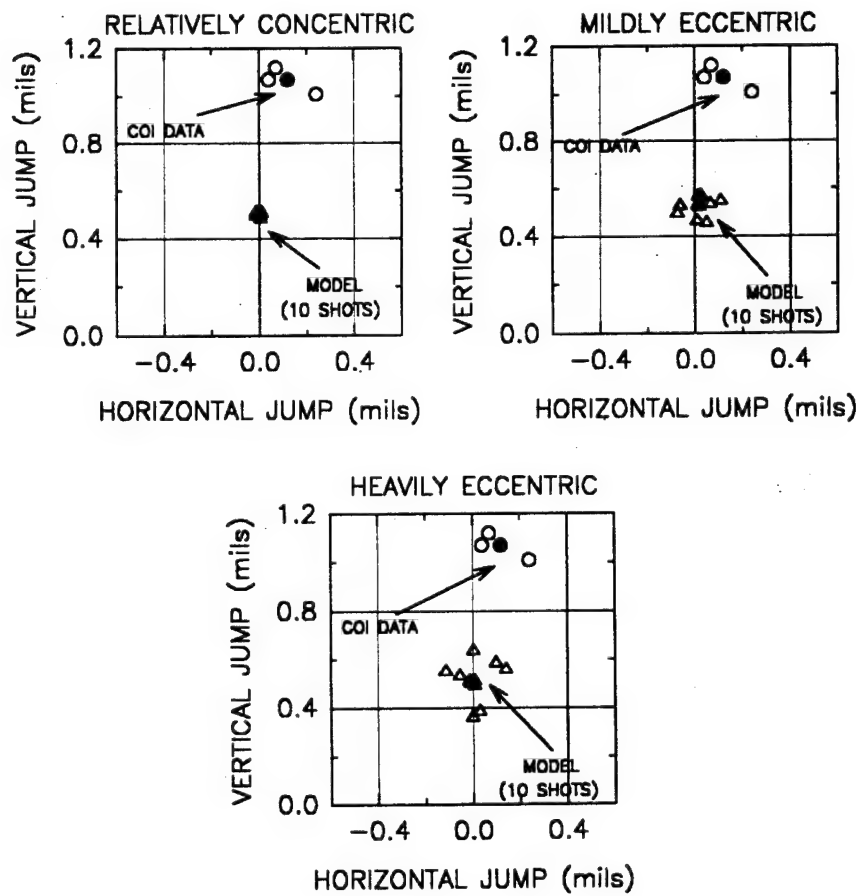


Figure 23a. Probabilistic analysis of gun jump: tube #4992.

120mm M256 ACCURACY STUDY PROBABILISTIC ANALYSIS

COI TEST DATA vs CALCULATED PROJO JUMP
for PROJECTILE STIFFNESS DISTRIBUTIONS
TUBE #4992 (STD INDEX)

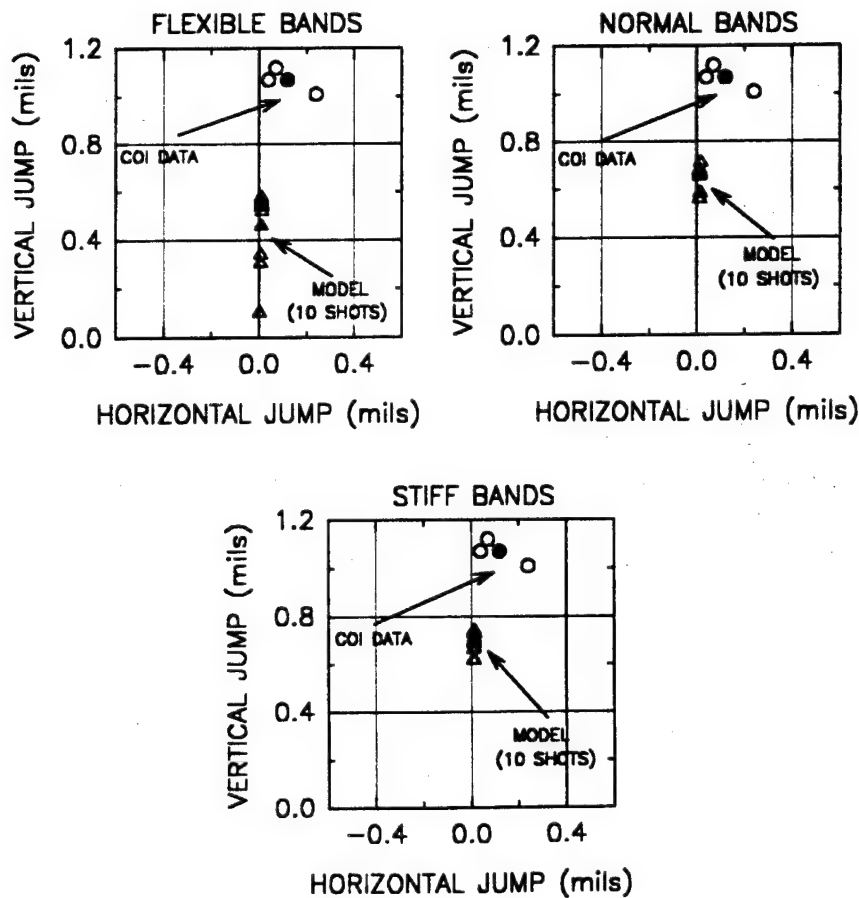


Figure 23b. Probabilistic analysis of projectile jump: tube #4992.

120mm M256 ACCURACY STUDY PROBABILISTIC ANALYSIS

COI TEST DATA vs CALCULATED GUN JUMP
for PROJECTILE ECCENTRICITY DISTRIBUTIONS
TUBE #4994 (STD INDEX)

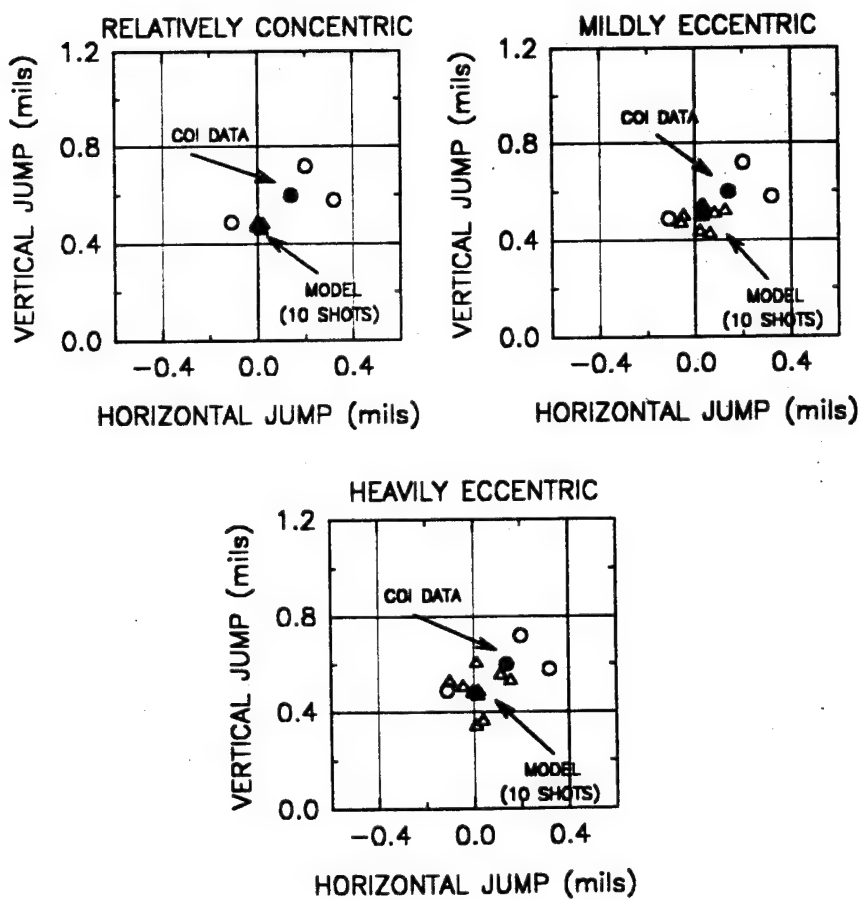


Figure 24a. Probabilistic analysis of gun jump: tube #4994.

120mm M256 ACCURACY STUDY PROBABILISTIC ANALYSIS

COI TEST DATA vs CALCULATED PROJO JUMP
for PROJECTILE STIFFNESS DISTRIBUTIONS
TUBE #4994 (STD INDEX)

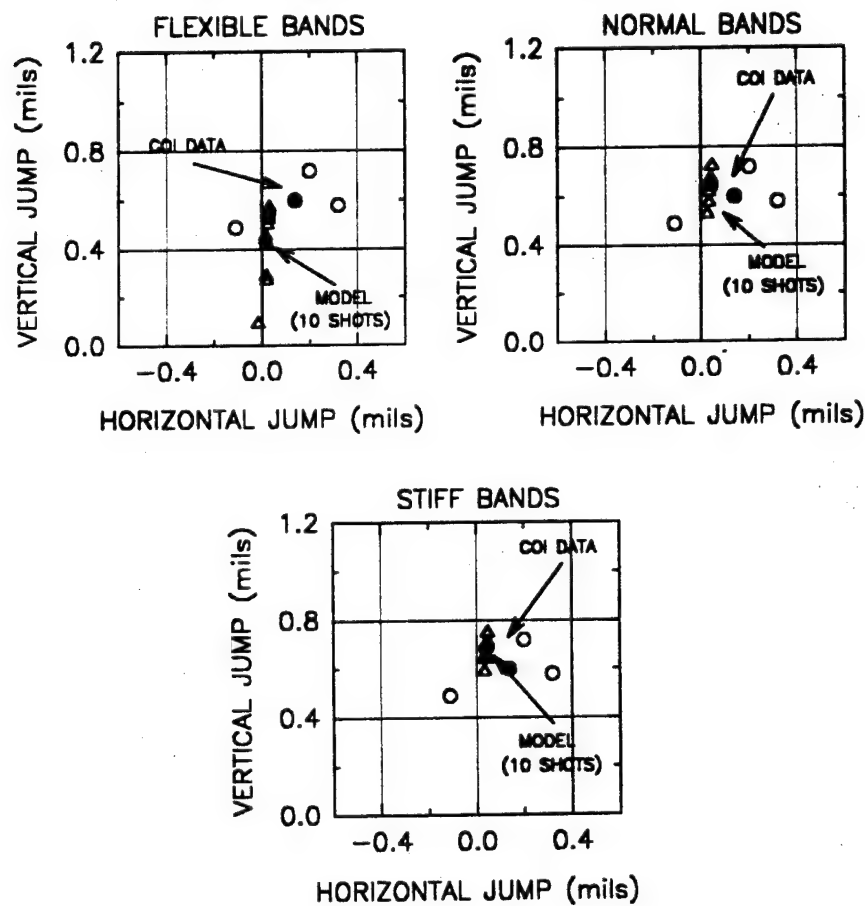


Figure 24b. Probabilistic analysis of projectile jump: tube #4994.

120mm M256 ACCURACY STUDY PROBABILISTIC ANALYSIS

COI TEST DATA vs CALCULATED GUN JUMP
for PROJECTILE ECCENTRICITY DISTRIBUTIONS
TUBE #4996 (STD INDEX)

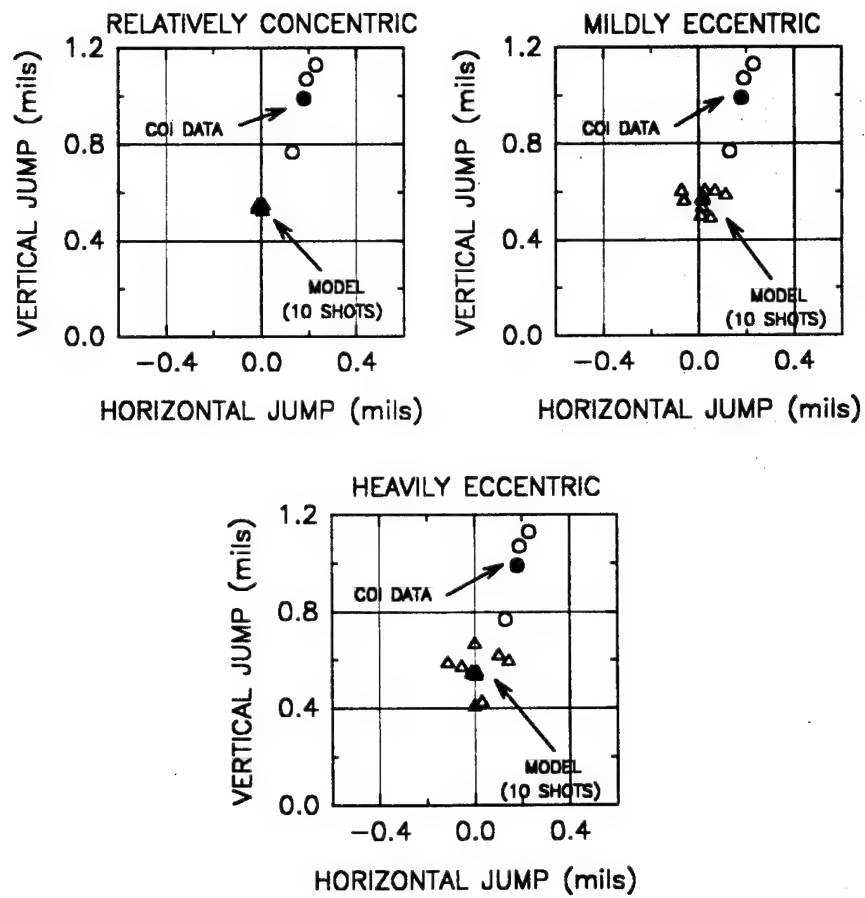


Figure 25a. Probabilistic analysis of gun jump: tube #4996.

120mm M256 ACCURACY STUDY PROBABILISTIC ANALYSIS

COI TEST DATA vs CALCULATED PROJO JUMP
for PROJECTILE STIFFNESS DISTRIBUTIONS
TUBE #4996 (STD INDEX)

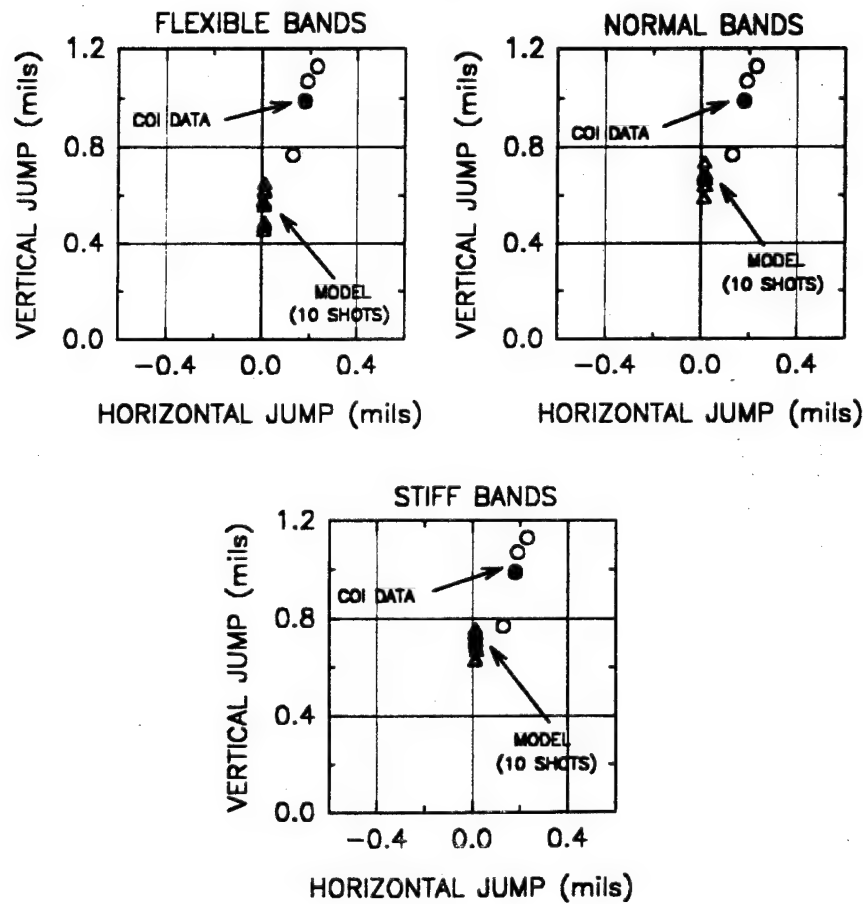


Figure 25b. Probabilistic analysis of projectile jump: tube #4996.

Correlation of Dynamic Results to COI Test Data

The results of the present study indicate that the projectile band stiffness rather than its eccentricity interact with the tube's profile to produce the calculated exit conditions of the round. For eccentric rounds, the response distributions are the same regardless of the tube, whereas their mean values are only mildly tube dependent. In the remainder of this section the SIMBAD mean value responses of projectile jump due to band stiffness are discussed in light of the COI firing data.

Figure 26 presents the mean values of the exit responses for the three band stiffness distributions for all ten tubes. The DIT tubes are indicated by the solid triangles, whereas the STD tubes are indicated by hollow triangles. The data certainly shows the effect that band stiffness has upon exit response. For the case of flexible bands (upper left in the figure), the spread in the mean exit values is quite large compared to either the normal or stiff band distributions. Recalling that the same distributions were used for each tube, the response to the flexible distribution appears to be intermingled among both DIT and STD tubes. In other words, there is no gravitation of the response to the type of profile indexing method. However, as the band stiffness becomes greater, the responses tend to migrate according to index. For the case of stiff bands, the responses for four of the five DIT tubes are located extremely close to the point 0.10-mils horizontal by 0.50-mils vertical. For all five of the STD tubes, the responses are located near the point 0.00-mils horizontal by 0.70-mils vertical. The spread for this group, however, is greater than that of the DIT group.

Presumably, as the band stiffness increases (note: the normal band stiffness distribution most closely represents the experimental work of Lyon (ref 11)) the location of the exit response begins to approach the actual COI patterns of the shots. (Refer to Figure 3 for the COI data.) Recalling, the mean COI value for four of the five DIT tubes were at the point 0.25-mils horizontal by 0.60-mils vertical, and all five STD tubes had a COI average of 0.10-mils horizontal by 0.85-mils vertical. What we hope to conclude is the existence of a constant offset vector (COV) which, when added vectorially to the exit condition of the shot, reproduces the impact location of the round at the target. If such a characteristic exists, the aim point for a particular tube, projectile, and charge could be adjusted based upon the results of a dynamic analysis and the COV for the gun and round being used. For example, a dynamic analysis indicates that the muzzle jump of a particular projectile and tube combination is 0.50-mils horizontal by 0.15-mils vertical, and the COV has been determined as -0.15-mils horizontal by 0.23-mils vertical. The aim point should be set at -0.35-mils horizontal $(-(0.50 - 0.15))$ by -0.38-mils vertical $(-(0.15 + 0.23))$. Owing to the fact that other mitigating factors exist (i.e., contribution of sabot discard, etc.) that affect the flight of a round, it is hoped that these factors are constant in the COV for a given projectile. This being the case, the calculation of a COV using projectile exit calculations is quite feasible. The data and calculations will be queried to see if a COV approach is possible.

120mm M256 ACCURACY STUDY PROBABILISTIC ANALYSIS

CALCULATED PROJECTILE JUMP AVERAGES
by TUBE GROUP and BAND STIFFNESS

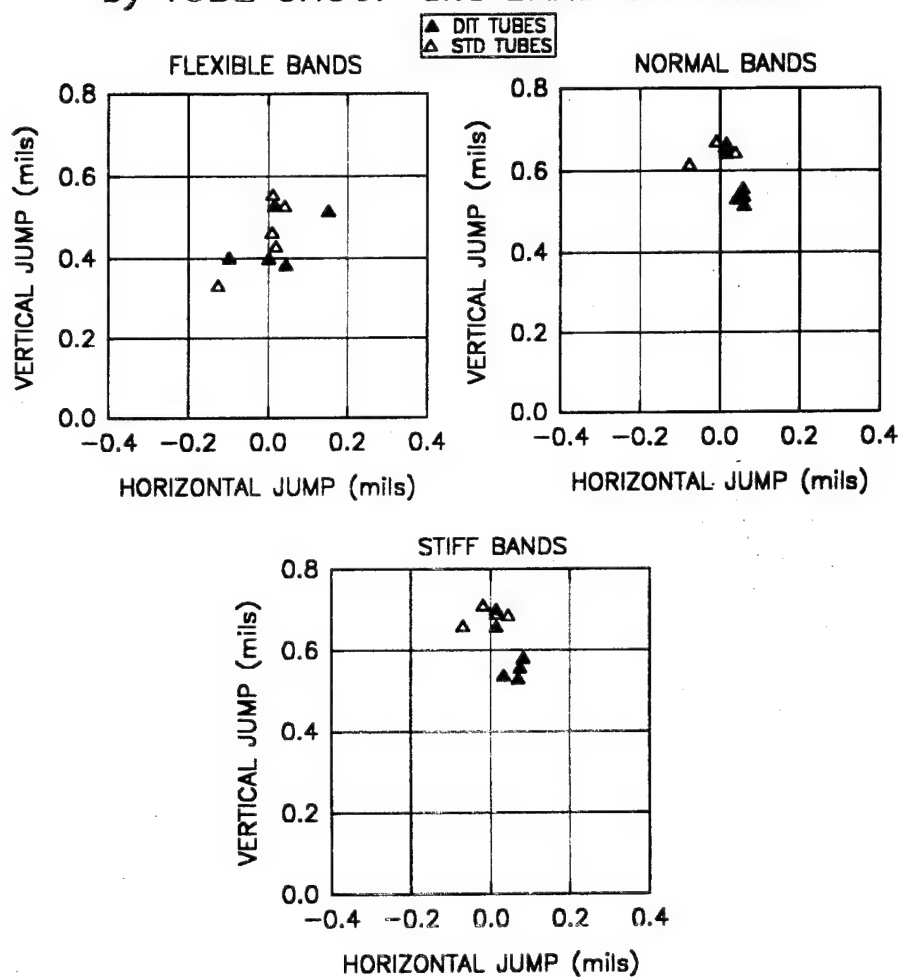


Figure 26. Probabilistic analysis: projectile jump averages.

Define the individual offset vectors (IOV) as the vectorial difference between the mean COI values and the mean projectile exit conditions for each tube at a given band stiffness distribution. The results of these calculations are shown in Figure 27. Unlike the actual COI values, which tended to gravitate by type of profile index, the IOVs tend to fall into two groups (defined by elliptical enclosures) that contain both DIT and STD tubes and two DIT 'flyer' tubes. The spread within each group is large for the case of flexible bands and becomes much smaller as band stiffness increases. The most populated group contains five tubes--three of which are the STD type. The mean value for this group resides at the point 0.30-mils horizontal by 0.50-mils vertical for the case of flexible bands and finally settles at the point 0.20-mils horizontal by 0.30-mils vertical for the stiff band distribution. At this point the spread among the five points is roughly a diameter of 0.25 radians. The IOV responses for the second most populated group reside very close to the axis in the horizontal direction and progress from slightly above to slightly below in the vertical direction as band stiffness increases. Also, as band stiffness increases, the spread in the IOVs decreases. The two 'flyers', both of which are DIT tubes, reside at the outskirts of the graph and are relatively insensitive to the band stiffness distribution.

What conclusions may be drawn from this information? For five of the ten cases, the COV is well defined at 0.15-mils horizontal by 0.30-mils vertical. It may be argued that this COV value is common for many M256 tubes. This being the case, aim compensation vectors may be calculated for all tubes in this test and impact results plotted as target graphs. The results for the case of normal band stiffness distribution are shown in Figure 28.

Figure 28 presents the actual impact locations at the target if an aim compensation vector using the results of dynamic analysis and the calculated COV is employed. Eight of the ten cases fall within a 0.40-mils horizontal by 0.60-mils vertical rectangle centered slightly below the horizontal axis and through the vertical axis. The two 'flyer' rounds again reside on the outskirts of the graph. By comparing these results to the raw impact data in Figure 3, benefits may be realized in both the COI average and the spread among tubes. These same eight cases when mapped back to the actual COI graph reside in a rectangle of 0.40-mils horizontal by 0.80-mils vertical the center of which is 0.20-mils horizontal by 0.80-mils vertical. A slight improvement in the COI spread in the vertical direction is indicated.

A small but realizable consistency in tube-to-tube accuracy may be achieved by incorporating a detailed dynamic analysis for various combinations of tube and round (at specific temperature) and employing a COV that may be calculated from previous firing data and dynamic analysis.

120mm M256 ACCURACY STUDY PROBABILISTIC ANALYSIS

CALCULATED PROJECTILE JUMP OFFSETS
from AVERAGE COI TUBE DATA
by TUBE GROUP and BAND STIFFNESS

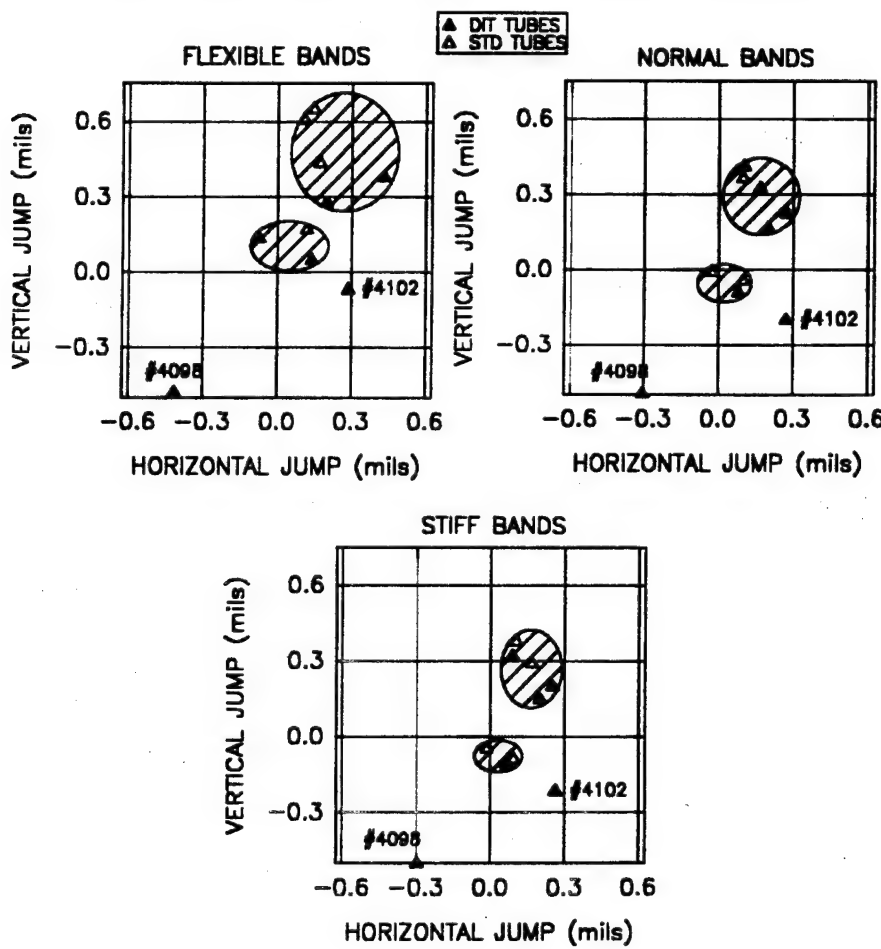


Figure 27. Probabilistic analysis: projectile jump offset.

120mm M256 ACCURACY STUDY PROBABILISTIC ANALYSIS

**CALCULATED CENTERS of IMPACT
from DYNAMIC and 'COV' ANALYSIS**

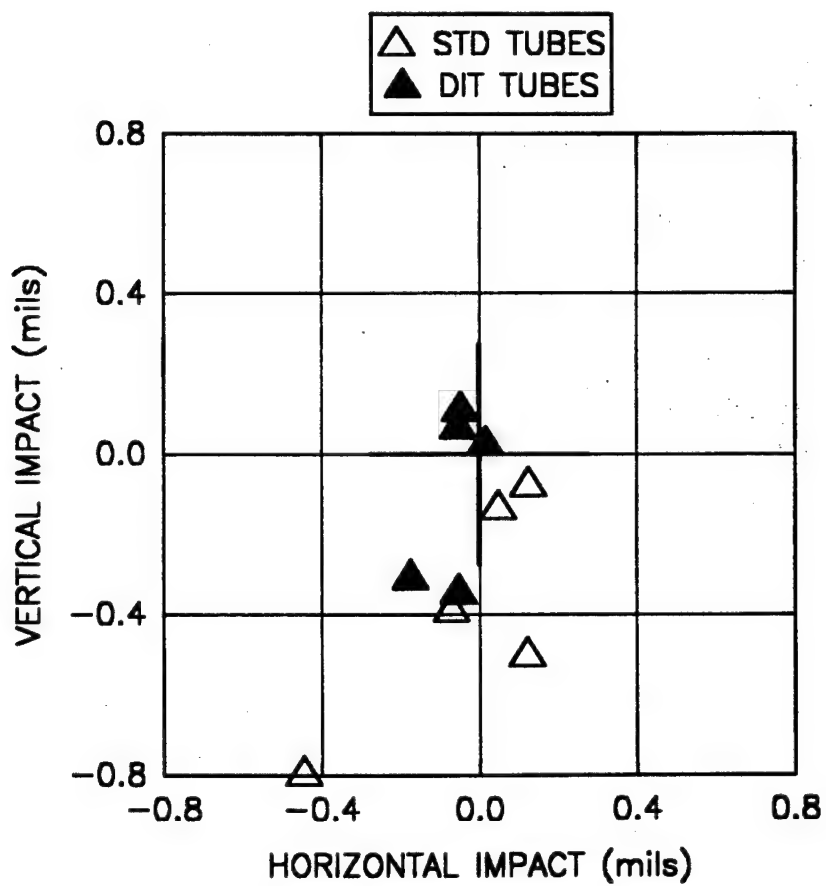


Figure 28. Probabilistic analysis: calculated centers of impact.

DISCUSSION AND CONCLUSIONS

The topics of gun dynamics, bore profile estimates, shot accuracy, probabilistic analysis, and a semi-empirical approach to estimating shot accuracy have been cited in this report. This section contains discussions of the analyses in which the above topics have been included and conclusions based upon the findings from these analyses. The main points of the report are discussed again in light of their relevance to the topics.

The first point discussed concerns the relevance that bore profile and curvature have upon tube acceptability through the use of gun dynamics. Granted, it is impossible to manufacture perfectly straight gun tubes due to their slenderness ratios and propensity to warp during manufacture. Current inspection procedures place restrictions on the amount of profile deviation between measurement points and along the total length of the tube. The real culprit in regard to dynamic excitation is not profile straightness but local curvature. A gun tube may pass profile inspection, but it may possess high degrees of curvature along its entire length. A projectile forced to ride along this 'bumpy path' will most certainly cause self-induced vibration and vibration to the tube as well.

Bore profile data for the ten tubes used in the test were presented along with a method of determining a correct functional fit of the data points using the chi-square statistic. Parameters of this method include both the number of inspection points and the accuracy of the inspection readings. By twice differentiating the profile fitting function, tube curvature is calculated. This tube parameter, which was different for each tube, proved to be critical in each of the gun dynamics models. The intent of the DIT test was to verify a tube indexing method that enhances accuracy. Results from studying a portion of the data indicate a definite migration of shot impact locations dependent upon the indexing method. Only one round type at one propellant temperature was studied.

It may be concluded that a better method of specifying bore straightness based upon local and overall curvature needs to be developed. Possibly, the same type of algorithm to calculate profile and curvature used in this analysis may be incorporated in the inspection loop during tube manufacture. Curvature calculations may be reported as well as profile data. Acceptance criterion based upon curvature may be specified.

The second point discussed concerns the use of and correlation between two dynamics models to estimate shotfall patterns based upon exit dynamics. The models used are Benét's USM and Simatic's SIMBAD. A number of supposed sensitive parameters were identified and modelled using the two codes. The figure of merit for both models is the kinematic state of the tube's muzzle and/or projectile at shot exit. Muzzle or projectile jump is defined as the deviation from aim of the projected direction of the shot at exit. Since the USM employs a solid shot, projectile jump and muzzle jump are equal. SIMBAD uses a flexible shot, therefore, muzzle jump need not be the same as projectile jump.

The parameters include clearance between the mount and tube, ballistic variations within a given shot, gun tube bore curvature, stiffness of the projectile's bore riders, and projectile mass eccentricity. The conduction of an initial study determined the robustness of these unknown or unmeasured parameters. Results indicate that neither ballistic variations nor projectile mass

eccentricity in SIMBAD affect the figures of merit, therefore, these parameters were set to their nominal values for the remainder of the study. Both projectile and muzzle jump, however, were sensitive to all remaining parameters. The most sensitive was mount clearance. Engineering drawings were examined to determine a range of clearance due to tolerance stackup. For the full range of this parameter, projectile and muzzle jump varied considerably in the vertical plane and slightly in the horizontal plane. Bore curvature for each tube was unique. Muzzle and projectile jump values showed much sensitivity to this tube parameter. Jump values proved to be quite sensitive in both vertical and horizontal planes to projectile band stiffness in SIMBAD.

For both the solid and flexible shot, both SIMBAD and the USM predicted the same level of gun jump as mount clearance was incremented through its expected range. In SIMBAD projectile band stiffness coupled with bore curvature affected projectile and muzzle jump. A definite coupling exists between these two parameters since strikingly different projectile jump distributions were indicated as these parameters were tested. Muzzle jump for eccentric solid shots for both models indicated sensitivity to the level of this parameter, but a coupling to tube curvature did not exist.

The third point discussed concerns the use of probability theory to predict shot accuracy from the results of dynamic analysis. Since many of the system parameters were either unknown or not measured, one must resort to probabilistic analysis to generate system parameters needed in a dynamic model. In this type of analysis, the values of uncertain or unknown parameters are randomly drawn from an expected statistical distribution having a mean and standard deviation. Therefore, a given distribution of input values results in a distribution of output responses having its own mean and standard deviation values. The likelihood that a response occurs is cast as a probability; the higher the probability, the more likely the occurrence of the response.

For this study neither bore curvature nor mount clearance was considered to be random. The bore characteristics for each tube were set based upon the previously mentioned chi-square analysis. The mount clearance was set at 0.009 inch since it appears that this value is reasonable based upon the initial study. The projectile characteristics of band stiffness and mass eccentricity were considered to be random. For each, three separate distributions (ten values in each)--each possessing its own mean and standard deviation--were calculated and employed as model inputs. The USM was used to rate gun jump for mass eccentricity distributions, whereas SIMBAD was used to rate projectile jump for band stiffness distributions.

For the mass eccentric projectiles, response distributions were very tight for eccentricity distributions having small mean values (intuitively correct) and quite disperse for eccentricity distributions having large mean values. The response distributions, however, were not sensitive to the gun tube, since the same response distributions persisted for each tube. Based upon these findings, a coupling between eccentricity and bore curvature does not exist.

The same is not true for the case of projectile band stiffness. Projectile jump response distributions are widely dispersed for flexible band distributions and less dispersed for stiffer distributions. Each response distribution is unique for a given tube, therefore, coupling exists between bore curvature and projectile band stiffness. As the mean value for band stiffness increased, the response distributions became less disperse and approached the mean COI values for most tubes. This leads one to speculate as to the possibility of using probabilistic methods to

determine parameter values in a pure dynamic analysis to improve aiming corrections for a given tube and projectile type.

The fourth point discussed concerns the feasibility of using a semi-empirical approach for the prediction of shot accuracy. The empiricism involves the use of experimental shotfall data for a given round and temperature condition to establish a baseline COV. A small sample of test data that met the given criterion was used to determine feasibility. This calculated COV couples the rounds exit direction from the dynamic analysis to the projected impact location in angular measure. For fifty percent of the test samples, a definite COV exists. It resides in a small circular region (0.25 mils) slightly above and to the right of the aim point in cartesian coordinates. In retrospect, by using the COV method for the test rounds used in this study, a small but discernible improvement in impact locations could be realized.

Further study of this method to include more rounds and more gun tubes is warranted. It is recommended that this approach be continued with the intent of gaining improved accuracy (albeit slight) across the full family of rounds for our M1A1 tank.

REFERENCES

1. T.F. Erline and M.D. Kregel, "Modelling Gun Dynamics With Dominant Loads," Proceedings of the Fifth U.S. Army Symposium on Gun Dynamics, ARCCB-SP-87023, Benét Laboratories, Watervliet, NY, 23-25 September 1987, p. 150.
2. E. Schmidt, "Jump From the M1A1 Tank," BRL IMR 868, Ballistic Research Laboratory, Aberdeen Proving Ground, MD, 1987.
3. E. Schmidt, "A Method for Indexing Tank Cannon," BRL IMR 912, Ballistic Research Laboratory, Aberdeen Proving Ground, MD, 1988.
4. S.A. Wilkerson, "The Use of Advanced Structural Codes to Study Gun Dynamics," ARL-TR-49, Army Research Laboratory, Aberdeen Proving Ground, MD, 1993.
5. J. Bornstein, I. Celmins, P. Plostins, and E. Schmidt, "Techniques for the Measurement of Tank Cannon Jump," BRL-MR-3715 Ballistic Research Laboratory, Aberdeen Proving Ground, MD, 1988.
6. B. Held (CPT), D. Webb, and E. Schmidt, "Temperature Dependent Jump of the 120mm M256 Tank Cannon," BRL-MR-3297, Ballistic Research Laboratory, Aberdeen Proving Ground, MD, 1991.
7. D. Hopkins, "Modeling Gun Dynamics with Three-Dimensional Beam Elements," BRL-TR-3171, Ballistic Research Laboratory, Aberdeen Proving Ground, MD, 1990.
8. D. Rabern (Los Alamos National Laboratory) and K. Bannister, "Prediction by Finite Element Models of 120mm Sabot/Rod Structural Response During Launch," BRL-TR-3294, Ballistic Research Laboratory, Aberdeen Proving Ground, MD, 1991.
9. J. Bornstein and E. Schmidt, "The Sensitivity of Tank Main Gun Ammunition Accuracy to Propellant Temperature," BRL-MR-3923, Ballistic Research Laboratory, Aberdeen Proving Ground, MD, 1991.
10. B. Held (CPT) and T.F. Erline, "Dynamics of the Balanced Breech System for the 120mm Tank Main Gun," BRL-TR-3186, Ballistic Research Laboratory, Aberdeen Proving Ground, MD, 1991.
11. D. Lyon, "Radial Stiffness Measurements of 120-mm Tank Projectiles," ARL-TR-392, Army Research Laboratory, Aberdeen Proving Ground, MD, 1994.
12. B. Held (CPT), "Variability in Tank Gun Accuracy Due to Recoil Variation," BRL-TR-3309, Ballistic Research Laboratory, Aberdeen Proving Ground, MD, 1992.
13. D. Webb, J. Thomas, and R. Carter, "M1A1 Tank DIT Experiment: Analysis and Results," BRL-MR-3962, U.S. Army Lab Command, Aberdeen Proving Ground, MD, 1992. CONFIDENTIAL

14. G. Borse, *FORTRAN 77 and Numerical Methods for Engineers*, PWS-Kent Publishing Company, Boston, 1985, pp 469-71.
15. R. Gast, "Analytical Comparison of the Accuracy of Tank Weapons," ARDEC Technical Report, ARCCB-TR-89023, Benét Laboratories, Watervliet NY, September 1989.
16. R. Gast, "Normal Modes Analysis of Gun Vibration by the Uniform Segment Method," ARDEC Technical Report, ARCCB-TR-87033, Benét Laboratories, Watervliet NY, November 1987.
17. *Simulation of Barrel Dynamics: Users Manual*, Danby Engineering, Cirencister, United Kingdom, 1992.
18. R. Gast, "Modal Analysis of the Dynamic Flexure in Tank Weapons," PhD Thesis, Rensselaer Polytechnic Institute, Troy, NY, May 1988.

TECHNICAL REPORT INTERNAL DISTRIBUTION LIST

	<u>NO. OF COPIES</u>
CHIEF, DEVELOPMENT ENGINEERING DIVISION	
ATTN: AMSTA-AR-CCB-DA	1
-DB	1
-DC	1
-DD	1
-DE	1
CHIEF, ENGINEERING DIVISION	
ATTN: AMSTA-AR-CCB-E	1
-EA	1
-EB	1
-EC	1
CHIEF, TECHNOLOGY DIVISION	
ATTN: AMSTA-AR-CCB-T	2
-TA	1
-TB	1
-TC	1
TECHNICAL LIBRARY	
ATTN: AMSTA-AR-CCB-O	5
TECHNICAL PUBLICATIONS & EDITING SECTION	
ATTN: AMSTA-AR-CCB-O	3
OPERATIONS DIRECTORATE	
ATTN: SMCWV-ODP-P	1
DIRECTOR, PROCUREMENT & CONTRACTING DIRECTORATE	
ATTN: SMCWV-PP	1
DIRECTOR, PRODUCT ASSURANCE & TEST DIRECTORATE	
ATTN: SMCWV-QA	1

NOTE: PLEASE NOTIFY DIRECTOR, BENÉT LABORATORIES, ATTN: AMSTA-AR-CCB-O OF ADDRESS CHANGES.

TECHNICAL REPORT EXTERNAL DISTRIBUTION LIST

<u>NO. OF COPIES</u>	<u>NO. OF COPIES</u>		
ASST SEC OF THE ARMY RESEARCH AND DEVELOPMENT ATTN: DEPT FOR SCI AND TECH THE PENTAGON WASHINGTON, D.C. 20310-0103	1	COMMANDER ROCK ISLAND ARSENAL ATTN: SMCRI-ENM ROCK ISLAND, IL 61299-5000	1
ADMINISTRATOR DEFENSE TECHNICAL INFO CENTER ATTN: DTIC-OCP (ACQUISITION GROUP) BLDG. 5, CAMERON STATION ALEXANDRIA, VA 22304-6145	2	MIAC/CINDAS PURDUE UNIVERSITY P.O. BOX 2634 WEST LAFAYETTE, IN 47906	1
COMMANDER U.S. ARMY ARDEC ATTN: SMCAR-AEE SMCAR-AES, BLDG. 321 SMCAR-AET-O, BLDG. 351N SMCAR-FSA SMCAR-FSM-E SMCAR-FSS-D, BLDG. 94 SMCAR-IMI-I, (STINFO) BLDG. 59	1 1 1 1 1 2	COMMANDER U.S. ARMY TANK-AUTMV R&D COMMAND ATTN: AMSTA-DDL (TECH LIBRARY) WARREN, MI 48397-5000	1
PICATINNY ARSENAL, NJ 07806-5000		COMMANDER U.S. MILITARY ACADEMY ATTN: DEPARTMENT OF MECHANICS WEST POINT, NY 10966-1792	1
DIRECTOR U.S. ARMY RESEARCH LABORATORY ATTN: AMSRL-DD-T, BLDG. 305 ABERDEEN PROVING GROUND, MD 21005-5066	1	U.S. ARMY MISSILE COMMAND REDSTONE SCIENTIFIC INFO CENTER ATTN: DOCUMENTS SECTION, BLDG. 4484 REDSTONE ARSENAL, AL 35898-5241	2
DIRECTOR U.S. ARMY RESEARCH LABORATORY ATTN: AMSRL-WT-PD (DR. B. BURNS) ABERDEEN PROVING GROUND, MD 21005-5066	1	COMMANDER U.S. ARMY FOREIGN SCI & TECH CENTER ATTN: DRXST-SD 220 7TH STREET, N.E. CHARLOTTESVILLE, VA 22901	1
DIRECTOR U.S. MATERIEL SYSTEMS ANALYSIS ACTV ATTN: AMXSY-MP ABERDEEN PROVING GROUND, MD 21005-5071	1	COMMANDER U.S. ARMY LABCOM MATERIALS TECHNOLOGY LABORATORY ATTN: SLCMT-IML (TECH LIBRARY) WATERTOWN, MA 02172-0001	2
		COMMANDER U.S. ARMY LABCOM, ISA ATTN: SLCIS-IM-TL 2800 POWER MILL ROAD ADELPHI, MD 20783-1145	1

NOTE: PLEASE NOTIFY COMMANDER, ARMAMENT RESEARCH, DEVELOPMENT, AND ENGINEERING CENTER,
BENÉT LABORATORIES, CCAC, U.S. ARMY TANK-AUTOMOTIVE AND ARMAMENTS COMMAND,
AMSTA-AR-CCB-O, WATERVLIET, NY 12189-4050 OF ADDRESS CHANGES.

TECHNICAL REPORT EXTERNAL DISTRIBUTION LIST (CONT'D)

<u>NO. OF COPIES</u>	<u>NO. OF COPIES</u>		
COMMANDER U.S. ARMY RESEARCH OFFICE ATTN: CHIEF, IPO P.O. BOX 12211 RESEARCH TRIANGLE PARK, NC 27709-2211	1	WRIGHT LABORATORY ARMAMENT DIRECTORATE ATTN: WL/MNM EGLIN AFB, FL 32542-6810	1
DIRECTOR U.S. NAVAL RESEARCH LABORATORY ATTN: MATERIALS SCI & TECH DIV CODE 26-27 (DOC LIBRARY) WASHINGTON, D.C. 20375	1	WRIGHT LABORATORY ARMAMENT DIRECTORATE ATTN: WL/MNMF EGLIN AFB, FL 32542-6810	1

NOTE: PLEASE NOTIFY COMMANDER, ARMAMENT RESEARCH, DEVELOPMENT, AND ENGINEERING CENTER,
BENÉT LABORATORIES, CCAC, U.S. ARMY TANK-AUTOMOTIVE AND ARMAMENTS COMMAND,
AMSTA-AR-CCB-O, WATERVLIET, NY 12189-4050 OF ADDRESS CHANGES.
